Establishment of a Co-culture System of human Macrophages and hMSCs to Evaluate the Immunomodulatory Properties of Biomaterials

Etablierung eines Co-Kultur-Systems von humanen Makrophagen und hMSCs zur Bewertung der Immunmodulatorischen Eigenschaften von Biomaterialien

Doctoral thesis for a doctoral degree
at the Graduate School of Life Sciences,
Julius-Maximilians-Universität Würzburg,
Section: Biomedicine

submitted by

Tina Tylek

from Borna

Würzburg 2019

Submitted on:

Members of the Thesis Committee

Chairperson:

Primary Supervisor: Prof. Dr. Jürgen Groll

Supervisor (Second): Prof. Dr. Franz Jakob

Supervisor (Third): Prof. Dr. Andreas Beilhack

Date of Public Defence:

Date of Receipt of Certificates:

Table of Contents

Table of Contents

Table of Contents

List of Figures

List of Figures

List of Tables

Aims and Motivation

Aims and Motivation

The innate immune response to foreign bodies is one of the major concerns, which needs to be addressed when new biomaterials are designed. The outcome of this response decides whether the biomaterial will be integrated, leading to proper healing or will be encapsulated and in the worst case rejected and thus fail to fulfill its desired function [1-3]. Macrophages are key players of the innate immune response. They are highly plastic cells, which can polarize into several subtypes with pro- and anti-inflammatory/pro-healing functions [4]. Their polarization state and the transition from the pro- to the anti-inflammatory type is crucial for the healing outcome. Thus, the macrophage response has often been addressed when the influence of biomaterial properties on the immune response was investigated *in vitro* [5, 6].

Nonetheless, macrophages are not the only cell type involved in these immune reactions, and therefore, *in vitro,* mono-cultures cannot comply with the complexity of *in vivo* processes. To overcome this, co-cultures of two or more cell types should be performed. However, to this date, there is a lack of established co-culture systems that can assess the immune response to biomaterials.

Mesenchymal stromal cells (MSCs) represent one cell type involved in this complex regeneration process, and previous studies have demonstrated their extensively immunomodulating properties [7-9]. However, their impact as endogenously derived MSCs on macrophages in the context of implanted biomaterials is mostly unclear.

Therefore, the overall aim of this thesis was to establish a functional co-culture system of primary human monocyte-derived macrophages and primary human MSCs (hMSCs) for an improved assessment of the immune response to biomaterials.

The experiments were performed with primary human cells to mimic the *in vivo* situation more closely and to be able to draw more accurate and clinically relevant conclusions. As biomaterial, precisely ordered, fiber-based scaffolds produced by the technique of Melt electrowriting (MEW) [10-12] were used. These scaffolds were manufactured and provided by a co-worker (Carina Blum) of the Department of Functional Materials in Medicine and Dentistry for the biological experiments within this thesis.

Aims and Motivation

Accordingly, the present thesis can be divided into four major parts:

1) The evaluation of the macrophage response to MEW-PCL fiber-based scaffolds (Title: Precisely Defined Fiber Scaffolds with 40 µm Porosity Induce Elongation-driven M2-like Polarization of Human Macrophages (**Chapter 2**))

2) The identification of cell-cell communication modes (Title: Cell communication modes and bidirectional mitochondrial exchange in direct and indirect macrophage/hMSC co-culture models (**Chapter 3**)),

3) The establishment of a suitable culture medium (Title: Platelet lysate outperforms FCS and human serum for co-culture of primary human macrophages and hMSCs (**Chapter 4**)), and

4) The establishment of a detailed operating procedure for the co-cultivation on MEW-PCL fiber-based scaffolds (Title: Protocol for a co-culture set up of human macrophages and hMSCs to assess the macrophage response to fiber scaffolds (**Chapter 5**)).

Chapter 1 gives an introduction and an overview of the relevant literature dealing with macrophages, their involvement in innate immunity, and the complexity of their interaction with hMSCs. Additionally, this chapter highlights the importance of a coordinated immune response to biomaterials and how this can be achieved.

The aim of **Chapter 2** was to evaluate the effects of MEW-PCL fiber-based scaffolds on the macrophage polarization by different pore geometries and pore sizes without adding differentiation factors. The potential of scaffolds with pore sizes around 40 µm had been already shown in other studies, albeit with non-fibrous setups [13]. Thus, the biomaterial design rationale for this thesis was to create scaffolds within this pore size range with the technique of MEW. Thereby, using fiber-based scaffolds with small fiber diameters (2 µm) allowed for the investigation of scaffolds with a high pore volume to fiber surface area.

First, the geometry-dependent macrophage response was tested using scaffolds of different pore shapes. Secondly, the importance of pore sizes ranging from 100 µm to 40 µm was investigated on box-shaped scaffolds. Here, differences on structural and molecular levels were tested.

Chapter 3 focuses on the identification, whether macrophages and hMSCs are actively interacting with each other. Therefore, mitochondria transfer was examined qualitatively

and quantitatively in direct and indirect (by conditioned media and transwell) co-culture systems. Moreover, the cellular structures involved in these mechanisms were examined by scanning electron microscopy. In addition, to demonstrate the immunomodulating properties of hMSCs on macrophages, the phagocytic activity of macrophages was analyzed after co-cultivation.

Due to the different standard cultivation media and serum supplements for the *in vitro* cultivation of human macrophages (RPMI-1640 GlutaMAX^{TM}, supplemented with human serum (hS)) and hMSCs (DMEM F-12 GlutaMAX^{TM}, supplemented with fetal calf serum (FCS)), a suitable co-culture medium had to be established **(Chapter 4)**. Based on the already demonstrated potential of human platelet lysate for the cultivation of hMSCs [14, 15], the influence of hS, FCS and human platelet lysate (hPL) was evaluated on macrophages in mono-cultures as well as in the co-culture of macrophages and hMSCs. To compare the potential of these sera in cell culture, macrophages were tested for differences in their morphology, adherence behavior, and differentiation potential. Due to the aim of achieving a relatively equal distribution and functional co-culture, the cell numbers and phenotype of both cell types were examined in direct co-culture. Furthermore, gene expression changes were quantitatively ascertained, and the phagocytic activity of macrophages was analyzed in order to evaluate the maintenance of the immunomodulating properties of hMSCs in the different sera. Previous studies had mentioned that heparin was obligatory in cell cultures to prevent a gelation effect [16]. However, heparin is also known to affect the polarization of macrophages [17]. Thus, hPL with and without the addition of heparin was used to investigate the influence and necessity of heparin in cultures with macrophages.

Chapter 5 is based on the results of the previous parts. Here, a step-by-step protocol for the co-cultivation of human macrophages and hMSCs on scaffolds has been developed. A MEW-PCL scaffold with a pore size of 60 μm was used as a representative biomaterial. Firstly, a setup for optimal cultivation conditions in indirect and direct co-culture on scaffolds has been developed. Subsequently, to study the co-culture phenotype and the interaction of both cell types with the material, protocols, already used for 2D co-culture, have been adapted.

Finally, the concluding discussion of all four parts with a closer look at future perspectives is outlined in **Chapter 6**.

Chapter 1

Introduction

1.1. The role of macrophages and mesenchymal stromal cells in inflammation and healing

The development of inflammation is the first response of the host body to an infection or an injury [18]. A highly ordered inflammation cascade and its outcome under normal wound conditions determine the healing outcome [19]. Numerous cell types and proteins are involved to ensure proper elimination of pathogens and regeneration of the damaged tissue [20]. However, disorders in this complex system triggered by alterations in the wound environment can lead to impaired healing, like in chronic wounds [21]. Moreover, foreign bodies such as implanted biomaterials cause an inflammatory response. For proper healing and to prevent rejection of the material, it is necessary that the inflammatory reaction is not prolonged [1].

The understanding of these mechanisms is evolving continuously, and thus further investigations can expand the knowledge of inflammation and wound healing dependent on different circumstances.

1.1.1. Macrophages

1.1.1.1   Innate immune system

The human immune system can be divided into two parts: the adaptive and the innate immune system [22]. The adaptive immune system is based on antigen-specific reactions mainly by T- and B-Lymphocytes, which are in interaction with macrophages and natural killer cells. In contrast, the innate immune system is the hosts' first defense line against invaders, encompassing physical barriers, as skin or mucosa, as well as cells and proteins, such as neutrophils, mast cells, eosinophils, monocytes, macrophages, complement factors, cytokines, and acute-phase proteins [23, 24]. Which cells and factors are involved, the order of their intervene, and which ultimately are critical to success, depends strongly on the nature and location of the wound and infection [25]. When invaders, like pathogens or foreign bodies, enter the body by a skin wound, monocytes, and macrophages, play a major part in inducing inflammatory reactions [26]. Thereby, circulating blood monocytes, evolving from the bone marrow via several intermediate cell types, are important cells of the innate immunity, which differentiate into macrophages through entering the tissue site [27]. Subsequently, on-site macrophages perform various functions [28], which are further described in the following section.

1.1.1.2.   Macrophage functions and populations

Due to their phagocytic activity, macrophages were first mentioned as "big eaters" in the late 19th century by Elie Metchnikoff [29]. In the following years, macrophages were recognized as key players of the immune system with pivotal roles in inflammation and immunity[30, 31]. Thereby, they fulfill several functions like, as the name suggests, the phagocytosis of pathogens, apoptotic cells, and debris [32] and the production of a broad range of cytokines dependent on the environmental stimuli [33]. Moreover, they are involved in tissue homeostasis, tissue remodeling, and metabolic functions [30, 34]. In addition, macrophages can interact with B-and T-cells of the adaptive immune system by the presentation of antigens on their surfaces [35]. Therefore, macrophages are part of both the innate and the adaptive immune system. Macrophages are characterized as highly plastic cells due to their phenotypical and functional heterogeneity dependent on the environment and tissue source.[36] Basically, macrophages can be divided into two different populations based on their occurrence: tissue-resident and monocyte-derived macrophages [37, 38].

The primary phenotypical regulator for tissue-resident macrophages is the surrounding tissue itself, which has been suggested to influence the gene expression pattern independently of the macrophage origin of either bone marrow, yolk sac or fetal liver [39, 40]. In nearly all tissues, adapted macrophage phenotypes can be found, e.g., brain, spinal cord – microglia [41]; lung – alveolar macrophages [42]; liver – Kupffer cells [43]; spleen – splenic macrophages [44]. According to their respective tissue environment, these adapted cells fulfill specific functions and respond diversely to inflammation processes. Furthermore, some tissue-resident macrophages can proliferate *in vivo* and thereby restore cell loss in inflammation [39, 45].

While tissue-resident macrophages are particularly important for tissue homeostasis [46], monocyte-derived macrophages are mainly participating in the initiation and resolution of inflammation caused by pathogens, foreign bodies, wounds, or injuries [47]. As the name suggests, this class of macrophages maturates from circulating blood monocytes entering the tissue at the inflammation site [48]. Here, macrophages can respond to a variety of stimuli in different circumstances by polarization into different phenotypes, which are described further below, and are even able to switch between them [49].

1.1.1.3.   The heterogeneity of macrophages

Because of the heterogeneity in polarization, macrophages were classified into specified groups. Based on the released cytokines by the Th1 and Th2 helper cell response, macrophages, which were associated with either the Th1 or Th2 response, are commonly classified as M1 [50, 51] and M2 [52, 53], respectively. Whereas the M1, as classically activated macrophages, are characterized as the pro-inflammatory type, M2, as alternatively activated macrophages, are defined as the anti-inflammatory, pro-healing type [54]. However, this classification system is extremely simplified and represents only extremes on a scale. In particular, in *in vivo* situations, macrophages can adapt a variety of functional phenotypes in response to environmental changes [30]. Several suggestions for a more exact classification have been made, for example, based on their functionality into classically activated, wound-healing, and regulatory macrophages [55, 56]. Furthermore, a classification of macrophages into several subtypes based on the stimuli affecting them and on the outcome of their gene expression and cytokine release has been proposed (Figure 1) [57]. Contributions to this system are mainly established in *in vitro* studies, and due to the steadily increasing knowledge in macrophage polarization, additions and alterations to the system are occasionally made. The next part will focus mainly on the stimuli-based classification established to date.
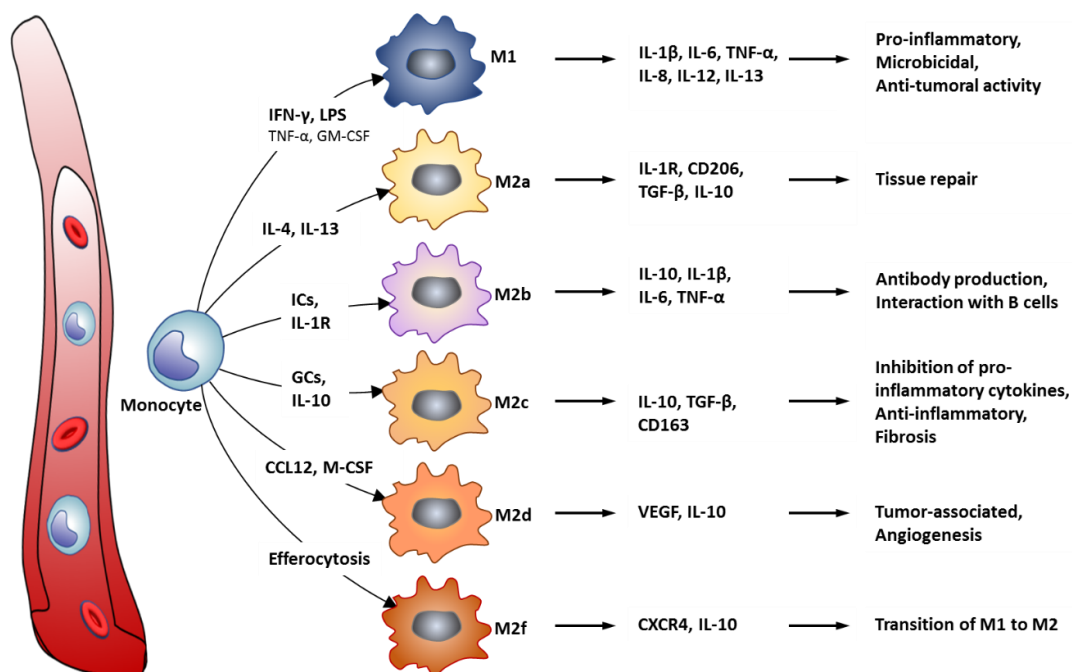
Figure 1. Scheme of macrophage polarization. Depending on the stimuli, macrophages polarize into different subtypes, each with specific expression patterns and functions. Redrawn and simplified from references [58], information added from reference [59].

1.1.1.4.   M1 type – Stimuli and Responses

Stimuli of different origins, signaling pathways, and receptors have been found to induce inflammation similarly. One of the major stimuli for a characteristic M1 differentiation, connected with the Th1 response, is the cytokine Interferon-γ (IFN-γ). This factor is produced by other immune cells, such as natural killer cells and neutrophils [60], as well as macrophages themselves [61]. Specific gene expression programs including the genes for cytokine receptors, cell activation markers, and cell adhesion molecules are controlled by IFN-γ [57, 62]. To initiate an *in vitro* M1 polarization, a combination of IFN-γ and bacterial lipopolysaccharides (LPS) is commonly used [63]. TNF-α, a further cytokine associated with the Th1 response, as well as the granulocyte macrophage colony-stimulating factor (GM-CSF) are also known to stimulate the M1 polarization [64],[65]. M1-differentiated macrophages are characterized by the production of pro-inflammatory-related cytokines, such as IL-1α, IL-1β, IL-6, TNF-α, IL-8, IL-12, IL-13, as well as by a low secretion of the anti-inflammatory cytokine IL-10 [57]. However, the influence of cytokines has always to be assessed in the respective context due to possible effects in both inflammation and healing processes. Functionalities of M1 macrophages are the removal of pathogens by the activation of the NADPH oxidase system and, thus, the production of reactive oxygen species (ROS) [66]. M1 macrophages have a strong microbicidal and anti-tumor activity. However, as they also impair tissue regeneration and wound healing, this has to be balanced by a regulative mechanism inducing pro-regenerative M2 macrophage polarization [67].

1.1.1.5.   M2 type – Stimuli and Responses

The polarization into M2 macrophages is more complex than that of M1 type macrophages. Accordingly, several subsets with different functionalities and expression patterns have been described: the well-established M2a, M2b, M2c, and M2d types and the only recently suggested M2f type.

The polarization into the M2a type is stimulated either by IL-4 or IL-13, which are cytokines associated and produced by Th2-related cells, such as mast cells, eosinophils, and macrophages themselves. IL-4 is known to stimulate macrophage fusion and to decrease their phagocytic activity [68]. Macrophages of this subset are characterized by a high expression of the anti-inflammatory mannose receptor CD206, of the decoy receptor IL-1 receptor II (IL-RII), and IL-1 receptor antagonist (IL1Ra) [69, 70]. Late M2a macrophages express suppressors of the IL-1β pro-inflammatory activity [71]. Due to a

lack of NO-production, M2a cells are compromised in microbicidal activity [72]. By producing proline and polyamine they stimulate collagen formation, induce cell growth, and participate thereby in tissue repair [69, 73].

The phenotype of M2b was reported for the first time in 2002 by Mosser and colleagues as a macrophage type, which differs significantly from the M1 and M2 populations described before [74]. Stimuli for the polarization of this type of macrophages are immune complexes (IC), toll-like receptor (TLR) agonists, or IL-1 receptor ligands [69, 70]. They can be roughly described as a mixture of M1 and M2 macrophages due to their expression and secretion pattern, including both anti (IL-10) and pro-inflammatory (IL-1β, IL-6, and TNF-α) cytokines [69, 74]. M2b macrophages are the only type of macrophages interacting with B-cells by the sustained production of antibodies and thus are an essential part of the adaptive immune system [74, 75].

The M2c macrophage type is induced by IL-10 or glucocorticoids (GCs), whereby GCs are produced and released as a reaction to various stress factors, like pain, starvation or infection and are essential for homeostasis [69, 76]. Moreover, M2c cells are characterized by a high release of anti-inflammatory IL-10, the scavenger molecule CD163, and the pro-fibrotic factor TGF-β1. Hence, they are regarded as deactivated macrophages according to their main property of downregulating pro-inflammatory cytokines, such as IL-1, IL-4, IL-5, IL-6, IL-8, IL-12, TNF-α, and pro-inflammatory mediators (iNOS,). Furthermore, these macrophages show strong anti-inflammatory activities against apoptotic cells [77, 78].

Tumor-associated macrophages (TAMs), or M2d, represent the fourth M2 macrophages type [79, 80]. Their differentiation and recruitment to the tumor site is stimulated by chemotactic factors such as CCL12 or monocyte colony-stimulating factor (M-CSF). On-site, they release high levels of anti-inflammatory IL-10 and only low levels of pro-inflammatory IL-12, IL-1β, TNF-α and IL-6 [81, 82]. The accumulation of M2d macrophages is related to a high release of pro-angiogenic factors like vascular endothelial growth factor (VEGF), which promotes angiogenesis [83].

Another M2 subtype has recently been detected following the phagocytosis of apoptotic cells, in particular, neutrophils, referred to as efferocytosis. Thereby, macrophages change their phenotypical expression pattern, e.g., by the up-regulation of the chemokine receptor CXCR4 [59]. This phenotypical switch is assumed to be related to the deactivation of macrophage inflammatory responses and thereby fosters their resolution. Suggestions have been made to call this phenotype M2eff or, according to M2a-d, M2f.

1.1.1.6. Spontaneous differentiation *in vitro*

The adherence of monocytes, *in vivo* as well as *in vitro*, is always associated with the differentiation and maturation into macrophages. For *in vitro* purposes, differentiation factors are often used to induce polarization into the previously described subtypes. Besides that, the polarization can also occur spontaneously, i.e., without the commonly used differentiation additives, based on environmental factors, such as cell culture media, different culture substrates, and 2D or 3D surfaces [84, 85]. In the present work, the term M0 describes this type of spontaneously polarized macrophages.

1.1.2. Mesenchymal stromal cells

1.1.2.1. Characteristics and functions

Mesenchymal stromal cells (MSCs) are spindle-shaped, plastic-adherent cells, which can be isolated from various tissues, such as bone marrow, adipose tissue, dental pulp, or umbilical cord blood. MSCs are characterized by their potential to differentiate into various cell types, like adipocytes, chondrocytes, osteoblast, muscle cells or tenocytes [86, 87]. However, the stemness of MSCs has been controversially discussed due to the inhomogeneous cell population obtained after cell isolation. Therefore recently, the term "mesenchymal stromal cells" has more and more replaced "mesenchymal stem cells" [88]. Despite the cells of the MSC lineage lack a universal marker set, the accepted surface markers CD105, CD73, and CD90 are present on the cells, and they do not express surface markers of leukocytes such as CD45, CD34, CD14, CD19, and CD3 [86, 89].

Due to their capability to adhere well onto plastic surfaces in contrast to other stromal cells, adherence selection is most often used as a method for their isolation. Isolated bone marrow mononuclear cells are therefore placed in a plastic tissue culture-treated flask and maintained for approximately 2-3 days at 37 °C in MSC growth medium. Subsequently, non-adherent cells will be washed off, the medium will be changed, and the remaining cells are defined as MSCs [90-92].

1.1.2.2. Immunomodulatory properties of MSCs

Besides their potential to differentiate into various tissue cells, MSCs are known to interact with cells of the immune system at several levels, either directly or by soluble factors [93]. Thus, MSCs show high potential for (cell) transplantations, the treatment of

autoimmune diseases as well as in the modulation of inflammatory responses. By interactions with the complement system, MSCs can promote their migration towards the site of inflammation, their resistance to oxidative stress, their proliferation, and their apoptotic protection [8]. Furthermore, by binding the complement component C3 they suppress the proliferation of peripheral blood mononuclear cells and by the expression of complement inhibitors, MSCs can protect themselves from the lytic activity of the complement system [9]. In response to the cellular microenvironment, MSCs show distinct phenotypes and affect the immune system differently [94]. Thereby, they either exert a pro- or an anti-inflammatory phenotype and thus take part in immunoregulation as well as tissue repair and regeneration [95]. MSCs with a predominantly pro-inflammatory characteristic are related to early infection and inflammation processes where they secrete pro-inflammatory cytokines, such as IL-6, IL-8, IFNβ or GM-CSF, involved in neutrophilic invasion, and CCL2, CCL3, and CCL12, which lead to an enhanced monocyte recruitment and thus differentiation into M1 macrophages [7, 9]. Furthermore, by releasing GM-CSF, MSCs help to maintain macrophages in their M1 state and enhance thereby bacterial clearance and early wound healing reactions [96]. In their anti-inflammatory state, activated by the exposure to TNF-α or TLR3 by immune cells, like macrophages, MSCs interact via soluble factors with numerous immune cells [9]. Thus, they suppress mast cell activation and reduce TNF-α production as well as stem cell factor induction by the upregulation of COX2 and Prostaglandin E2 (PGE2) [97]. Additionally, MSCs can interfere with natural killer (NK) cell cytotoxicity and inhibit the maturation of monocytes into dendritic cells (DCs) as well as the direct activation of DCs. Furthermore, macrophages and MSCs work together to maintain homeostasis and to act against microbial activities [98, 99]. Thereby, both cell types interact in various ways and influence each other, as described in the following section.

1.1.3. Interaction of macrophages and MSCs – co-cultivation as a technique for *in vitro* investigations

1.1.3.1. Interaction between macrophages and MCSs

Macrophages and MSCs take part in numerous cell-mediated events. Of particular interest is the influence in and on emerging microenvironments [100]. In this context, the terms MSC-educated macrophages and macrophage-associated MSCs are used to describe the cross-talk between both cell types (Figure 2) [101-103].

As a result of the interaction with MSCs, macrophages adapt an M2-like phenotype, secreting less TNF-α and higher amounts of IL-10 and CCL18, and show an increased phagocytic activity [104]. Due to the expression of the M2-associated surface markers CD163 and CD206, but the further release of pro-inflammatory cytokines such as IL-6, the impact of MSCs is considered to be an environmental stimulus for macrophages, which polarizes them into a specific subtype [105]. Studies reported that this effect is mainly orchestrated by Prostaglandin E2 (PGE2) and its role in paracrine regulation [106]. Furthermore, the effects of MSCs on macrophages are driven by the TNF-α-stimulated-gene (TSG6) and indoleamine2,3-dioxygenase (IDO), which were shown to enhance the polarization into the alternative macrophage type both, *in vitro* and *in vivo* [103, 107]. These stimulating, anti-inflammatory properties of MSCs make them an attractive tool for cell therapies [108, 109].

The macrophage-associated MSCs show a higher capacity for migration due to their increased expression of the corresponding receptors [110, 111]. In addition, these MSCs are pro-angiogenic and secrete the cytokines IL-6 and CXCL10 [100, 101]. The impact of macrophages on MSCs differs depending on their polarization. While M1 macrophages lead to in the end to MSC apoptosis, M2 macrophages enhance their migration, viability, and proliferation [112, 113].

Macrophages and MSCs are involved, as single populations but also together, in inflammatory responses and tissue repair. Studies demonstrated the contribution of MSCs in tissue repair of several degenerative and inflammatory diseases as resident or implanted cells, interacting with the environment by biologically active mediators [100, 114]. MSCs from the bone marrow, driven by signals from damaged tissue, migrate to the site of the inflammation and help to initiate a proper immune response, which is essential for the subsequent healing of the tissue [95, 115]. Moreover, MSCs release plenty of angiogenic growth factors, such as VEGF, HGF, or PDGF-β, which recruit and activate cells involved in the later regenerative phase of the immune response, e.g., macrophages, which in turn attract fibroblasts and further MSCs for tissue remodeling [100].

In vitro and *in vivo* studies on the crosstalk of macrophages and MSCs distinguish between those MSCs that are part of the therapy itself (direct cell administration or cell implantation together with biomaterials) and endogenously derived host MSCs, which arrive at the site of injury or implantation during the healing process [5]. While several studies investigated the impact of administered MSCs on macrophages, so far little

knowledge has been gained about the impact of MSCs on the macrophage response, in particular in the context of implanted biomaterials.
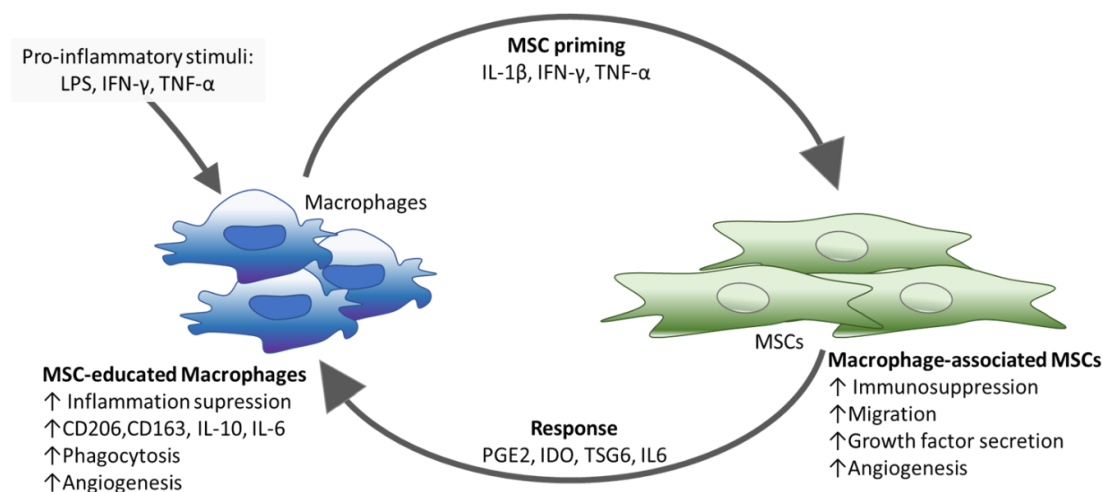
Figure 2. Interaction of macrophages and MSCs in regeneration and healing. *By interacting with inflammatory factors (LPS, TNF-α), macrophages polarize into the M1 subtype and release pro-inflammatory cytokines (IL-1β, IFN-γ), which stimulate MSCs to become immunosuppressing, pro-angiogenic and to release growth factors. MSCs respond by releasing prostaglandin E2 (PGE2), TNF-α-stimulated gene (TSG6) and indoleamine-2,3-dioxygenase (IDO). This stimulates macrophages to differentiate into a specific M2-like subtype characterized by the release of IL-6 and IL-10 and the expression of CD206 and CD163, an increased phagocytic activity and pro-angiogenic functions. Based on reference [111].*

1.1.3.2. Co-culture as an *in vitro* model

To understand certain events like the interaction of macrophages and MSCs *in vivo*, *in vitro* studies are performed. Thereby, cellular processes can be analyzed more easily and in more detail, taking advantage of a tightly controlled environment, which is not possible *in vivo*. Furthermore, the compliance of these *in vitro* studies with ethic laws is achieved more easily due to the redundancy of animal experiments. However, to properly mimic the *in vivo* cellular reactions, a mono-culture study in 2D is often insufficient. Therefore recently, approaches for a better assessment, like 3D cultures, e.g., in spheroids [116], or the co-cultivation of two or more cell types [117] have been suggested.

To investigate the interactions between macrophages and MSCs, firstly, a co-culture setup is mandatory, in which both cell types are viable and show similar behavior as in their mono-cultures. Secondly, both cell types need to be able to interact and communicate with each other within this culture system.

1.1.3.3. Principles of co-cultures

A co-culture system is defined as a cell cultivation setup of two or more different cell populations with a certain degree of contact between them [117]. The use of co-culture systems to study natural or artificial interactions of different cell types has countless applications such as infection studies, creating experimental models and biomimetic environments (like artificial tissues), studying natural interactions, drug testing or improving cultivation success for distinct cell types [118-120]. Furthermore, the co-cultivation of human cells could aid and transfer cell events more rapidly and more efficiently to the appropriate *in vivo* system, and hence reduce animal experiments for exploring and testing human biomedicals.

Co-culture systems can differ depending on the number of cell populations, the similarity between these cell populations, the degree of their separation, and the duration of the co-cultivation [117]. Commonly, co-cultures are performed with two cell types in order to manage the level of intricacy regarding the molecular interactions and their analysis as well as the establishment of a stable system. Furthermore, bi-cultivation outperformed an increased number of cell populations in co-cultures [121]. Cell types in co-cultivation can vary from very similar, e.g., from the same species or even the same cell type differing only in gene expression patterns, to very different cells like those from different species [117].

Besides the use of different cell types for the desired co-culture, a significant influence on the outcome by the degree of contact between them has to be considered for the respective intent. Various technical methods for a mixed (direct co-culture) or separated (by microfluidics, Petri dishes, on solid supports, or indirect via conditioned media) co-culture were established. If the intended application demands a mixed co-culture, e.g., to preserve the physiological behavior of mammalian cells and tissue or for invasion and recruitment assays, growth medium optimization will usually be required [85, 122].

1.1.3.4. Cell-cell communication

Distinct circumstances make cells of the same as well as of different types communicate with each other via multiple, specific ways *in vivo* as well as *in vitro* (Figure 3). One way to communicate is by soluble factors, such as cytokines and chemokines, which are released from one cell and detected by another via its specific membrane receptors [123]. Cytokines are for example involved in the regulation of inflammation, cell activation, cell migration, cell proliferation, apoptosis, and hematopoiesis [124]. Another way of cell

communication, mainly between T- or B-cells and an antigen-presenting cell, are immunological synapses. These allow for the directed secretion and integration of positive as well as of negative signals to regulate the response intensity [125].

Moreover, cells interact through gap junctions with each other in direct contact and can thereby transfer small molecules [126]. The communication via extracellular vesicles (EVs) is another important way of communication and signal transduction between cells. Depending on their size, EVs can be divided into exosomes (40 -100 nm) and microvesicles (100 - 1000 nm) and can deliver pro-peptides, cytosolic proteins, microRNAs, mRNAs, and even organelles from one cell to the other [126, 127]. For instance, the transfer of mitochondria between different cell types, including macrophages and MSCs, has been proven to occur via EVs [128, 129]. Thereby, mitochondria transfer from MSCs has been related to the increase of ATP levels and the enhancement of phagocytic activity of macrophages [130]. Additionally, mitochondria and other cell materials like vesicles, organelles, and signaling molecules can be transferred via direct contact through tunneling nanotubes (TNTs) [123].
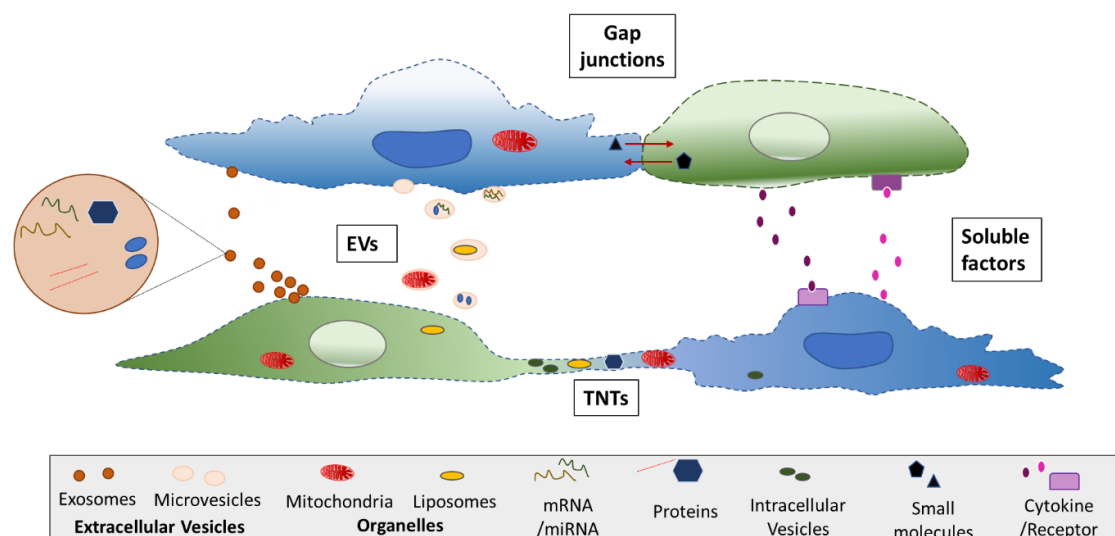
Figure 3. Cell-cell communication modes. *Mechanisms of cell communication can occur directly (gap junctions, tunneling nanotubes (TNTs) or indirectly (extracellular vesicles (EVs), soluble factors). Based on references [123, 127, 131].*

TNTs are open-ended or connexin-containing protrusions and consist of F-actin surrounded by plasma membrane. They have diameters in the range of 50 - 200 nm with varying lengths of up to several folds of the cell diameter [132] and thus, in contrast to gap junctions, direct communication is possible over a long distance [133]. The formation

of TNTs can be induced by, e.g., inflammation, infection or morphogenesis [134], and via the formation of more than one TNT towards different cells, a cellular network can be established. Many cell types, including MSCs and the most immune cells, are able to form such cellular connections and thereby can interact directly with each other [131, 135]. So far, however, many questions on the function and structure of TNTs are still open and require further investigation.

1.2. The host response to biomaterials

1.2.1. Development and order of events

After an injury and the occurrence of a wound, a related host immune response always takes place intending to restore the damaged tissue fully. Thereby, the order of events, as well as the appearance of the involved cells, usually follows a similar course. However, dependent on the trigger, e.g., a lesion or a biomaterial implantation, alterations in the order and outcome might arise. This work will mainly focus on cell interactions, which occur after the implantation of biomaterials.

The engraftment of a biomaterial induces a host response to the implant that determines the outcome of the integration as well as the biological performance of the implant (Figure 4) [2]. This response can be divided into different stages: in the protein adsorption, the early inflammation phase, and the resulting foreign body response.

After the grafting of biomaterials, their surfaces immediately adsorb a variety of blood plasma proteins, followed by the development of a provisional matrix. The subsequent inflammation phase, including the acute and chronic inflammation, is at the beginning mainly determined by the appearance of neutrophils, which enter the wound site via the bloodstream. By signals released from active neutrophils as well as through their apoptosis, mononuclear cells like monocytes and lymphocytes may initiate the chronic inflammatory response at the site of implantation. Thereby, monocyte-derived macrophages are among the key players of the initial inflammatory reaction, and their cellular response to the implanted biomaterial determines, during the foreign body reaction phase, whether a fibrous capsule formation or the resolution of the inflammatory process and hence tissue regeneration will take place [2, 3]. Therefore, dependent on the biomaterial design and its properties, the host response may be influenced to improve the healing outcome and to prevent a rejection. Accordingly, the stages of the host response described below in detail still need further assessment in correlation with newly designed biomaterials.
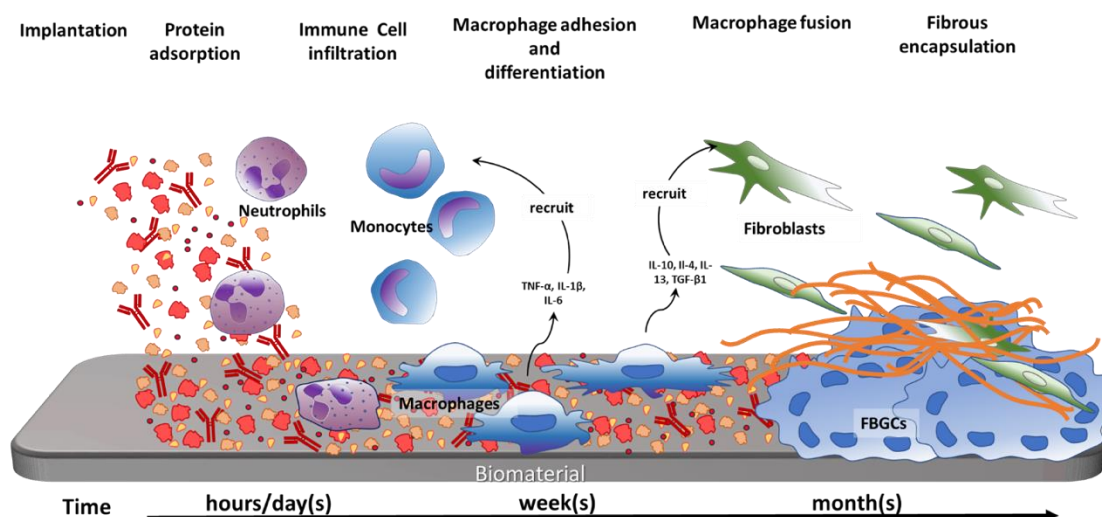
Figure 4. Host response to biomaterials. After implantation, the biomaterial is immediately adsorbed by numerous proteins, which activate the immune cell infiltration. When monocytes adhere, they differentiate into macrophages, which then polarize into different subtypes. During an extended foreign body reaction, macrophages fuse to form foreign body giant cells. Tissue cells, such as fibroblasts and mesenchymal stromal cells, get recruited, resulting in a fibrous encapsulation of the biomaterial. Based on references [2, 3, 136].

1.2.1.1.   Protein adsorption

The surfaces of synthetic biomaterials are generally not bioactive themselves, and the adsorbed proteins instead provide the bioactivity following the exposure of these surfaces to biologicals fluids like blood and saliva or cell culture medium [137]. Only after the adsorption of proteins, such as albumin, fibrinogen, complement, fibronectin, vitronectin, and γ globulin, inflammatory cells are able to recognize the material as a foreign body and thus start the initiation of cellular responses [138]. Presumably, the types, levels, and surface conformations of the adsorbed proteins are pivotal regulators of the tissue reaction to such implants [3]. Concomitant with the protein adsorption, a provisional matrix around the biomaterial surface, defined as the first clot at the interface of tissue and material, is formed by the deposition of acute-phase serum proteins as well as proteins released from degranulated platelets [3]. The presence of mitogens, chemo-attractants, cytokines, growth factors, and other bioactive agents within the provisional matrix furnishes a rich milieu of activating and inhibiting substances capable of modulating macrophage activity along with the proliferation and activation of other cell populations in the inflammatory and wound healing responses [139]. Therefore, this environment may be regarded as a naturally derived, biodegradable release system.

1.2.1.2. Inflammation phase

The acute phase of inflammation is mainly mediated by the adsorbed protein layer on the material surface as well as by mast cell degranulation and thus histamine release and fibrinogen adsorption. While this leads to the attraction of neutrophils entering the tissue via the blood, the released amounts of interleukin IL-4 and IL-13 from mast cells determine whether the subsequent foreign body response results in prolonged or attenuated manifestation [3]. By the secretion of chemokines and cytokines, their degranulation and their attempt to phagocytose foreign substances, neutrophils create an acute inflammatory environment [140]. During the first 2 - 3 days, neutrophils are present at the biomaterial interface and are involved in the degradation of the implant material by releasing oxidants. Moreover, neutrophils secrete pro-inflammatory cytokines, which induce the recruitment of monocytes, their adherence to the surface, and thereby their differentiation into M1 macrophages [60, 141].

Additionally, neutrophils are also crucial for prompting the transition of macrophages from M1 into M2 [142]. Starting after 24 h, neutrophils become apoptotic and discharge compounds such as nucleotides or chemokines, which act as signals for macrophages to remove them by efferocytosis [143, 144]. This process has several functions: besides hindering apoptotic neutrophils from unloading their cytotoxic content that could provoke tissue lesions and contribute to an enhanced inflammation response, efferocytosis facilitates the rebuilding of the tissue [145, 146]. With the shift from pro-inflammatory to anti-inflammatory macrophages, anti-inflammatory cytokines are released, which reduce the degradative capacity of immune cells and promote tissue remodeling via the migration and proliferation of fibroblasts or mesenchymal stromal cells at the wound site [3].

1.2.1.3. Foreign Body Reaction

If the foreign body exceeds a certain size (50 nm), phagocytotic cells will be unable to internalize it and will instead undergo the so-called frustrated phagocytosis [147]. As a result, toxic agents are released into the environment and can also damage the surrounding tissue [148]. Since most of the implanted materials do not fit into this phagocytable range, frustrated phagocytosis is an often-occurring phenomenon. Together with the phenotypical transition from pro- to anti-inflammatory macrophages, implanted materials often trigger macrophage membrane fusion resulting in the formation of foreign body giant cells (FBGCs) [136]. The formation of these cells, also

driven by the release of IL-4 and IL-13, is a common host response to biomaterials [2, 3, 136]. Depending on their response to the material's special properties, FBGCs can act as a barrier at the tissue/material interface and eventually lead to a rejection of the implant. Due to the secreted, pro-fibrotic factors, fibroblasts are recruited to the site of the material and attempt to repair the damaged tissue by the deposition of collagen type I and collagen type III [2, 149]. However, a profuse secretion of pro-fibrotic factors can lead to a fibrotic deposition of extracellular matrix (ECM) and the encapsulation of the biomaterial and hence, to the deterioration of the implant and the loss of its desired function [150, 151].

1.2.2. Modulation of the host response

Due to the common issue of the immune response to biomaterials, which are intrinsically used to enhance regeneration, several approaches to improve the outcome after implantation have been made. While a transient, initial pro-inflammatory state is helpful and necessary, a prolonged inflammation deteriorates the proper healing and the subsequent regeneration. Therefore, strategies have been examined, which aimed to harness the beneficial features of the immune response while they attenuate the potentially harmful aspects [2, 5]. Attempts to modulate the immune responses by presenting signals or stimuli have been performed with different methods: gene or drug delivery, cell transplantation, biomaterial modulation or combinations thereof.

1.2.2.1.   Modulation of the macrophage polarization and response by biomaterials

As key players of the host response, macrophages with their capability of switching between polarization states have been often addressed by biomaterial cues to assess the modulation of the immune response. Signals and stimuli can be transferred to the cells by different biochemical cues in their environment, such as interaction with other cell types or extracellular matrix components. Furthermore, biophysical cues, like external forces or inherent material properties, can influence cellular behavior. Accordingly, for the successful generation and development of immunomodulating biomaterials, it is crucial to understand macrophage polarization states at different stages of the host immune response. Although a prolonged polarization into the pro-inflammatory M1 type is correlated with a deteriorated healing, an initial inflammatory phase is needed. Although an early switch into the pro-healing M2 state is desired, a strongly intensified M2 presence would lead to detrimental foreign body giant cell formation [152].

Biomaterial-induced cues can be classified as inherent, i.e., induced by the biomaterial itself, or as consequent, i.e., by the microenvironment's reaction because of the biomaterial implantation (Figure 5) [5].
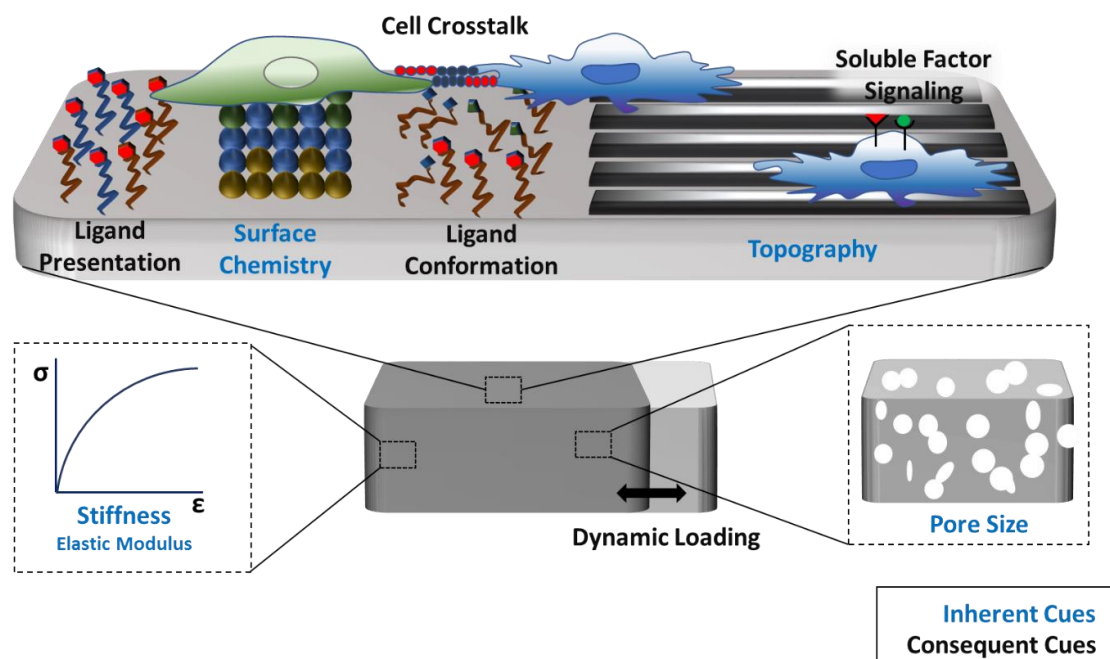
Figure 5. Biomaterial-based modulation of macrophage response. Macrophage polarization can be affected by inherent (blue) or consequent (black) cues. Redrawn and simplified from reference [5].

Consequent cues include dynamic loading as biophysical cue as well as biochemical cues, such as protein adsorption and hypoxia, by the implantation of the biomaterial. After implantation, biomaterials can undergo dynamic loading by pulsing vessels or due to their proximity to contracting muscles, which might provoke mechanical strain of the surrounding cells resulting, for example, in the upregulation of pro-inflammatory cytokines by macrophages [153, 154]. Moreover, the adsorption of selective proteins, as well as the conformation of their ligands on the biomaterial surface, can alter the macrophage polarization [155]. Furthermore, other cells, like MSCs, either transplanted or attracted to the implant site, can influence the macrophage response consequently [9, 95, 104].

If biomaterials are modulated biophysically or biochemically prior to implantation in order to influence the immune response, the term inherent cue will be used. As (bio)chemical modifications, for example, extracellular matrix proteins can be used to control the integrin adhesion of monocytes and thereby either prevent M1 polarization or promote M2 differentiation [156-158]. Furthermore, biomaterials can be designed to present or to release anti-inflammatory molecules, such as dexamethasone [159], heparin [160], and cytokines like IL-4 and IL-10 [49, 157, 161], respectively, resulting in the

modulation of the macrophage response. Biophysical cues, such as mechanical properties, topography or 3D geometries, have also been shown to stimulate macrophage polarization. Accordingly, stiffer hydrogels promoted macrophage adhesion but also increased the pro-inflammatory immune response compared to softer gels [162].

Furthermore, porous structures have already been described to influence the polarization of macrophages *in vivo* [13]: A concave-structured hydrogel, based on poly(2-hydroxyethyl methacrylate) (pHEMA) with a highly ordered architecture and exactly equally-sized pores of up to 40 µm, showed a pronounced infiltration of murine macrophages being mainly directed towards the healing phenotype. However, the scaffold fabrication method, used in this study, was limited to the production of scaffolds with a bimodal pore size distribution, originating from the diameter of the templating spheres and their contact areas. Hence, an unambiguous correlation between one defined pore size and the effects on innate immune cells was hardly possible. In contrast, extrusion-printed porous scaffolds of chitosan with diagonally orientated fibers have been reported to promote the anti-inflammatory macrophage phenotype. Thereby, these scaffolds decreased the pro-inflammatory cytokine release, whereas the secretion of pro-inflammatory markers by macrophages on constructs with orthogonally arranged fibers was enhanced [163]. In addition, McWorther *et al.* (2013), as well as Chen et al. (2010), have reported considerable effects of micro- and nano-topographical features towards the M2 macrophage polarization [164-166], when murine macrophages were triggered to adopt an elongated phenotype by these setups.

1.2.2.2.   Adaptions of scaffold geometry by melt electrowriting

The additive manufacturing technique of Melt electrowriting (MEW) (Figure 6) is an especially suitable and advantageous approach to generate 3D scaffolds as it enables the production of highly defined scaffold geometries built of fibers with diameters in the lower micrometer range [167]. In detail, defined pore sizes, as well as pore interconnectivity, have been achieved when directly-written fiber substrates were generated by MEW in a layer-by-layer fashion [10, 168]. Due to the elevated temperatures during the manufacturing procedure, cells cannot be processed simultaneously with MEW. Nevertheless, the Department of Functional Materials in Medicine and Dentistry (Würzburg) has also demonstrated the ability of cells to attach, infiltrate, and proliferate upon seeding onto MEW substrates, which renders these scaffolds suitable for various tissue engineering applications [168-170]. The most widely investigated polymer with a

well-established printing behavior for MEW is poly(ε-caprolactone) (PCL). Depending on the application, defined melt electrowritten PCL constructs with pore sizes ranging from several micrometers to several millimeters, and fiber diameters between 800 nm to 50 µm [170, 171] have been described. Already in 2013, melt electrowritten fiber scaffolds with small average inter-fiber distances of 46 ± 22 µm have enabled sufficient fibroblast penetration. However, the high standard deviation clearly indicated the irregular pore size distribution and the lack of precise stacking of the fibers upon each other [172]. The fiber deposition accuracy is mainly affected by dielectric shielding and residual charges around each deposited fiber [173]. On the one hand, this limits the discrete deposition of any two fibers to a minimal distance of a few tens of micrometers, depending on the fiber diameter, process parameters, and the type of polymer used. On the other hand, it allows for the direct contact and precise stacking of fibers.

With the ability to create scaffolds in this precisely defined manner, the investigation of cellular responses to morphological changes arising from the scaffold geometry is possible.
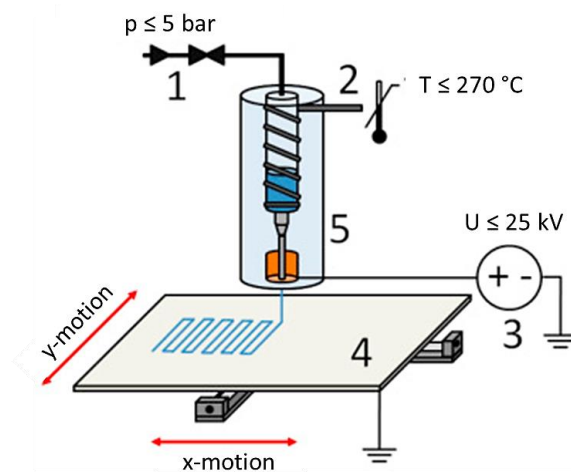
Figure 6. Schematic drawing of a MEW device. 1) Nitrogen gas pressure-assisted feeding system 2) Electrical heating system 3) High voltage source 4) Computer-aided movable collector plate 5) Syringe with molten polymer and needle tip with electrode. Adapted from reference [171]

Chapter 2

Precisely Defined Fiber Scaffolds with 40 µm Porosity Induce Elongation-driven M2-like Polarization of Human Macrophages

Chapter 2 is based on a manuscript, which is currently in revision (journal: Biofrabrication).

Authors: Tina Tylek*, Carina Blum*, Andrei Hrynevich, Katrin Schlegelmilch, Tatjana Schilling, Paul D. Dalton, Jürgen Groll

The chapter is based on the work of the author of this thesis Tina Tylek, who performed all biological experiments, data evaluation and composition of the biological parts of this manuscript.

*: shared author contributions

Chapter 2

The author contributions to the original research article are as follows:

Contributor	Contributions
Tina Tylek	Conceived the research; performed and analyzed data of all biological experiments; wrote the manuscript
Carina Blum	Conceived the research; performed and analyzed data of all experiments concerning Melt electrowriting (MEW) and characterization of scaffolds; wrote the manuscript
Andrei Hrynevich	Provided support for MEW; revised and provided feedback on the manuscript
Katrin Schlegelmilch	Conceived the research and helped to supervise the project
Tatjana Schilling	Helped to supervise the project; revised and provided feedback on the manuscript
Paul D. Dalton	Provided support for MEW; revised and provided feedback on the manuscript
Jürgen Groll	Conceived the research; revised and provided feedback on the manuscript

2.1. Abstract

Macrophages are key players of the innate immune system that can roughly be divided into the pro-inflammatory M1 type and the anti-inflammatory, pro-healing M2 type. While a transient initial pro-inflammatory state is helpful, a prolonged inflammation deteriorates a proper healing and subsequent regeneration. One promising strategy to drive macrophage polarization by biomaterials is precise control over biomaterial geometry. For regenerative approaches, it is of particular interest to identify geometrical parameters that direct human macrophage polarization.

For this purpose, melt electrowriting (MEW) was advanced towards the fabrication of fibrous scaffolds with box-shaped pores and precise inter-fiber spacing from 100 μm down to only 40 μm. These scaffolds facilitate primary human macrophage elongation accompanied by differentiation towards the M2 type, which was most pronounced for the smallest pore size of 40 μm. These new findings can be important in helping to design new biomaterials with an enhanced positive impact on tissue regeneration.

2.2. Introduction

Influencing or ideally directing the innate immune response after implantation remains one of the major challenges in the development of biomaterials and the design of three dimensional (3D) scaffolds [174]. The early phase of the immune reaction is characterized by protein adsorption to the biomaterial´s surface, followed by a provisional matrix formation [3]. The subsequent acute inflammation involves neutrophil recruitment to the injury site from the bloodstream. This neutrophil response after biomaterial implantation commonly resolves within several days and overlaps with the subsequent arrival of mononuclear cells such as monocytes and lymphocytes that can initiate the chronic inflammatory response at the site of implantation [175]. Thereby, monocyte-derived macrophages are among the key players of the initial inflammatory reaction and overall response to the implanted biomaterial, determining whether a fibrous capsule formation or the resolution of the inflammatory process and hence tissue regeneration will take place [5].

Macrophages are highly plastic and can roughly be divided into two main subtypes depending on their functionality and spatial occurrence: the "classically activated" M1 and the "alternatively activated" M2 phenotype [4]. The M1 macrophages typically release high amounts of pro-inflammatory cytokines such as IL-1β, IL-8, and TNF-α, show microbicidal activity as well as a high phagocytic activity and produce reactive nitrogen and oxygen species [176, 177]. This M1 macrophage action always provokes an inflammatory response after biomaterial implantation and is mandatory as an initial step for proper wound healing and tissue regeneration. However, the extended presence of M1 macrophages leads to severe foreign body responses as well as granuloma and fiber encapsulation resulting in a chronic inflammatory response and failure of the biomaterial's integration.[6]

In contrast, M2 macrophages release anti-inflammatory cytokines such as IL-10 and are characterized by the expression of scavenger (CD163) as well as mannose receptors (CD206) [178, 179]. Furthermore, they comprise a range of different subsets (M2a, M2b, M2c) with functionalities ranging from regulation to wound healing [180]. While the M2a and M2b subgroups fulfill immune regulatory functions, the M2c subset is crucial for tissue remodeling and the suppression of inflammatory immune responses by the secretion of TGF-β1 and IL-10 [31, 69]. These factors contribute to the vascularization of regenerative biomaterials and inhibit the formation of fibrous tissue, which significantly

improves the integration and performance of the biomaterial to fulfill its intended function [4].

For tissue-regenerative applications, it is therefore of importance that biomaterials can attenuate the pro-inflammatory response and to promote macrophage polarization into the regenerative type. One strategy to generate immunomodulating biomaterials are (bio)chemical modifications at the material surface. For example, extracellular matrix proteins can be used to control the integrin adhesion of monocytes and thereby either prevent M1 polarization or promote M2 differentiation [156-158]. Furthermore, biomaterials can be designed to present as well as to release anti-inflammatory molecules, such as dexamethasone[159], heparin[160], and cytokines like IL-4 or IL-10 [49, 157, 161], respectively, or to bind pro-inflammatory cytokines by functionalized electrospun fiber surfaces with neutralizing antibodies[181] to modulate the immune response.

Another strategy to influence the immune response involves physical cues, such as material stiffness, surface roughness, topography, or microstructure of the biomaterial. Accordingly, stiffer hydrogels promoted macrophage adhesion but also increased the pro-inflammatory immune response compared to softer gels[162]. Furthermore, porous structures have already been described to influence the polarization of macrophages *in vivo* [13]. A concave-structured hydrogel, based on poly(2-hydroxyethyl methacrylate) (pHEMA) with a highly ordered architecture and regularly-sized pores of up to 40 μm, showed a pronounced infiltration of murine macrophages being mainly directed towards the healing phenotype. However, the scaffold fabrication method used in this study yielded scaffolds with a bimodal pore size distribution, originating from the diameter of the templating spheres and their contact areas in dense packing. Hence, an unambiguous correlation between a defined pore size and effects on innate immune cells is difficult.

Also, extrusion-printed porous scaffolds of chitosan with diagonally orientated fibers generating triangular-like pores with filament diameters of 75 ± 5 μm as well as inter-filament spacings of 165 ± 5 μm, were shown to promote the anti-inflammatory macrophage phenotype. These scaffolds decreased the pro-inflammatory cytokine release of macrophages, whereas the secretion of pro-inflammatory markers by these cells on box-shaped constructs with orthogonally arranged fibers was enhanced [163].

In addition, McWorther *et al.* (2013), as well as Chen et al. (2010), had reported considerable effects of micro- and nano-topographical features towards the M2 macrophage polarization [164-166], when murine macrophages were triggered to adopt an elongated phenotype by these setups. While this effect of elongation and the

correlation with a thereby induced M2 polarization could be described in 2D for murine macrophages by either micropatterning or stimulation with IL-4 [166], this behavior could so far not be triggered for primary human macrophages. For human macrophages, the induced polarization in 2D by differentiation factors leads to a pronounced elongated shape rather for M1 (LPS/INF-γ) than for M2 (IL-4 or Dexamethasone) macrophages [182, 183]. It has furthermore been shown that the outcome of morphology and polarization of human macrophages differs between 2D and 3D environments [184, 185]. However, the elongation of human monocyte-derived macrophages on 3D scaffolds and the effects on differentiation and polarization has so far been unexplored. One potential reason is the lack of suited scaffold fabrication methods.

The additive manufacturing technique of melt electrowriting (MEW) is an especially suitable and advantageous approach in this context as it enables the production of highly defined scaffold geometries built of fibers with diameters in the lower micrometer range [167]. In detail, defined pore sizes, as well as pore interconnectivity, have been achieved when directly-written fiber substrates were generated by MEW in a layer-by-layer fashion [10, 168]. The Department of Functional Materials in Medicine and Dentistry has also demonstrated the ability of cells to attach, infiltrate, and proliferate upon seeding onto MEW scaffolds, of interest for various tissue engineering applications [168-170]. The most widely investigated polymer for MEW processing is poly(ε-caprolactone) (PCL), which is compatible with both *in vivo* and *in vitro* applications [11]. Defined melt electrowritten PCL constructs with pore sizes ranging from several micrometers to several millimeters, and fiber diameters between 800 nm to 50 μm [170, 171] have been previously described. The fiber deposition accuracy is one limitation of MEW, especially regarding the stacking height [186] and is mainly affected by dielectric shielding and residual charges around each deposited fiber [173]. On the one hand, this limits the discrete deposition of any two fibers to a minimal distance of a few tens of micrometers, depending on the fiber diameter, process parameters and the type of polymer used. On the other hand, this electrostatic attraction of fibers assists in the precise stacking of fibers to a certain height.

In the present study, the precision of MEW was advanced to allow for the fabrication of 3D porous fiber scaffolds with several adjustable but defined geometries that comprise one consistent pore size down to 40 μm throughout each construct. Box-shaped constructs with pore sizes ranging from 40 to 100 μm were then seeded with primary human peripheral blood-derived macrophages. The analysis of the cell behavior on these

scaffolds regarding cell morphology, gene expression, cytokine release, surface marker expression, and phagocytic activity provided for the first time clear evidence of elongation-driven human macrophage polarization in 3D scaffolds. Specifically, the data shows the correlation between small pore sizes and the cells' increased elongation behavior as well as their enhanced differentiation towards a pro-healing M2 macrophage phenotype. Altogether, this suggested an extended geometry-based healing effect for those 3D scaffolds with the smallest pore size tested and might set the stage for planning future promising biomaterial designs of clinical relevance.

2.3 Results

2.3.1. Spontaneous macrophage polarization depends on scaffold geometry

Melt electrowriting (MEW) was applied to produce 3D fiber scaffolds made of PCL. The scaffolds differed in their design, i.e., square, triangular, roundish, and disordered geometries were produced (Data not shown, dissertation Carina Blum (unpublished)), which was accompanied, to a certain extent, by different fiber diameters.

The cultivation of monocyte-derived macrophages on MEW scaffolds with different geometries for seven days resulted in different cell morphologies as detected by SEM (Figure 7 a-d). Whereas macrophages developed an elongated and stretched phenotype across the pores on box-shaped scaffolds (Figure 7a), their cultivation on triangle-shaped scaffolds (Figure 7 b) led them to adapt the scaffold morphology and to span the gap between adjacent fibers. On round-structured scaffolds, with a larger fiber diameter (10 µm) (Figure 7 c) compared to the other geometries (2 - 3 µm), macrophages developed no predominant morphology. Some cells were flattened with complete contact of the material-facing cell surface to individual fibers, while others had developed a rather spherical phenotype and some cells stretched across these roundish pores. After cultivation on randomly structured morphologies (Figure 7 d), macrophages grew into the individual pores spanning several layers of the scaffold. The gene expression profiles detected after seven days of spontaneous differentiation (Figure 7 e) were dependent on the different scaffold geometries. Macrophages cultivated on box-shaped scaffolds showed a stronger downregulation of the M1 markers IL-1β and IL-8 in parallel with the highest upregulation of the M2 marker CD163 when compared to all other geometries. Scaffolds with a roundish morphology provoked the smallest M1 marker downregulation and a significant decrease of M2-specific CD163 compared to box-shaped and disordered pores. Macrophages cultivated on triangle-shaped scaffolds slightly decreased the IL-8 and slightly increased the CD163 expression, compared to the day one reference sample of monocytes/macrophages (expression level set to 1). The expression of the M2 marker IL-10 was diminished over time for all examined morphologies.
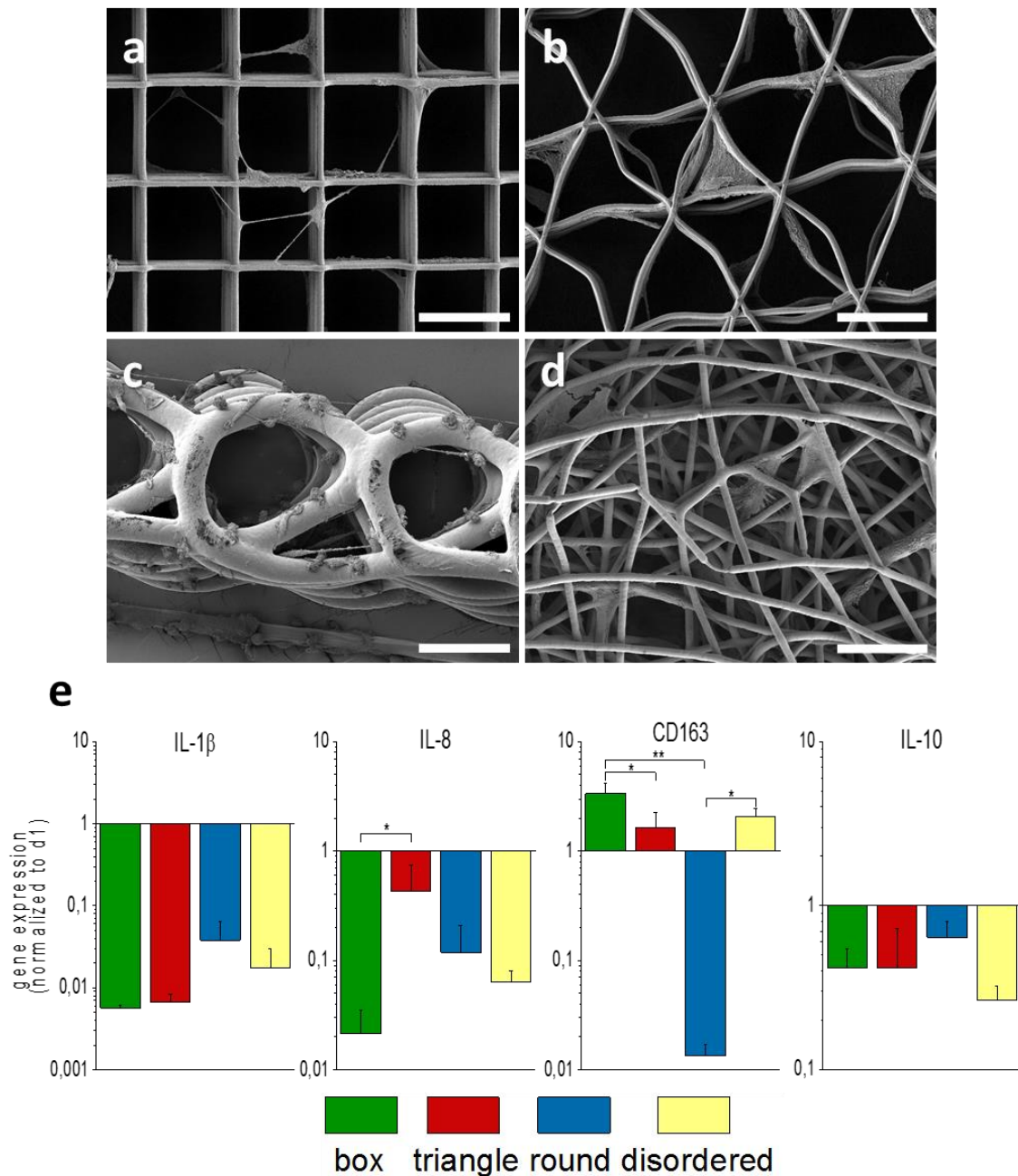
Figure 7. Morphology and gene expression profile of spontaneously differentiated macrophages on PCL scaffolds with different geometries. The cellular morphology of macrophages cultivated for seven days was observed via SEM on scaffolds with a box-shaped (a), triangle-shaped (b), round-shaped (c), and randomly disordered scaffold (d) geometry, scale bar = 50 μm. Gene expression analysis via qPCR (e) suggested spontaneous differentiation of macrophages on all tested scaffold geometries over time (compared to the reference sample (monocytes/macrophages at day 1 on the corresponding scaffold type). While both M1 markers, IL-1β and IL-8, were decreased after cultivation on the scaffolds, the M2 markers, CD163 and IL-10, rather increased, except for the roundish geometry, or experienced only a mild reduction compared to day 1. The fold changes of gene expression are given as logarithmic values with the expression of the corresponding day 1 set to 1 (mean ± SD, n = 3). *p <0.05; **p < 0.01.

2.3.2. Human macrophages can adapt an elongated morphology on box-shaped 3D scaffolds

For further experiments, box-shaped scaffolds consisting of perfectly parallel and perpendicular fibers with pores ranging from 40 to 100 µm in both x- and y-direction, were established (data not shown, see dissertation of co-worker Carina Blum). Based on the technical feasibilities of easy scaffold handling as well as controllable printing behavior, the optimal stacking height of the fibers was determined for each pore size and ranged from 20 to 60 layers (Table 1). The PCL scaffolds exhibited a high flexibility, as has been shown previously [187].

Table 1. Combinations of pore size and number of stacked layers. *Simplified from [Dissertation of Carina Blum].*

Box spacing [µm]	Number of layers in x- and y-direction
100	30 each
80	20 each
60	18 each
50	15 each
40	10 each

SEM imaging after seven days of cultivation showed that macrophages were able to stretch along single fibers and to bridge pores by reaching perpendicular as well as parallel fibers in each scaffold to a certain degree. (Figure 8 a-e). With increasing pore size, more roundish as well as flattened cells were observed on the scaffold walls. Vice versa, higher numbers of elongated macrophages with long cellular extensions were detected on scaffolds with decreasing pore sizes. On scaffolds with a pore size of 40 µm more than 50 % of the cells were elongated with an average length of about 80 µm. With increasing pore sizes, the number of elongated cells reduced down to 20 % for the fiber distance of 100 µm. This was accompanied by an increase of rounded as well as flattened cells being neatly attached to the scaffold walls. The length of the elongated cells did no longer significantly decrease from a pore size of 60 µm upwards and was maintained at an average of about 50 µm (Figure 8 f, g).

On all tested scaffolds, similar amounts of DNA, and thus cell numbers were determined at the examined time point, which excluded any cell density-associated bias on the analysis (Figure 9).
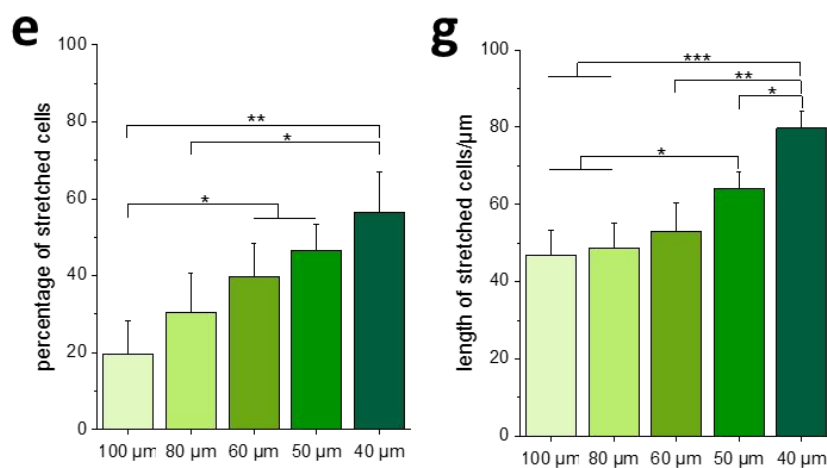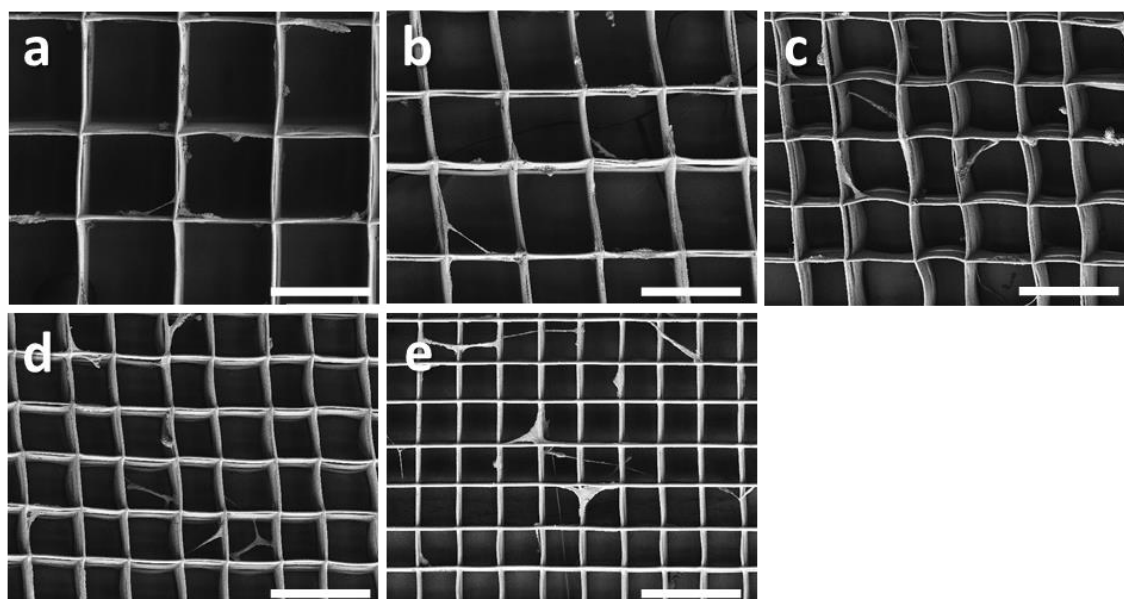
Figure 8. Cellular morphology and elongation behavior of macrophages after seven days of cultivation on 3D PCL scaffolds. Macrophage morphology was examined via SEM on scaffolds with pore size of 100 µm (a), 80 µm (b), 60 µm (c) 50 µm (d), and 40 µm (e), scale bar = 100 µm. Cell numbers and the of percentage of elongated cells (f) as wells as the lengths of elongated cells (g) were determined via ImageJ (mean ± SD, n = 3), *p <0.05; **p < 0.01, ***p < 0.001
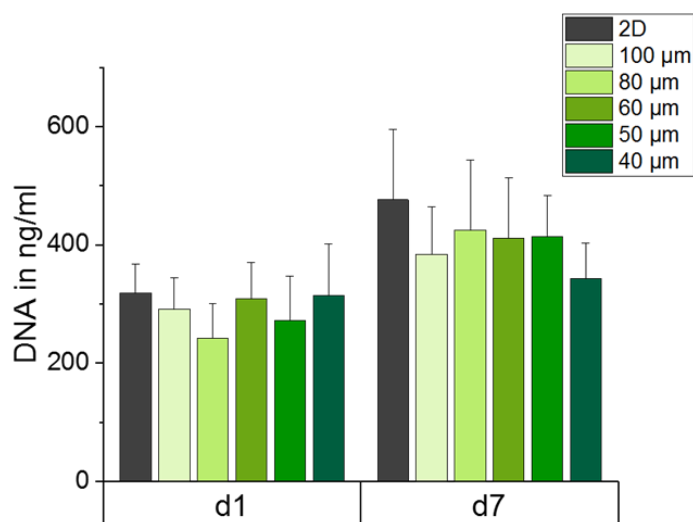
Figure 9. DNA amount of macrophages after one and seven days of cultivation on PCL film (2D) and PCL porous scaffolds with pore sizes ranging from 40 μm to 100 μm. *mean ± SD, n = 3*

2.3.3. Pore size of box-shaped scaffolds directs the spontaneous differentiation and phagocytic activity of human macrophages

The outcome of the spontaneous differentiation of monocyte-derived macrophages after seven days on scaffolds with varying pore sizes of 40 μm - 100 μm as well as on 2D PCL films was compared to macrophages cultured for one day on the corresponding scaffold/film type (Figure 10).

Concerning the expression of the M1 markers IL-1β and IL-8, porous scaffolds triggered a significant downregulation compared to the 2D control. Among the different scaffold types, no significant expression differences were obtained. In contrast, an elevated expression of the M2 markers CD206 and CD163 on scaffolds with a pore size of 40 μm and 50 μm was detected while increasing pore sizes diminished and even reverted the effect into a decline of gene expression for CD206 and CD163. The expression of the M2 marker CD163 was significantly upregulated after the cultivation of macrophages on scaffolds with a pore size of 40 μm - 60 μm. However, the larger the pores, the smaller was the augmentation of the CD163 gene expression, which even turned into a decrease for pores of 80 μm and 100 μm. Macrophages on the 2D control showed minimal up- or downregulation of the M2 macrophage differentiation markers over the time of seven days. Albeit, when considering the corresponding 2D reference sample, the IL-10

expression of macrophages was at a similar steady-state level on 40 µm scaffolds and was further reduced on scaffolds with larger pores.
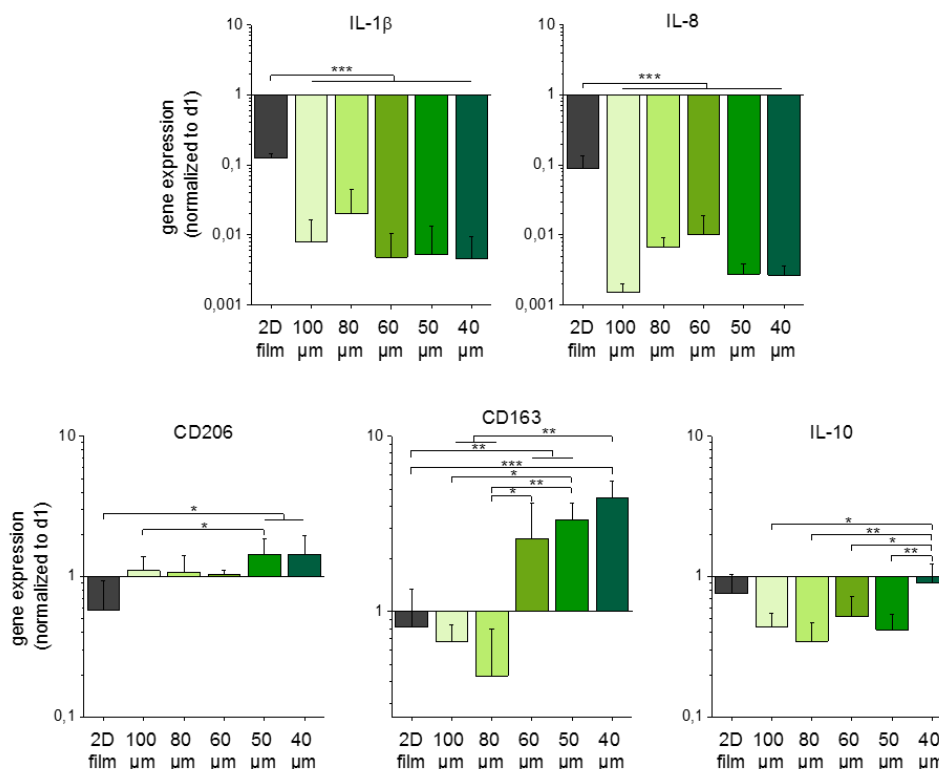
Figure 10. Gene expression profile of spontaneously differentiated macrophages on scaffolds with varying pore sizes. Gene expression was analyzed via qPCR. Spontaneous differentiation was observed on all tested scaffolds with pores ranging from 40 µm to 100 µm. Gene expression of the M1 markers, IL-1β and IL-8, as wells as of the M2 markers, CD206, CD163, and IL-10, were examined. On scaffolds with smaller pores, M2 marker expression was upregulated, while all 3D scaffolds led to a pronounced reduction of M1 marker expression. (mean ± SD, n = 3). *p <0.05; **p < 0.01, ***p < 0.001

The IL-1β, IL-8, IL-6, and IL-10 cytokine release by macrophages was examined after three and seven days of cultivation on box-shaped scaffolds with varying pore sizes and on 2D PCL films (Figure 11).

On all porous scaffolds, the release of IL-1β had declined after seven days. The cultivation on the 2D films did not affect the IL-1β release over time, which was consistently much higher than for samples derived from box-shaped scaffolds. Similar results, comparing 2D films and porous scaffolds, were ascertained for the release of IL-8. A significantly higher release of IL-6 was determined after three days of cultivation, comparing the 2D control with scaffolds of 40 µm and 50 µm pore size, respectively. After seven days, macrophages on 40 µm scaffolds released the lowest amount of IL-6. Interestingly of all porous scaffolds, macrophages on scaffolds with 60 µm pores showed the highest release of IL-6 as well as of IL-1β after three days. The amount of released IL-10 was significantly higher

after seven days on scaffolds with 40 µm pores compared to all other samples. Macrophages cultured on 50 µm and 100 µm box-shaped scaffolds showed a significant decrease of IL-10 from day 3 to day 7.
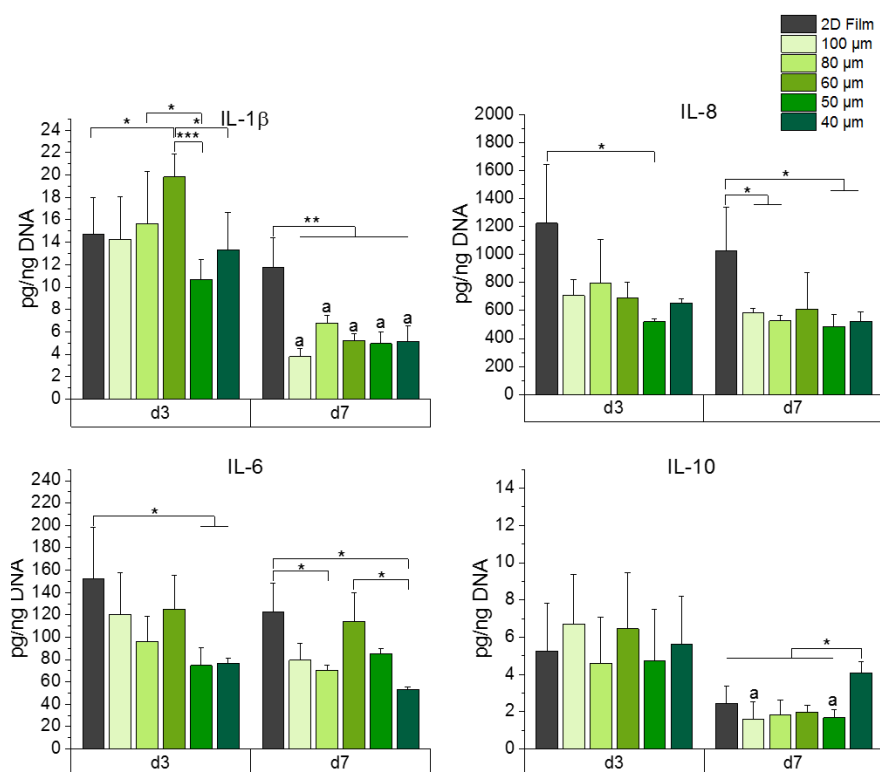
Figure 11. Cytokine release of spontaneously differentiated macrophages. *The cytokine release of IL-1β, IL-8, IL-6, and IL-10 was measured using supernatants of macrophages cultivated on a 2D PCL film and 3D MEW PCL scaffolds, respectively, with pores ranging from 40 µm to 100 µm. The amounts of released cytokines were normalized to the DNA content of the corresponding sample. (mean ± SD, n = 3). *p <0.05; **p < 0.01, ***p < 0.001; ªp < 0.05 vs d1, same culture condition.*

After seven days on all 3D scaffolds with pores ranging from 40 µm to 100 µm as well as on 2D PCL films as a control, the macrophages co-expressed the M2-specific surface markers CD206 and CD163 (Figure 12). The immunofluorescence stainings depicted that both markers were more highly expressed on scaffolds with pores of 40 µm to 60 µm than on scaffolds with 80 µm and 100 µm pores. Interestingly, elongated cells showed a more intense fluorescent staining.
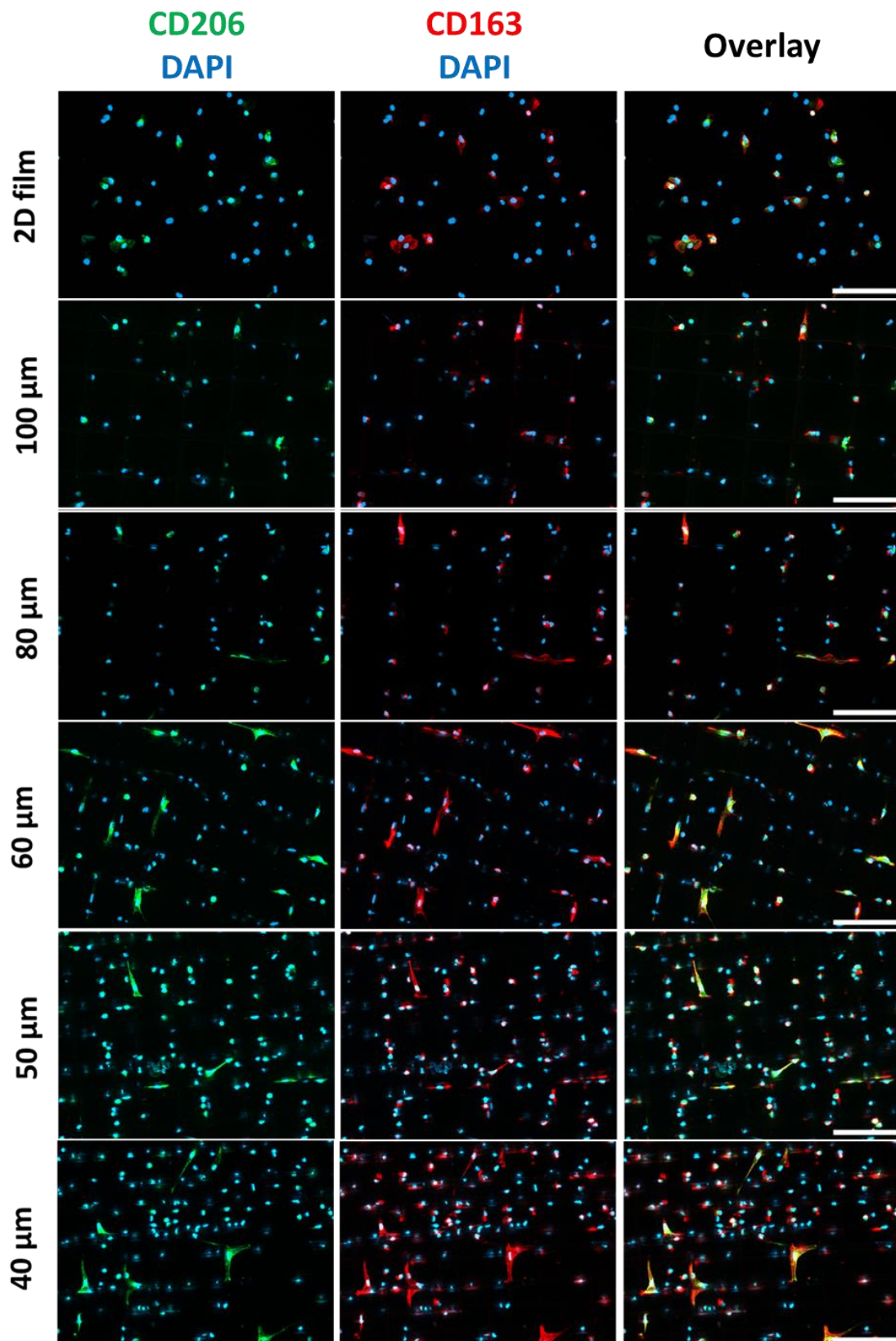
Figure 12. Immunofluorescent staining of the M2-characteristic surface markers CD206 and CD163. *On 2D PCL scaffolds (control) as well as melt electrowritten 3D scaffolds with varying pore sizes from 40 μm to 100 μm, cultivated macrophages were stained against CD206 (green, left panel) and CD163 (red, mid-panel) after seven days of spontaneous differentiation. The overlay of both channels is shown in the right panel. For counterstaining of the nuclei, DAPI (blue) was used. Scale bar = 100 μm*

The phagocytic activity of macrophages cultured on box-shaped scaffolds with varying pore sizes was augmented on day 1 (Figure 13) when pore sizes increased from 40 µm to 80 µm as detected by the corresponding elevated bead uptake. Macrophage cultivation on the smallest pores of 40 µm and 50 µm showed an initial tendency on day 1 to decrease phagocytosis compared to 2D PCL films, while larger pores enhanced the bead uptake. Between pore sizes of 60 µm and 100 µm, no further significant differences were observed. After a culture period of seven days, the number of phagocytosed beads was decreased significantly for pore sizes of up to 80 µm compared to 2D PCL films, and even the largest pore size of 100 µm showed the same tendency. Thereby, no further differences between the varying 3D scaffold types were observed.
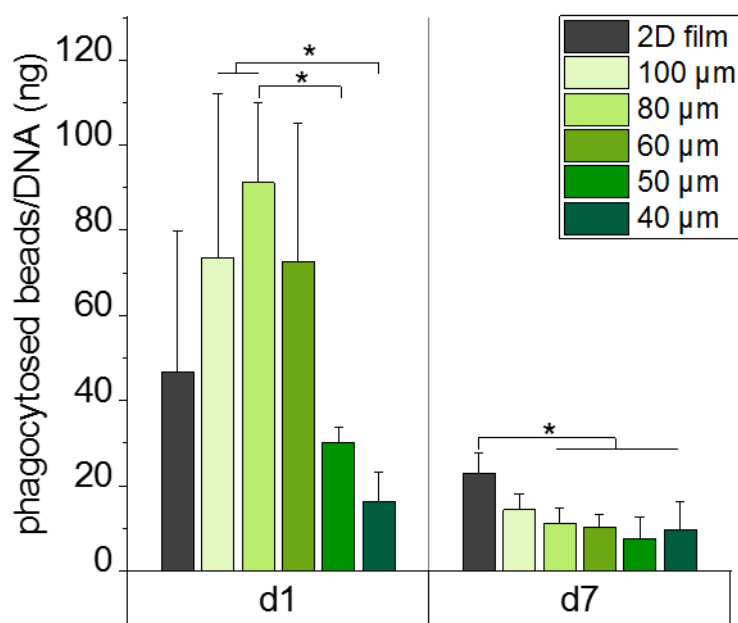
Figure 13. Phagocytic activity of macrophages cultivated on 3D MEW scaffolds with pores ranging from 40 µm - 100 µm. *The phagocytic activity of macrophages cultivated on 2D PCL films (control) and on 3D PCL scaffolds for one and seven days was detected via the uptake of fluorescent beads counted via fluorescence microscopy and normalized to the DNA content of the corresponding film/scaffold type. After one day of cultivation higher phagocytic activity was observed on scaffolds with pore sizes of 60 µm − 100 µm compared to scaffolds with smaller pores. After seven days, a significant decrease of phagocytic activity for the cultivation on porous scaffolds was detected. (mean ± SD, n = 3). **p < 0.01; ***p < 0.001*

2.4. Discussion

Immediately after implantation, a biomaterial is exposed to the body's immune response, which particularly involves the action of macrophages arriving from the bloodstream at the wound. An immediate but transient inflammation is important for healing. The switch in polarization of macrophages into the regenerative, M2 type is, however, mandatory to overcome the pronounced inflammatory response, and therefore is one of the major concerns in the fabrication and design of new biomaterials [5]. Besides biochemical modifications with cytokines or matrix proteins that may activate macrophage polarization [161, 188], macrophages are able to differentiate spontaneously depending on mechanical cues like stiffness, topography or 3D geometry of the biomaterials [13, 164, 185, 189-192]. Hence, in the present study, the influence of different, precisely manufactured scaffold morphologies produced by melt electrowriting (MEW) was investigated on the spontaneous differentiation of primary human monocyte-derived macrophages. The investigations proved an association between pore sizes, cellular elongation, and polarization towards the regenerative M2 type of human macrophages.

The studies of Bryers *et al.* [13] who demonstrated that a pHEMA sphere template scaffold with uniform and homogeneously distributed 34 μm pores supported murine macrophage polarization towards the M2 type, and Sussman *et al.* [189], who demonstrated a reduction of the foreign body reaction by such scaffolds in a murine model of skin healing *in vivo*, was used as basis for the scaffold design rationale of this study. For the reproducible fabrication of such scaffolds in high quality, the MEW technique was advanced and successfully generated PCL scaffolds with regular inter-filament distances down to 40 μm. In contrast to the cast scaffolds mentioned above, that only allow for a limited variety of pore shapes, in this study, also the production of scaffolds with different porous geometries via the precise and uniform deposition of individual PCL fibers was successfully established.

Previously, polylactic acid scaffolds with triangular-like, diagonal pores triggered macrophages to polarize into an M2-like phenotype *in vitro*, which was accompanied by a reduced release of pro-inflammatory cytokines when compared to chitosan box-shaped, orthogonal pore constructs [163]. These diagonally ordered scaffolds were, however, prepared with conventional additive manufacturing technologies resulting in filament diameters of 75 ± 5 μm as well as inter-filament spacings of 165 ± 5 μm. Nonetheless, the

comparison of chitosan scaffolds with diagonal and orthogonal structures with filament diameters of 250 ± 30 µm and spacings of 380 ± 60 µm and 600 ± 93 µm, respectively, did not lead to significant differences. The setup described in this former report with relatively big fiber diameters and large spacings might not be the optimum 3D environment to study changes in macrophage behavior: The relatively small macrophages (diameter of 20 µm - 30 µm as roundish phenotype [193]) are supposed to get readily in contact with the fibers and thus can be affected by the material itself, but they might not sense the different, rather over-dimensioned geometries. Considering this previous study, PCL scaffolds with triangle- and box-shaped morphology were produced, however, with distinct smaller pore sizes and fiber diameters. Box-shaped MEW scaffolds have already been described in previous studies [13, 170, 171, 194]. Here, the manufacturing procedure was improved regarding the significantly smaller pore size of the scaffolds, with the previously smallest pore size described being 90 µm [171].

Furthermore, the production of scaffolds with round pores from PCL fibers to assess the role of biomaterial surface curvature was successfully established. These scaffolds made of PCL were limited to a larger pore size (around 70 µm) and fiber diameter (around 10 µm). Additionally, to allow for better comparison of the within this study newly established, highly ordered scaffolds with previous studies using random scaffold geometries [195, 196], the MEW procedure was adjusted to produce randomly disordered scaffolds that mimic electrospun fiber constructs.

The pro-inflammatory cytokine release of macrophages on cylindrical pores diminished over time, but the concurrent decrease of the anti-inflammatory cytokine release rather hinted at an overall non-polarized macrophage type. This is in accordance with the presence of a broad range of different cell morphologies on these constructs (Figure 7 d). It has been assumed that the flattened and the spherical cell morphology on the round-shaped scaffolds results from the larger fiber diameter. Thus, the comparably small cells could be hindered to recognize the 3D topography of the entire scaffolds. This would rather restrict them from interacting with their immediate pericellular environment, i.e., only with the surface of a single fiber.

As concluded from the gene expression analyses, the most promising setup for the support of spontaneous differentiation towards the M2 type are the box-shaped scaffolds. Here, macrophages showed the highest expression of the M2-specific surface marker CD163 compared to all other scaffold types. Furthermore, both tested M1 markers (IL-1β,

IL-8) were strongly downregulated to the lowest levels of all scaffolds. Together with the occurrence of stretched cells on the scaffolds used in this thesis, this is in accordance with the study of McWorther *et al.* (2013), who proved an elongated phenotype to trigger murine macrophages into an M2-like polarization [166].

Guided by these outcomes, the subsequent experiments were focused on the box-shaped MEW scaffolds and aimed to investigate the influence of these porous scaffolds and their different pore sizes on macrophage polarization potential. This is the first time that MEW scaffolds with a defined small pore size of 40 μm and excellent stacking quality, resulting in highly ordered structures that have been produced. As for all defined pore sizes of 40 μm, 50 μm, 60 μm, 80 μm, and 100 μm, the manufacturing procedure outperformed previously described techniques regarding the accuracy and reproducibility of fiber deposition. In particular, this was a prerequisite to perform the biological experiments within this study, since it enabled the consistent immunological evaluation of the scaffold geometries.

As smaller pores for box-shaped scaffolds supported the stretched and elongated M2-like macrophage type (Figure 8), it was hypothesized that smaller pore sizes, separated by walls and built of relatively thin (2 μm - 3 μm) fibers, prompt the cells to interact with the scaffold at several sites. In addition, smaller pore sizes appear to facilitate the formation of elongated macrophages, since the cells can more easily bridge the gaps between the fibers unlike on scaffolds with 80 or 100 μm pore sizes. To the best of my knowledge, this study is the first, which put pore sizes of highly ordered scaffolds into context with the elongation behavior of macrophages.

M2-specific markers (CD163, CD206, and IL-10; Figure 10-7) were higher expressed and released on scaffolds when using smaller pores and decreased with increasing pore size. In particular, higher CD163 expression was thought to correlate with the higher percentage and length of elongated macrophages, which is in accordance with previous studies[164, 165] using murine cells in a structured 2D environment and hence can be transferred to the events in human primary macrophages in 3D. IL-10, a main anti-inflammatory cytokine[197], was released in significantly higher amounts, especially for macrophages cultured on box-shaped scaffolds with 40 μm pores. Furthermore, the particularly intense staining of elongated cells for these M2 markers indicated that this morphology change induced by smaller pore sizes increases the differentiation towards the M2 type. As the gene expression of the tested M1 markers (IL-1β, IL-8) was strongly downregulated on all box-shaped scaffolds with significant differences to the 2D control,

which showed a slighter decrease, this suggests an anti-inflammatory differentiation effect of porous MEW scaffolds over the period of seven days. Additionally, the 2D PCL control showed a larger potential for stimulating the release of pro-inflammatory cytokines over the whole culture period, which is in accordance with previous studies, where flat films led to an increased formation of fibrous capsules [185] or an enhanced pro-inflammatory outcome [195] compared to porous 3D electrospun fiber scaffolds. Moreover, based on the decreased release of IL-6 and IL-8 on scaffolds with 40 μm and 50 μm pores on day three, scaffolds with smaller pores were assumed to amplify the anti-inflammatory response.

The phagocytosis of pathogens, but also of foreign bodies, is a central task of macrophages. In literature, it is controversially discussed whether the phagocytic activity is induced by the M1 [198]- or the M2 type [199, 200] of macrophages. However, these studies were conducted in a conventional 2D culture, and a transfer of this knowledge to 3D culture setups is hardly possible. One previous study described an increased phagocytic activity of M1-induced macrophages in a 3D nano-scaffold based on collagen and chitosan [201] that correlates slightly with findings of this thesis. With a decrease of pore size and especially on scaffolds with 40 μm and 50 μm, the initial phagocytotic activity was significantly lower compared to scaffolds with larger pores (Figure 13). Based on the results of a lower initial proinflammatory response to smaller pore scaffolds, this was also suggested to result in a decreased phagocytic activity at day one. Therefore, the increased phagocytosis was assumed to be associated with a rather pro-inflammatory response. Moreover, concordantly with the reduced pro-inflammatory cytokine release, less phagocytic activity appeared on the 3D scaffolds compared to the 2D control after seven days, which further highlighted the benefits of porous scaffolds.

Conclusion

In this study, it could be demonstrated that fiber scaffolds with precisely controlled pore sizes between 40 μm and 100 μm lead to the elongation of adherent primary human macrophages, accompanied by a polarization towards the anti-inflammatory M2 type. This effect was most pronounced for the smallest pores of 40 μm. The down-regulation of pro-inflammatory markers and the concomitant up-regulation of anti-inflammatory factors, as well as the cell elongation, were thereby increased with decreasing pore size. Thus, it could be shown, to best of my knowledge for the first time, that elongation-driven polarization of human macrophages towards a regenerative macrophage type can be

achieved by 3D scaffolds, provided that the scaffold geometry can be controlled precisely in cellular dimensions. These findings open a perspective to generate immunomodulatory pro-healing scaffolds solely through structural control, a strategy that can be applied for future biomaterial designs to improve tissue regeneration and wound healing.

2.5. Experimental section

2.5.1. Materials:

Medical-grade PCL (Corbion Inc, Netherlands, PURASORB PC 12, Lot# 1412000249, 03/2015) was used as received and handled as described elsewhere [12]. All other chemicals were purchased from Merck (Darmstadt, Germany) unless otherwise stated.

2.5.2. 3D PCL scaffold and 2D PCL film fabrication:

All samples were fabricated with a previously described, custom-built MEW printer [12] by Carina Blum. The main experiments in this study were performed with square box-shaped scaffolds, whose manufacturing parameters slightly differed from scaffolds with other geometries (data not shown, see dissertation Carina Blum). Briefly, PCL pellets for box-shaped scaffolds were molten in a syringe with a 30G nozzle (Nordson Deutschland GmbH, Germany) at up to 77 °C until entirely liquefied. A positive, 4.0 kV high voltage was applied to the nozzle while the collector plate was grounded. The distance between the nozzle and the collector plate was adjusted to 1.4 mm. The polymer melt was pushed through the nozzle by applying 2 bar air pressure on the entire syringe. The MEW head (heater, syringe, and nozzle) was held in a fixed position and straight fibers were printed onto a moving collector plate at a speed of 950 mm min-1. After the initial stabilization of the electrified polymer jet, the box-shaped scaffolds were directly written as 3D structures using a similar G-code motion path and filament deposition onto the collector plate as has been previously described [171]. The box-shaped scaffolds were further varied and differed in the pore size and the stacking height, as stated in Table 1.

A smooth PCL film was used as a 2D control, where PCL pellets were melted using a heat gun at a temperature of 90 °C. The film was drawn at a speed of 2 mm s-1 to a thickness of approximately 100 µm. For the cell culture experiments, PCL film disks with a diameter of 14 mm were used.

Prior to cell culture experiments, PCL scaffolds and films were sterilized in 70 % ethanol for 30 min, followed by extensive washing in Dulbecco´s phosphate-buffered saline (PBS).

2.5.3. Scaffold imaging and characterization:

For the scaffold imaging using a Zeiss Crossbeam 340 scanning electron microscope (SEM; Carl Zeiss Microscopy GmbH, Oberkochen, Germany), the samples were coated with a 3 nm thick conductive platinum layer in a Leica EM ACE600 sputtering unit (Leica Microsystems, Wetzlar, Germany) prior to SEM imaging. The straight-line selection tool of ImageJ software was used to measure pore size and fiber diameters. Measurements were taken at 20 random regions within each SEM image, and mean values were calculated.

2.5.4. Cell culture

All experiments were performed with the approval of the Local Ethics Committee of the University of Würzburg. Buffy coats were obtained from the Bavarian Red Cross (Blood donor service, German Red Cross, Wiesentheid, Germany) with the written informed consent of each blood donor.

Monocytes were isolated from human blood-derived buffy coats of healthy donors. Peripheral blood mononuclear cells were collected by density gradient centrifugation with Pancoll (Density: 1.077 g l-1; Pan-Biotech, Aidenbach, Germany). Monocytes were isolated via negative selection (Pan Monocyte Isolation Kit, Miltenyi Biotec, Gladbach, Germany). Cells were seeded onto the different scaffold types and the 2D-PCL control and cultivated for up to seven days in macrophage culture medium (RPMI-1640, GlutaMAX^{TM} (Thermo Fischer Scientific, Waltham, USA) with 10 % (v/v) of human platelet lysate [85] (hPL, PL Bioscience, Aachen, Germany) and 1 % (v/v) Penicillin-Streptomycin (Pen-Strep; 5,000 U ml-1) (Thermo Fisher Scientific, Waltham, USA) in tissue culture-treated 24-well plates (Nunc, Thermo Fischer Scientific, Waltham, USA) in a humidified atmosphere at 37 °C and 5 % CO_2. Monocytes differentiated spontaneously, i.e., without supplemented differentiation factors, into so-called M0 macrophages within this time.

In detail, 0.75 x 10^6 freshly isolated monocytes suspended in 50 µl were seeded onto each sample in a tissue culture-treated 24-well plate. While melt electrowritten scaffolds were subsequently incubated in a humidified atmosphere at 37 °C and 5 % CO_2 for 0.5 h to facilitate cell adhesion before an additional 1 ml cell culture medium was added, cells on the 2D PCL film were immediately supplied with 1 ml macrophage culture medium. To avoid cell loss, each scaffold was weighed down with a sterile plastic ring cut from a

serological pipette (Greiner BioOne, Kremsmünster, Austria) for the first two days of cultivation.

Each experiment was performed at least three times with independent primary donor material (n = 3).

2.5.5. Determination of DNA amount

The Quant-iT™ PicoGreen® dsDNA Reagent and Kit (Thermo Fisher Scientific, Waltham, USA) were used according to the manufacturer's manual employing the middle-range standard curve to determine the DNA amount that correlates with the number of adhered macrophages. In short, macrophages were cultivated on PCL films and scaffolds in 24-well plates in 1 ml macrophage culture medium per well in a humidified atmosphere at 37 °C and 5 % CO_2. After one and seven days, cells were washed once with PBS$^-$ and lysed in 1 ml 1 % Triton X-100 in PBS$^-$ for 1 hour at 4 °C. The standards and samples were excited at 485 nm and the fluorescence emission intensity was measured at 538 nm on a plate reader (Tecan, Männedorf, Switzerland).

2.5.6. Gene expression analysis

Total cellular RNA of macrophages was isolated using PeqGold Trifast™ (VWR, Darmstadt, Germany) in accordance with the manufacturer's protocol. Cell-laden scaffolds were placed into a fresh well to exclude any cells having possibly adhered to the cell culture plastic from further analysis. cDNA was generated with the High-Capacity cDNA Reverse Transcription Kit (Thermo Fisher Scientific, Waltham, USA) according to the manufacturer's manual. The mRNA expression levels of macrophages were analyzed via quantitative Real-Time PCR (qPCR) (StepOnePlus; Thermo Fisher Scientific, Waltham, USA) with SYBR™ Select Master Mix (Thermo Fisher Scientific, Waltham, USA). Each 10 µl qPCR reaction comprised 5 ng of cDNA and 200 nM primer sequences (Biomers, Ulm, Germany) (Table 2). For each cDNA sample, the threshold cycle (Ct) value of each target sequence was subtracted from the Ct value of the housekeeping mRNA RPS27a to derive ΔCt. Gene expression changes were calculated by the 2-ΔΔCt method. A control group of macrophages, as indicated in the figure legends, was used for normalization.

Table 2. Primer sequences

Name	Sequence 5' → 3'	Annealing temperature [°C]	Fragment size [bp]
RPS27A*			141
Forward	5'-TCGTGGTGGTGCTAAGAAAA-3'	61	
Reverse	5'-TCTCGACGAAGGCGACTAAT-3'		
IL-8			113
Forward	5'-CATACTCCAAACCTTTCCACCC-3'	61	
Reverse	5'-CTCTGCACCCAGTTTTCCTTG-3'		
IL-1β			120
Forward	5'-GACCTGAGCACCTTCTTTCCC-3'	61	
Reverse	5'-GCACATAAGCCTCGTTATCCC-3'		
CD163			85
Forward	5'-GTGCCTGTTTTGTCACCAGTTC-3'	61	
Reverse	5'-TTACACACCGTTCCCCACTCC-3'		
CD206			156
Forward	5'-TCCAAACGCCTTCATTTGCC-3'	61	
Reverse	5'-GCTTTTCGTGCCTCTTGCC-3'		
IL-10			130
Forward	5' CTTTAAGGGTTACCTGGGTTGC '3	61	
Reverse	5' TCACATGCGCCTTGACT '3		

*housekeeping gene

2.5.7. Cytokine quantification via Single-Analyte ELISArray Kits

The cytokine release of spontaneously differentiated macrophages cultivated on 2D PCL films and 3D scaffolds was tested via Single-Analyte ELISArray Kits (Qiagen, Hilden, Germany) after three and seven days of cultivation. The production of IL-1β, IL-8, IL-6, and IL-10 was analyzed in samples' supernatants according to the manufacturer's protocol. Thereby, the absorbance measured on a plate reader (Tecan, Männedorf, Switzerland) at 450 nm and corrected with the absorbance at the reference wavelength of 570 nm directly correlated with the amounts of cytokines. For the normalization to cell numbers, the DNA levels of macrophages on the corresponding scaffolds were determined as described above and taken into account.

2.5.8. SEM Preparation of biological samples

For SEM preparation after seven days of cultivation, samples were fixed with 6 % glutaraldehyde for 15 min on ice. Then samples were incubated two times with PBS⁻ on ice prior to their dehydration by a graded ethanol series (2 x 70 %, 2 x 90 %, 2 x 100 % (v/v)). After drying via hexamethyldisilazane, the samples were fixed on stubs and coated,

as mentioned above. For the determination of the percentage and individual length of stretched cells, 20 random images per scaffold were taken and analyzed via ImageJ.

2.5.9. Immunofluorescence staining of cell surface proteins

Macrophages were cultured either on the 2D PCL film or scaffolds for seven days and fixed with 4 % formaldehyde for two hours at room temperature (RT). The samples were washed twice with PBS and blocked with 2 % bovine serum albumin in PBS- for 30 min at RT. Primary antibodies against CD163 (#TA506380, OriGene, Rockville, USA; 1:100) and CD206 (#ab64693, Abcam, Cambridge, UK; 1:400) were applied for 2 h at RT in a humidified chamber. Subsequently, fluorescence-labeled secondary antibodies (Cy2^{TM}-conjugated AffiniPure Goat Anti-Rabbit or Cy3^{TM}-conjugated AffiniPure Goat Anti-Mouse (Jackson ImmunoResearch; Dianova, Hamburg, Germany) were applied for 30 min at RT. Samples were washed and mounted with "Immunoselect Antifading Mounting Medium" with DAPI (Dianova, Hamburg, Germany). Images were captured via fluorescence microscopy (Axio Observer, Zeiss equipped with epifluorescence optics and an MRm camera; Zeiss, Oberkochen, Germany).

2.5.10.   Phagocytosis assay

The phagocytic activity of macrophages was analyzed using 2 µm red fluorescence-labeled latex beads (Sigma-Aldrich, Munich, Germany). The beads were added to the macrophage culture in a ratio of 10 beads per seeded cell and incubated in a humidified atmosphere for 2 h at 37 °C and 5 % CO_2. Cell-laden 3D scaffolds as well the 2D controls were washed three times with serum-free macrophage culture medium to remove non-phagocytosed beads.

The phagocytotic activity was analyzed via fluorescence microscopy by counting engulfed beads of ten random pictures of each scaffold via ImageJ. To exclude beads attached to the scaffolds themselves, cell-free scaffolds were treated in the same way and the measured beads subtracted from those of the cell-laden scaffolds. For normalization, the DNA amount of the macrophages was determined for each scaffold, as described above.

2.5.11.   Statistics

Statistica (Statsoft, Hamburg, Germany) was used for statistical analyses. The two-sample t-test determined the statistical significance of qPCR data. For all other data, two-way analysis of variance (ANOVA) was performed. Results were considered to be significantly different at a p-value below 0.05.

Chapter 3

Cell Communication Modes and Bidirectional Mitochondrial Exchange in Direct and Indirect Macrophage/hMSC Co-Culture Models

Chapter 3 was published as original research article (Tina Tylek, Katrin Schlegelmilch, Andrea Ewald, Maximilian Rudert, Franz Jakob, Jürgen Groll. "Cell communication modes and bidirectional mitochondrial exchange in direct and indirect macrophage/hMSC co-culture models" in BioNanoMaterials, 2017, issue 3-4), reproduced from [128] as open access article distributed under the Creative Commons Attribution License which permits unrestricted use, distribution and reproduction in any medium. The article is based on the work of the author of this thesis Tina Tylek, who performed all experiments, data evaluation and composition of the manuscript.

The original text was slightly modified to improve readability.

Chapter 3

The author contributions to the original research article are as follows:

Contributor	Contributions
Tina Tylek	Designed research; performed and analyzed data of all experiments; wrote the manuscript
Katrin Schlegelmilch	Helped supervising and designing the project; revised and provided feedback on the manuscript
Andrea Ewald	Provided feedback on the manuscript
Franz Jakob	Provided cell material
Maximilian Rudert	Provided cell material
Jürgen Groll	Conceived the research; revised and provided feedback on the manuscript

3.1   Abstract

Macrophages are important cells of the innate immune system. They exhibit a high plasticity in phenotypes and play a major role in healing by initiating the early inflammatory reactions via the pro-inflammatory M1 phenotype. The anti-inflammatory M2 phenotype is assumed to induce regenerative processes and vascularization in subsequent tissue repair. Especially for regenerative processes, their interplay with multipotent human mesenchymal stromal cells (hMSCs) is decisive. Accordingly, *in vitro* co-culture models of these cell types are an important starting point for unraveling regenerative mechanisms. In this study, the use of direct co-culture, transwell-systems, and conditioned medium were compared to investigate the mitochondria transfer between the two cell types and the influence of hMSCs' presence on the phagocytic activity of macrophages. Using flow cytometry and fluorescence microscopy, the transfer of mitochondria in both directions: from hMSCs to macrophages and, most notably, also vice versa, was visualized. Both cell types release mitochondria and internalize them in direct contact via tunneling nanotubes, as well as in indirect contact due to extracellular vesicles (EVs). Mitochondria were non-directionally released into the medium and could be transferred via conditioned medium. After three hours of direct and indirect co-culture, the majority of the cells showed a mitochondrial uptake. Co-cultivation also led to an increase in the phagocytic activity of macrophages, with the highest phagocytic rate after 48 h and most pronounced in direct co-cultivation.

3.2. Introduction

Human monocyte-derived macrophages are crucial immune effector cells of the innate immune system. In addition to their function as first defense against microorganisms, they also serve to initiate and control the adaptive immune response [202]. They react specifically to alterations in their environment as well as on cellular signals and are divided into the pro-inflammatory M1 and the anti-inflammatory M2 type [179]. Influenced by other cell types or implanted biomaterials, they are able to switch between the differentiation types [203, 204].

Human mesenchymal stromal cells (hMSCs) are multipotent adult stem cells that can be isolated from several tissues. They reflect immune-modulatory properties, as they secrete chemotactic peptides and can change the macrophage phenotype into an anti-inflammatory M2-like type[95, 102, 114]. Furthermore, their stimulatory effect on phagocytic activity, a primary characteristic of macrophages, has been reported [114]. This process leads to internalization and killing of entering pathogens, removal of foreign particles or clearing of cell debris by macrophages, which is essential for host homeostasis [202]. Moreover, specific populations of bone and bone marrow resident macrophages with very remarkable plasticity have been recently described to contribute to bone healing and regeneration substantially. Upon tissue injury, both hMSCs and macrophages display several roles in the inflammatory and regenerative phases of healing as well as in the remodeling phases, during which tissue regeneration takes place. In the very early phase of bone healing, resident macrophages have even been demonstrated to be involved in efferocytosis, the removal of dying osteoblasts [205, 206]. Besides neutrophils and mast cells, such tissue-resident macrophages belong to the first cells that enter the wound site. There, they release chemokines for monocyte attraction, which subsequently differentiate into new macrophages and become part of the inflammatory processes [114, 152]. Through juxtacrine secretion of cytokines such as IL- 6 hMSCs are activated [207], migrate to the wound site, and regulate the inflammation by immunomodulatory functions, like suppression or production of chemokines [208, 209]. Due to the release of growth factors, hMSCs recruit other cell types like parenchymal cells, endothelial cells or fibroblasts, which start to proliferate in the wound area [210]. Later in the remodeling phase, macrophages can switch from the M1 into the M2 type [203]. Together with hMSCs that differentiate into different cell types depending on the environment, they take part in tissue regeneration.

After the implantation of biomaterials, the implant often gets encapsulated and separated from the host tissue during inflammation/regeneration phases (foreign body reaction) [3, 211]. Since macrophages and hMSCs are important cells for tissue regeneration processes, co-culture models of both cell types are often used to analyze reactions caused by specific biomaterials or environmental factors [12, 13]. In addition, *in vitro* co-culture systems are important for analyzing the direct influence of one cell type to another to mimic *in vivo* conditions and thus supporting the understanding of *in vivo* processes. There are three different options for performing co-culture systems. Via direct co-culture, it is possible to investigate the mutual interactions of cell populations in the same culture plate. Here the impact of direct contact and soluble non-directional components, respectively, cannot be distinguished. In a transwell-system, the cell populations are separated by a membrane, so the exchange effects of soluble factors can be examined as cells have no direct contact but are cultivated in the same culture medium [212]. By means of conditioned medium, the influence of spontaneously secreted factors onto a second, separated, cell population can be examined.

By the release of mitochondria, hMSCs are known to increase ATP levels or to enhance the phagocytic activity of alveolar macrophages [130]. They can also manage oxidative stress by depolarized mitochondria. The transfer of mitochondria can be achieved either by encapsulation in extracellular vesicles (EVs) or via so-called tunneling nanotubes (TNTs), which are tubular connections between cells [213-215]. The formation of nanotubes has also been described for macrophages. Here, they enable vesicular traffic to neighboring cells to induce the phagocytosis of apoptotic cells [132, 216]. However, the transfer and exchange of mitochondria by TNTs or other intercellular transport routes from macrophages to other cells is so far largely unexplored.

In the present study, the interactions and modes of communication between hMSCs and macrophages via different co-culture systems were investigated. Flow cytometry and fluorescence microscopy as characterization methods were used. Especially the analysis via fluorescence microscopy can be further used for co-culture studies on biomaterials and in 3D cultures. If the effect of eluates of biomaterials on the co-culture of macrophages and hMSCs is to be investigated, the analysis can also be carried out using flow cytometry. Moreover, the transfer of mitochondria from macrophages to hMSCs and vice versa, as well as the influence of hMSCs on the phagocytic activity of macrophages, was analyzed.

3.3. Results

3.3.1. Flow cytometry analysis of mitochondrial uptake after direct and indirect co-culture

To investigate the cell-cell contact during the co-culture of macrophages and hMSCs, the mitochondrial transfer from one cell type to the other via flow cytometry and fluorescence microscopy was examined. Therefore, one cell-type was stained with MitoTracker® Red, which is incorporated into the mitochondria of these cells. Once mitochondria are released or transferred through direct cell-cell contact, the dye sequestered in the cell organelle can be delivered to other cells. This mitochondrial uptake was analyzed by flow cytometric quantification. To distinguish macrophages from hMSCs after direct co-culture, macrophages were gated by positive CD45 staining using a specific, FITC-labelled antibody. After 3 h of direct co-cultivation, 100 % of the hMSCs population was positive for macrophage mitochondria and nearly 96 % of the macrophage population showed uptake of mitochondria derived from hMSCs. After 24 h these uptake rates remained stable in both investigated cell types (Figure 14).
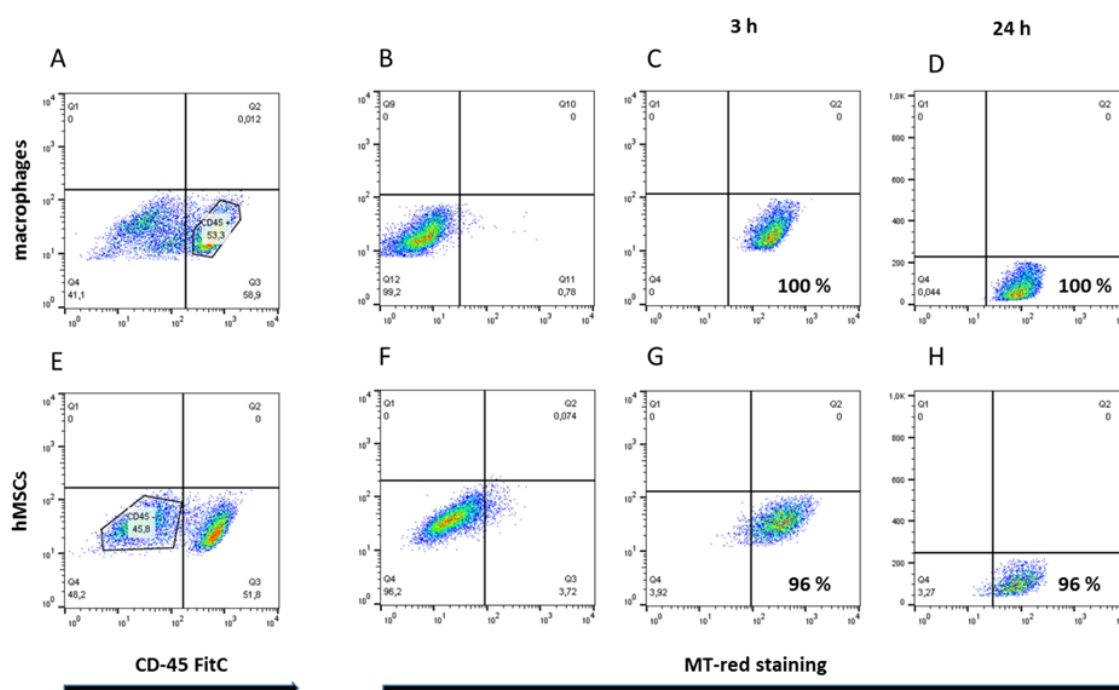
Figure 14. Flow cytometry analysis of mitochondrial transfer in direct co-culture from hMSCs to macrophages and vice versa (A-D: transfer from hMSCs to macrophages, E-H: transfer from macrophages to hMSCs). A: After the co-culture of macrophages and hMSCs, CD45+ macrophages were gated. B: Population of MitoTracker® Red (MT-red)-negative macrophages. C: 100 % of macrophages (CD45+) showed red fluorescence after 3 h of direct co-culture with MT-red-stained hMSCs D: After 24 h the staining of macrophages remained stable. E: CD45- hMSCs were gated. F: Population of MT-red-negative hMSCs. G and H: After 3 h and 24 h, respectively, 96 % of hMSCs (CD45-), showed red fluorescence when co-cultivated with MT-red-stained macrophages. Data are representative of three independent experiments. Moreover,

mitochondrial transfer without direct cell-cell contact through conditioned medium was detected. For this purpose, the cells were cultivated separately for 24 h before the conditioned culture media were interchanged (Figure 15). Here, the mitochondrial uptake was less pronounced compared to the direct co-culture but still increased during 24 h of exposure to conditioned medium up to 72 % for hMSCs and 61 % for macrophages.
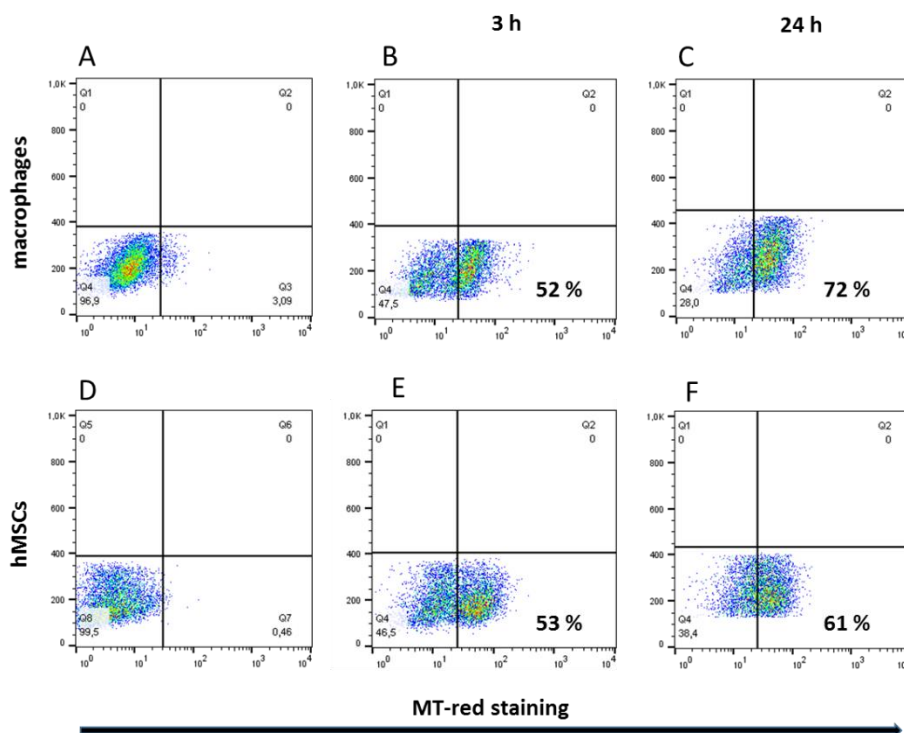
Figure 15. Flow cytometry analysis of mitochondrial transfer via conditioned medium from hMSCs to macrophages and vice versa. The conditioned medium of one MT-red-stained cell type was harvested and after centrifugation and sterile filtration applied to the unstained cell type. A: Population of MT-red-unstained macrophages. B and C: Previously unstained macrophages were treated with conditioned medium of MT-red-stained hMSCs. After 3 h (B), 52 % of macrophages showed red fluorescence, which increased up to 72 % after 24 h (C). D: Population of MT-red-unstained hMSCs. E: After 3 h in conditioned medium, 53 % of hMSCs displayed red fluorescent mitochondria, this rate increased up to 61 % after 24 h (F). Data are representative of three independent experiments.

3.3.2. Microscopic analysis of mitochondrial transfer in direct and indirect co-culture

For visualization of mitochondrial transfer, one cell type was stained with Cell Tracker® Green (CT-green) and the other one with MitoTracker® Red (MT-red). Therefore after co-culture, green fluorescent cells have not internalized mitochondria from the other cell type, while double-stained cells (green and red fluorescent) reflect cells after mitochondrial uptake from the respective other cell type (Figure 16 A and B). After 3 h of direct co-cultivation, most of the cells stained with CT-green possessed double staining in consequence of mitochondrial uptake.

Fluorescence microscopy visualized mitochondria transfer by direct cellular extensions, tunneling nanotubes (TNTs), from one cell type to the other (Figure 16 A and B) and by the release of extracellular vesicles (EVs), which apparently contain mitochondria (Figure 16 C and D). It could be shown that TNTs, starting at macrophages or hMSCs, contain small red fluorescent particles, when cells were stained with MT-red. These TNTs connect different cell types (Figure 16 A and B, white arrows) as well as cells from the same type. The isolated EVs showed red fluorescent mitochondria when the cell culture medium was taken from cultivated cells stained with MT-red. In cell culture medium from unstained cells (Figure 16 E) and cell culture medium, which contains MT-red (data not shown) but was not in contact with macrophages or hMSCs, no red fluorescent particles were found. Hence, the staining originates from released mitochondria.
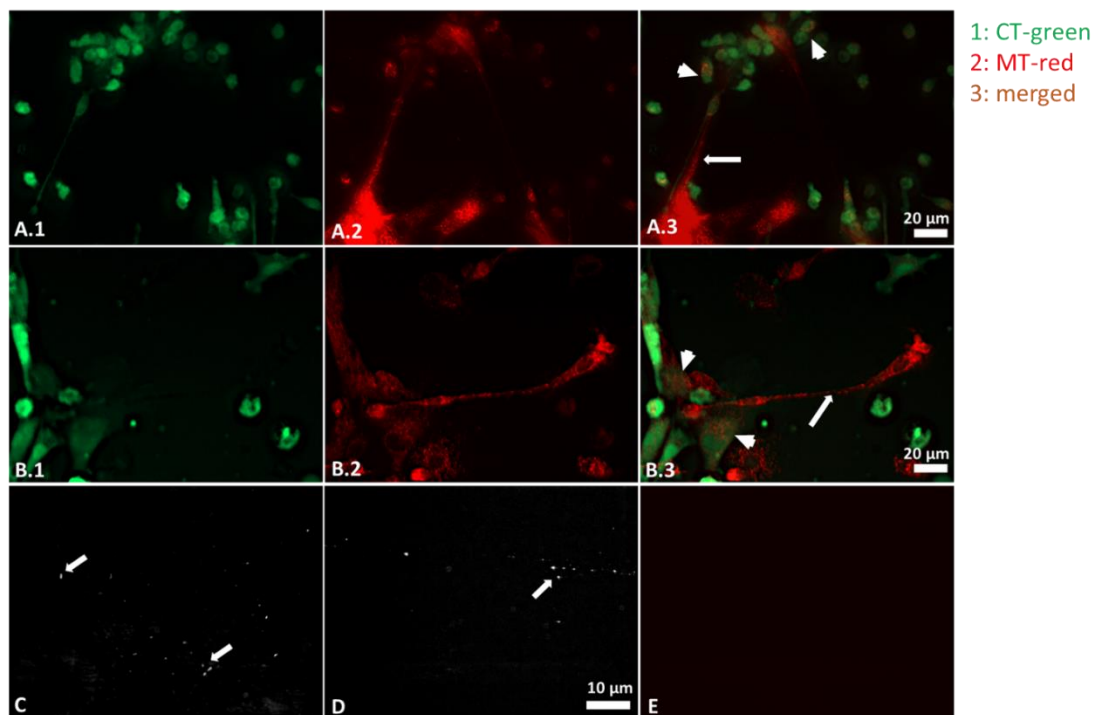
Figure 16. Mitochondrial transfer takes place via TNTs and EVs. A: Mitochondrial transfer from hMSCs to macrophages via TNTs after 24 h of co-culture. A.1: macrophages stained with non-transferable CT-green. A.2: MT-red-positive cells A.3: After 24 h of co-culture, transfer via TNTs was observed (white arrow), several macrophages showed double staining (white arrowheads). B: Mitochondrial transfer from macrophages to hMSCs. B.1: HMSCs were stained with CT-green: B.2: MT-red-labeled cells after 24 h of co-culture. B.3: During direct co-cultivation for 24 h, macrophages transferred mitochondria to hMSCs (double staining, arrowheads). Macrophages showed large TNTs (white arrow) forming a connection to hMSCs and containing stained mitochondria. C, D: Isolation of exosomes and EVs from cell culture medium derived from MT-red-stained macrophages (C) and hMSCs (D), respectively. Small fluorescent particles resemble stained mitochondria (white dots, arrows, image colored to grayscale for better visibility). In negative control samples (E), no labeled particles were detected. Scale bar A, B = 20 µm, C = 10 µm.

3.3.3. Scanning electronic microscopy of TNTs and EVs

For better visualization of TNTs and EVS of macrophages and hMSCs, scanning electron microscopic (SEM) images were taken (Figure 17). Macrophages and hMSCs were both co-cultured and mono-cultured. The formation of TNTs was demonstrated for macrophages and hMSCs, respectively (Figure 17 A). TNTs reach a length of up to 150 µm and a diameter of approximately 0.5-1 µm. After isolation of EVs from the cell culture supernatant of each mono-cultivation, small particles (approx. 1 µm) with a membrane-like structure were observed (Figure 17 B).
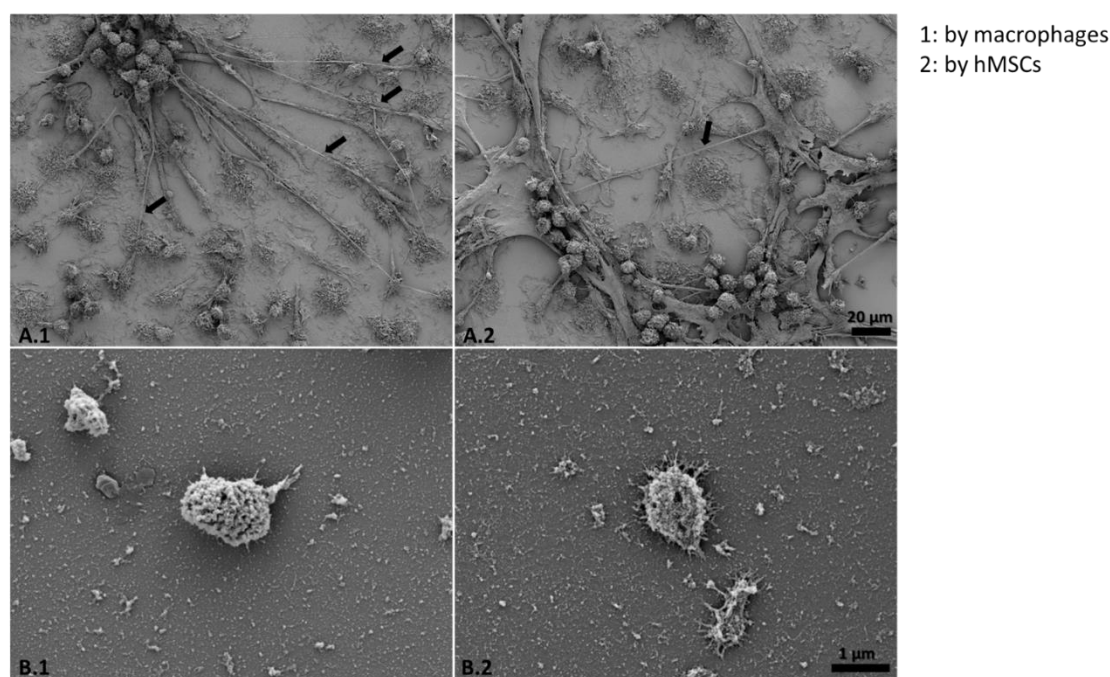
Figure 17. Scanning electron microscopic images (SEM) of TNTs and EVs from macrophages and hMSCs. A: TNT formation (black arrows) by macrophages (1) and hMSCs (2) after 24 h of co-cultivation. B: Small particles with a membrane-like structure after the isolation of EVs from the cell culture supernatant of macrophages (1) and hMSCs (2). Scale bar A = 20 µm, B = 1 µm.

3.3.4. Influence of co-culture on phagocytic activity of macrophages

To analyze the alteration of phagocytic activity of macrophages during co-cultivation with hMSCs, red-fluorescent latex beads with a size of 2 µm were used. The effects on phagocytosis were examined after direct contact co-cultures as well as after cultivation in the transwell system and conditioned medium, respectively. The beads were added to macrophages in the different co-cultivation set-ups (direct co-culture, conditioned medium, and transwell system with hMSCs on the transwell membrane, respectively) or to the control macrophages after several time points (3, 24, 48, 72 h) of mono-cultivation.

During this process, a strong increase in phagocytic activity, especially during direct co-culture (Figure 18), was observed. In addition, indirect co-culture by either conditioned medium or in the transwell system showed an increase of up to 8- and 4-fold, respectively, compared to mono-cultivated macrophage control. The most substantial effect on phagocytosis was detected after 48 h of direct co-cultivation, exceeding the uptake rate of cytokine-induced M1 and M2 differentiated macrophages in single cell type cultivation. After 72 h of co-cultivation, the phagocytic activity was comparable to control macrophages.
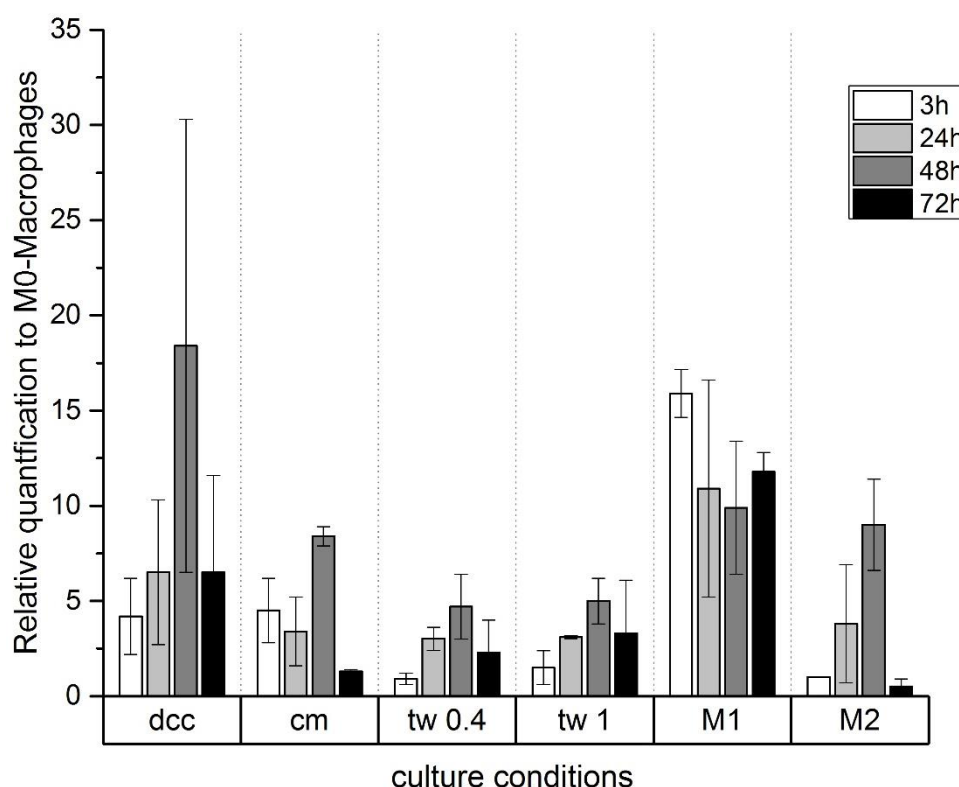
Figure 18. Effect of hMSCs on macrophage phagocytic activity (n=2). *Macrophages show an increase in phagocytosis of 2 μm sized latex beads after co-cultivation, either via direct co-culture (dcc), conditioned medium (cm) or in a transwell (tw) system (pore sizes: 0.4 μm; 1 μm) with hMSCs compared to mono-cultivated M0 macrophages. For comparability, induced M1 and M2 macrophages were also tested for phagocytic activity. The phagocytic rate was increased after co-cultivation for 48 h with values up to 18-fold in direct co-culture. After 72 h, the phagocytosis rate decreased to the level of unstimulated macrophages.*

3.4. Discussion

In the present study, the bidirectional mitochondrial transfer between macrophages and hMSCs after co-cultivation, and the increase of phagocytic activity of macrophages under these culture conditions was demonstrated.

It was shown, that at least two different mechanisms achieved the transfer of mitochondria: the transfer via EVs and TNTs, respectively, originated from hMSCs [213, 214, 217] as well as from macrophages. Mitochondrial transfer has been correlated in other studies for hMSCs with respiratory defects of cells where the donated intact or additional mitochondria support damaged cells [213, 214]. The results of this thesis uncovered mitochondrial transfer between different cell types also via indirect mechanisms without specificity for target cells. By the demonstrated presence of mitochondria-containing EVs using fluorescence microscopy, the conditioned medium provided by one cell type resulted in the uptake of mitochondria into acceptor cells by these vesicles (Figure 16 C and D). The mitochondria exchange took place very quickly. Within 3 h of co-cultivation, nearly all primarily unstained cells showed MT-red fluorescence (Figure 14 and Figure 15). This indicates rather an untargeted transmission and a general cell-cell communication than a cell-specific transfer.

In contrast to previous studies, which investigated the mitochondrial transmission of hMSCs only [213, 217], in this study, additionally, the transfer originating from macrophages was observed. The reasons behind the transport of mitochondria from macrophages to hMSCs needs further examination. One possible reason might be the acceleration of the inflammation reaction by exchanging information via mitochondria.

As opposed to other studies [213] that discovered the mitochondrial transfer from hMSCs to macrophages via the transwell system, this effect could not be detected in our experiments with pore sizes of 0.4 µm and 1 µm. The mentioned study lacks information about the pore size of the transwell system. Hence, larger pores might facilitate the transfer of mitochondria from the upper compartment to the lower one and, therefore, rather resemble the set up with conditioned medium.

Shown by the exchange of mitochondria, it is most likely that also signaling molecules or other organelles can be exchanged, which may lead to an enhanced reaction of hMSCs and possibly other cells in the surrounding tissue. Thus, the investigation of mitochondrial transfer can be used for the examination of cell-cell communication and interactions between macrophages and hMSCs.

For better visualization of TNTs and EVs, SEM analysis (Figure 17) was performed, and both types of structures arising from both macrophages and hMSCs could be observed. Two different sorts of TNTs have already been described in literature, one with a diameter of up to 0.7 μm, the other one with larger diameters (> 0.7 μm) [132]. Via the latter, cells can transport compartments of the cytoplasm and hence organelles like mitochondria [132]. Such TNTs with a diameter up to 1 μm emanating from macrophages and hMSCs were detected. Moreover, SEM images of pelleted EVs demonstrated small particles surrounded by a membrane-like structure with a size of 1 - 2 μm, as shown in other studies [218]. Thus, these vesicles may enable the indirect transfer of mitochondria. To monitor the biological effect of hMSC communication on macrophages, the phagocytic activity was used as a readout. Phagocytic activity of macrophages is a reaction against host pathogens, which are internalized and disposed of by this mechanism [219]. Within this thesis, phagocytosis was increased during co-cultivation of hMSCs with macrophages (Figure 18). The impact of hMSCs on macrophages and their phagocytic activity has already been shown in other studies [102]. Besides the known effects of direct contact, as shown by these authors, in this study, additionally, an effect of soluble factors either in a transwell system or the application of conditioned medium, which was generated from hMSC mono-cultures was demonstrated. These results show that in direct co-culture, macrophages displayed the highest increase of phagocytic activity, up to 11-fold compared to mono-cultivated M0 macrophages. This increase was achieved solely by co-cultivation with hMSCs without any differentiation factors provided to the macrophages, i.e., the presence of hMSCs was sufficient for this effect. Interestingly, the effect of hMSCs on macrophage phagocytosis exceeded the uptake rate of cytokine-induced M1 and M2 macrophages, respectively. Via indirect mechanisms, the increase in phagocytic activity was less pronounced than by direct co-cultivation, but still up to 6-fold higher compared to unstimulated control cells and hence approximately at the level of cytokine-induced M1 macrophages. These results suggest that the more pronounced the contact between macrophages and hMSCs becomes, the higher is the resulting phagocytic activity. The highest value for phagocytic activity was achieved after 48 h both, by direct and indirect co-cultivation. Moreover, it could be shown that after 72 h of co-cultivation, the phagocytic activity declined to the level of unstimulated macrophages. Therefore, it has to be assumed that after this time, the reaction by the *in vitro* co-culture between hMSCs and macrophages was completed.

To conclude, in this study, it could be detected that mitochondrial transfer did not only occur from hMSCs to macrophages but also vice versa and that this process was not restricted to direct contact between the cell types. Moreover, the increase in phagocytic activity of macrophages stimulated by hMSCs did not require direct contact, indicating a kind of paracrine mechanism.

Both, the evaluation of mitochondrial transfer and the phagocytic activity assay, are feasible and reliable methods for the analysis of cellular communication and interactions, which enable examinations on several biomaterials besides protein or RNA analysis methods. The mitochondrial transfer, especially by macrophages due to direct and indirect mechanisms, needs further investigations to understand the underlying process and subsequent impact.

3.5. Experimental section

3.5.1. Cell culture

All experiments were approved by the Local Ethics Committee of the University of Wuerzburg and with the informed consent of each donor patient.

Monocytes were isolated from human blood. For this purpose, peripheral blood mononuclear cells were collected by density gradient centrifugation with Pancoll (Density: 1,077 g/l; Pan-Biotech, Aidenbach (D)) from buffy coats (Blood donor service, German Red Cross, Wiesentheid (D)) of healthy donors. Monocytes were then isolated via negative selection (Pan Monocyte Isolation Kit, Miltenyi Biotec, Gladbach (D)) and were cultivated up to 7 days in macrophage culture medium (RPMI-1640, GlutaMAX^{TM} (Thermo Fischer Scientific, Dreieich (D)) with 10 % of human serum (pooled serum of 6 healthy donors) and 1 % Pen-Strep (Thermo Fischer Scientific, Dreieich (D)) in 12-well plates (Sarstedt, Nümbrecht (D)) in a humidified atmosphere at 37 °C and 5 % CO_2. Monocytes differentiated spontaneously, without differentiation factors, into macrophages within this time (M0-macrophages).

For induced differentiation of monocytes into M1 and M2 type macrophages, respectively, 1 µg/ml lipopolysaccharides (Sigma-Aldrich, Munich (D), M1) or 10^{-7} M dexamethasone (Sigma-Aldrich, Munich (D), M2) were used.

Human mesenchymal stromal cells (hMSCs) from trabecular bone were isolated from the femoral heads of patients undergoing total hip arthroplasty via plastic adherence and regularly verified due to their differentiation potential into osteoblasts and adipocytes [220]. Obtained cells were cultured in DMEM F-12 GlutaMAX^{TM} medium (Thermo Fischer Scientific, Dreieich (D))) with 10 % fetal calf serum (Thermo Fischer Scientific, Dreieich (D)), 100 U/ml penicillin and 100 mg/ml streptomycin (Thermo Fischer Scientific, Dreieich (D)) and 50 µg/ml L-ascorbic-acid-2-phosphate (Sigma Aldrich, Munich (D)) in 175 cm^2 cell culture flasks (Greiner Bio-One, Kremsmuenster (D)). For passaging, hMSCs were washed once with 1 x Dulbecco's Phosphate-Buffered Saline (PBS-) (Thermo Fisher Scientific, Dreieich (D)), incubated for 5 min each in PBS-/EDTA (0.54 M) (Sigma Aldrich, Munich (D)) and Trypsin-EDTA (0.05 %) (Thermo Fischer Scientific, Dreieich (D)) in a humified atmosphere at 37 °C, 5 % CO_2. After stopping the enzyme reaction with culture medium supplemented with serum, cells were centrifuged at 1000 rpm for 5 min at room temperature. For experiments, undifferentiated hMSCs in passage 2 were used.

3.5.2.   Co-culture experiments

Three different experimental set-ups were used to analyze the influence of macrophages and hMSCs to each other. For experiments with conditioned medium, macrophages and hMSCs were cultivated separately in macrophage culture medium. After 24 h, the conditioned medium of each cell type was collected, centrifuged (4000 rpm, 10 min, 20 °C), and supplied to the other cell type for further experiments. For co-cultivation experiments in different transwell systems (ThinCertTM, Greiner Bio-One, Kremsmuenster (D), 0.4 µm and 1 µm pore size), monocytes were isolated and cultivated for 3 days in macrophage culture medium in a well plate/transwell membrane. Subsequently, hMSCs were then added to the macrophages (ratio 1:4) in the same medium in a transwell membrane/well plate on day four for a co-culture period up to 3 days. To investigate direct cell contact effects, monocytes were cultivated for 3 days after isolation in macrophage culture medium and then enriched with hMSCs (ratio 1:4) and co-cultivated for up to 3 days.

3.5.3.   Mitochondrial transfer

Mitochondrial transfer from one cell type to the other was analyzed by flow cytometry (FACSCaliburTM, BD Bioscience, Heidelberg (D)) and fluorescence microscopy. The cell types were stained either with 200 nM MitoTracker® Red CMXRos (Thermo Fischer Scientific, Dreieich (D)) for 30 minutes at 37 °C and the other one with 50 nM non-transferable CellTracker^{TM} CMFDA green (Thermo Fischer Scientific, Dreieich (D)) or vice versa, and after that washed three times with PBS. The staining was performed at least 1 h before starting the experiments. The transfer was followed via fluorescence microscopy (Axio Observer, Zeiss equipped with epifluorescence optics and a black/white AxioCam MRm).

For flow cytometry, cells were scraped off from the well bottom using a cell scraper. Human macrophages were additionally stained with anti-CD45 (FITC) (Mitenyi Biotec, Bergisch Gladbach (D)) or the corresponding isotype control (Mitenyi Biotec, Bergisch Gladbach (D)). For analysis, macrophages were gated for CD45 positive (CD45+) and hMSCs CD45 negative (CD45$^-$) cells.

3.5.4. Isolation of extracellular vesicles (EVs)

EVs were isolated with Total Exosome Isolation Reagent (from cell culture medium) (Thermo Fischer Scientific, Dreieich (D)). For this purpose, macrophages, and hMSCs, respectively, were stained with MitoTracker-red and cultured for 24 h in macrophage cultivation medium. Culture medium was collected and processed according to the manufacturer's instructions. The obtained pellet was resuspended in 50 μl of PBS- and examined for red fluorescent mitochondria in these vesicles by fluorescence microscopy. Culture medium from unstained cells as well as culture medium supplemented with MitoTracker-red (without cell contact), served as negative controls.

3.5.5. Scanning electron microscopy (SEM)

For sample preparation, macrophages and hMSCs were co-cultivated for 24 h on polystyrene coverslips. The pellet of isolated EVs was smeared on glass coverslips. Specimen were fixed for 30 min in 6 % glutaraldehyde (Sigma Aldrich, Munich (D)) in PBS on ice followed by dehydration in ascending ethanol concentrations (each 2x for 10 min: 70 %, 90 % and 100 %) and incubation for 2x 15 min in hexamethyldisilazane (Sigma Aldrich, Munich (D)). After air-drying, samples were fixed on stubs and coated with 2 nm platinum by Leica EM ACE600 sputter coater (Leica microsystems, Wetzlar (D)). Samples were analyzed, and images were taken via a Zeiss Crossbeam 340 scanning electron microscope (Zeiss, Oberkochen (D)).

3.5.6. Phagocytosis assay

Phagocytic activity of macrophages was analyzed using 2 μm sized, red-fluorescence labeled latex beads (Sigma-Aldrich, Munich (D)). Beads were opsonized in pooled human serum for 30 minutes prior to addition to macrophages in a ratio of 10 beads per cell and incubated in a humidified atmosphere for two hours at 37 °C and 5 % CO_2. Cells were washed three times with serum-free macrophage culture medium to remove non-phagocytosed beads. For cell counting, the cell nuclei were stained with the DNA dye Hoechst 33342 (Sigma-Aldrich, Munich (D)). Bead uptake and cell count were analyzed by inverted fluorescence microscopy. Cells and phagocytosed beads were counted using Image J software (NIH, Bethesda, USA). For each experimental setting, 10 random pictures with 10 x magnification were exploited. Phagocytosed beads for each experimental setting were normalized to 5000 cells.

Chapter 4

Platelet Lysate Outperforms FCS and Human Serum for Co-Culture of Primary human Macrophages and hMSCs

Chapter 4 was published as an original research article (Tina Tylek, Tatjana Schilling, Katrin Schlegelmilch, Maximilian Ries, Maximilian Rudert, Franz Jakob, Jürgen Groll. "Platelet lysate outperforms FCS and human serum for co-culture of primary human macrophages and hMSCs" in Scientific Reports, 2019), reproduced from [85] as open access article distributed under the Creative Commons Attribution License which permits unrestricted use, distribution and reproduction in any medium. The article is based on the work of the author of this thesis Tina Tylek, who performed all experiments, data evaluation and composition of the manuscript.

The original text was slightly modified to improve readability.

Chapter 4

The author contributions to the original research article are as follows:

Contributor	Contributions
Tina Tylek	Designed research; performed and analyzed data of all experiments; wrote the manuscript
Tatjana Schilling	Helped to supervise the project; revised and provided feedback on the manuscript
Katrin Schlegelmilch	Helped supervising and designing the project; revised and provided feedback on the manuscript
Maximilian Ries	Performed experiments of osteogenic differentiation of hMSCs (data not shown in this thesis)
Franz Jakob	Provided cell material
Maximilian Rudert	Provided cell material
Jürgen Groll	Conceived the research; revised and provided feedback on the manuscript

4.1. Abstract

In vitro co-cultures of different primary human cell types are pivotal for the testing and evaluation of biomaterials under conditions that are closer to the human *in vivo* situation. Especially co-cultures of macrophages and mesenchymal stromal cells (MSCs) are of interest, as they are both present and involved in tissue regeneration and inflammatory reactions and play crucial roles in the immediate inflammatory reactions and the onset of regenerative processes, thus reflecting the decisive early phase of biomaterial contact with the host. A co-culture system of these cell types might thus allow for the assessment of the biocompatibility of biomaterials. The establishment of such a co-culture is challenging due to the different *in vitro* cell culture conditions. For human macrophages, medium is usually supplemented with human serum (hS), whereas hMSC culture is mostly performed using fetal calf serum (FCS), and these conditions are disadvantageous for the respective other cell type. It could be demonstrated that human platelet lysate (hPL) can replace hS in macrophage cultivation and appears to be the best option for co-cultivation of human macrophages with hMSCs. In contrast to FCS and hS, hPL maintained the phenotype of both cell types, comparable to that of their respective standard culture serum, as well as the percentage of each cell population. Moreover, the expression profile and phagocytic activity of macrophages was similar to hS.

4.2. Introduction

Monocytes and macrophages evolving thereof are cells of the innate immunity, which can be found in most tissues of the human body [221]. Macrophages are highly plastic cells, which can change their polarization in response to various signals. Thus, several classes could be described based on their expression and phenotypical profile [30, 77]. The two main sub-populations are the classically (M1), or alternatively (M2) activated macrophages [222]. The M1 type is characterized by the expression of proinflammatory cytokines, like IL-1β, IL-6, IL-8 or TNF-α, microbicidal activity, and the production of reactive nitrogen and oxygen intermediates [57].

In contrast, M2 macrophages are mainly involved in tissue remodeling and immunoregulatory processes. In addition, they show a high phagocytic activity, the expression of scavenging receptors, e.g., CD163, mannose receptors, e.g., (CD206), or anti-inflammatory cytokines like IL-10 [223]. During *in vitro* studies, it is also possible to differentiate macrophages spontaneously, i.e., without the addition of differentiation factors, into the so-called M0 type only by environmental factors like specific materials or due to co-cultivation with other cell types [84].

Cells that tightly interact with macrophages *in vivo* are mesenchymal stromal cells (MSCs) [224-226]. These adult multipotent stem cells can differentiate into various cell types, like osteoblasts [227], chondrocytes [228] and adipocytes [229]. They are known for switching the phenotype of proinflammatory macrophages into the anti-inflammatory M2 type, and thus are part of tissue regeneration and wound healing processes together with the latter [230-232]. Accordingly, the crosstalk of both cell types is often analyzed in biomaterial research. Here, the particular interest is to investigate, whether there are any changes in macrophage polarization or MSCs differentiation in *in vitro* as well as *in vivo* studies depending on the designed biomaterial [226, 233-235], eventually with the aim to evolve design criteria for biomaterials to favor or even provoke a healing response after implantation.

So far, the majority of *in vitro* studies that examine the interaction of either hMSCs or macrophages with biomaterials rely on cell mono-culture. One issue hindering the establishment of an *in vitro* co-culture, especially of these cell types, is the cultivation in different culture media. While human monocytes and macrophages are most commonly cultivated in RPMI-1640 with human serum [84, 232, 236], hMSCs are usually cultivated in MEM-based media supplemented with fetal calf serum (FCS) [237-239]. Recent studies

have already shown that hMSCs can also be cultivated in medium with human platelet lysate (hPL) instead of FCS, without the loss of their differentiation potential and immunomodulatory effects [240, 241].

PL can be prepared via freeze-thaw cycles of platelets and subsequent centrifugal separation of the debris from all the bioactive platelet factors [14, 242, 243]. These include, for example, the platelet-derived growth factor (PDGF), transforming growth factor (TGF)-β1, vascular endothelial growth factor (VEGF), epidermal growth factor (EGF), attachment factors, and enzymes [244]. Like macrophages and hMSCs, platelets are part of tissue regeneration processes [245]. While platelets coagulate and degranulate upon wounding, they release bioactive factors. These lead to inflammation and thus neutrophil and macrophage activation, fibroblast, smooth muscle cell, and MSC recruitment, as well as collagen synthesis and angiogenesis, resulting in tissue regeneration [14].

Hence, especially for *in vitro* studies in the field of tissue regeneration and biomaterial research, the use of platelet lysate could mimic the natural environment of an *in vivo* situation better than other commonly used supplements and showed beneficial effects, when incorporated in biomaterials [246, 247]. When PL is used as a serum supplement, it is, however, often described that heparin has to be added to prevent the coagulation of the medium in cell cultures [16]. However, heparin is also known to stimulate macrophage polarization [17, 248], which is unfavorable for the analysis of their spontaneous differentiation. In the present study, thus, the use of PL as an alternative for macrophage *in vitro* cultivation as well as for co-culture experiments with hMSCs was investigated. Furthermore, the need for heparin as a substitute in both culture systems was analyzed.

4.3. Results

4.3.1. Macrophage cultivation in RPMI-1640 medium with different sera

4.3.1.1. Influence of different sera on cellular phenotype, adhesion and viability

Possible differences regarding the maturation and phenotype characteristics of monocytes/macrophages after cultivation in RPMI-1640 GlutaMAX^{TM} medium supplemented with 10 % hS, 10 % FCS, and 10 % hPL +/- heparin, respectively, were analyzed by inverted light microscopy after a culture period of seven days (Figure 19 A). After maturation, several macrophages in medium with hS (Figure 19 A.2) showed a round shape with a diameter size of approximately 20 µm. In addition, cells with long cellular extensions were observed in this media condition. Macrophages in media supplemented with hPL +/- heparin showed similar morphologies compared to hS (A.3,4). In contrast, the cultivation of macrophages in medium with FCS (A.1) yielded a markedly different phenotype with flattened cells with a diameter of up to 50 µm. The difference in the cell numbers of macrophages in hS and hPL compared to macrophages cultivated with FCS was quantified via the measurement of the DNA amounts after one, three and seven days of culture (Figure 19 B). The DNA amount and thus, cell numbers increased over time from day one to day seven of cultivation in all culture media. Since macrophages do not proliferate *in vitro*, higher cell numbers reflect a stronger cell adhesion to the plastic surface with time. Thereby, in media supplemented with hS and hPL +/- heparin, cell adhesion was at least 2-fold (d7, approx. 1 µg/ml DNA) elevated compared to that in medium with FCS (0.42 µg/ml DNA). Cell viability was not affected as indirectly analyzed via flow cytometry for the apoptotic cell marker 7AAD (Figure 20).
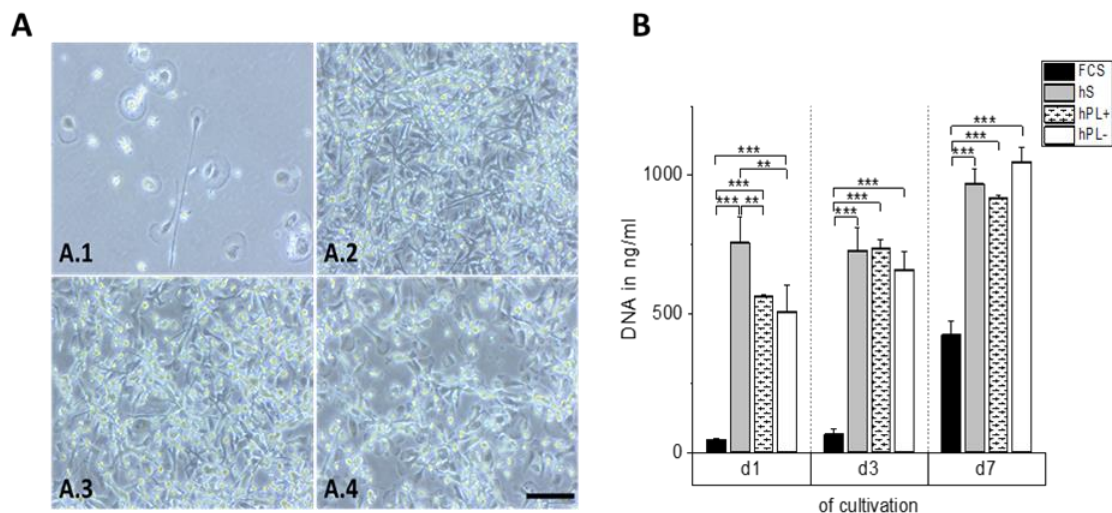
Figure 19. Phenotype and adhesion of spontaneously differentiated macrophages. *The phenotype (A) of macrophages after seven days of cultivation in medium with hS (A.2), hPL + heparin (A.3), and hPL - heparin (A.4) was similar, while macrophages cultivated in medium with FCS showed a markedly different morphology (A.1). The analysis of DNA amounts (B) corresponding to cell numbers, provided information about cell adhesion behavior (mean ± SD, n = 3). Scale bar = 100 μm. **p < 0.01, ***p < 0.001*
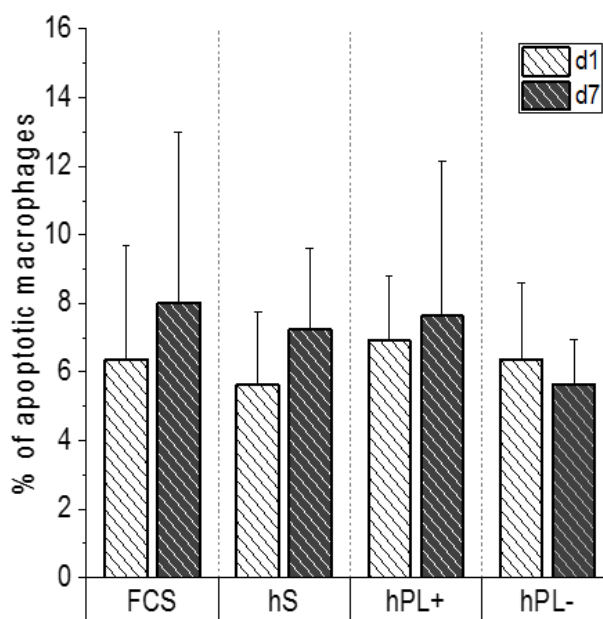
Figure 20. Proportion of apoptotic macrophages in different media conditions. *Positively stained macrophages for the apoptotic cell marker 7AAD were normalized to total cell numbers. The comparison of all four media supplements did not yield significant differences in cell viability (mean ± SD, n = 4).*

4.3.1.2. Gene and protein expression of spontaneously/non-induced and induced differentiated macrophages in reply to different sera and supplements

Gene expression analysis was performed after seven days of cultivation of spontaneous, non-induced (M0) and lipopolysaccharide (LPS)/ dexamethasone (Dex)- induced (M1/M2) macrophages in media supplemented with either hS, hPL +/- heparin or FCS (Figure 21 A) via qPCR. According to the gene expression patterns of IL-1β, IL-8, CD206 and CD163, it was able to show that non-induced (M0) macrophages differentiate spontaneously in all media. Compared to the reference sample of macrophages on day one (expression level set to 1), the expression of IL-1β and IL-8 decreased, while the expression of CD206 increased. In M0 cell cultures with hPL, spontaneously differentiated macrophages showed differences in M2 marker expression to those cultivated in hS- and FCS-supplemented cultures. In particular, a decrease of CD163 and an increase of CD206 expression was observed for hPL-supplemented cultures. Induced differentiated macrophages were able to differentiate into both subtypes in all culture conditions. An upregulation of M1 markers and a downregulation of M2 markers in induced M1 differentiated macrophages, and vice versa for M2 differentiated cells compared to spontaneously differentiated ones were detectable. Interestingly, macrophages cultured in medium supplemented with hPL reflect a more similar expression pattern to cells in hS- than in FCS-containing media. The addition of heparin showed no significant differences.

For further analysis of the M0, M1 and M2 polarization, the protein expression of IL-1β and CD206 was determined via flow cytometry after seven days of cultivation (Figure 21 B). In hS as well as in hPL +/- heparin, differentiation into the M1 and M2 type macrophages was confirmed. Accordingly, for M1 macrophages, the M1 marker expression of IL-1β increased significantly up to 37-fold compared to M0 and M2 type macrophages. For the M2 type macrophages, the specific M2 marker CD206 was expressed by 80 % of the cells. This corresponds to a 3- (M0) and 5-fold (M1) increase, respectively, compared to the other macrophage types. Thereby, the tested serum supplements did not result in significant differences in marker gene expression within the same differentiation condition. Flow cytometry of macrophages in FCS-supplemented media failed due to low cell numbers adhering to the well plates and was therefore omitted in this assay (Figure 22).
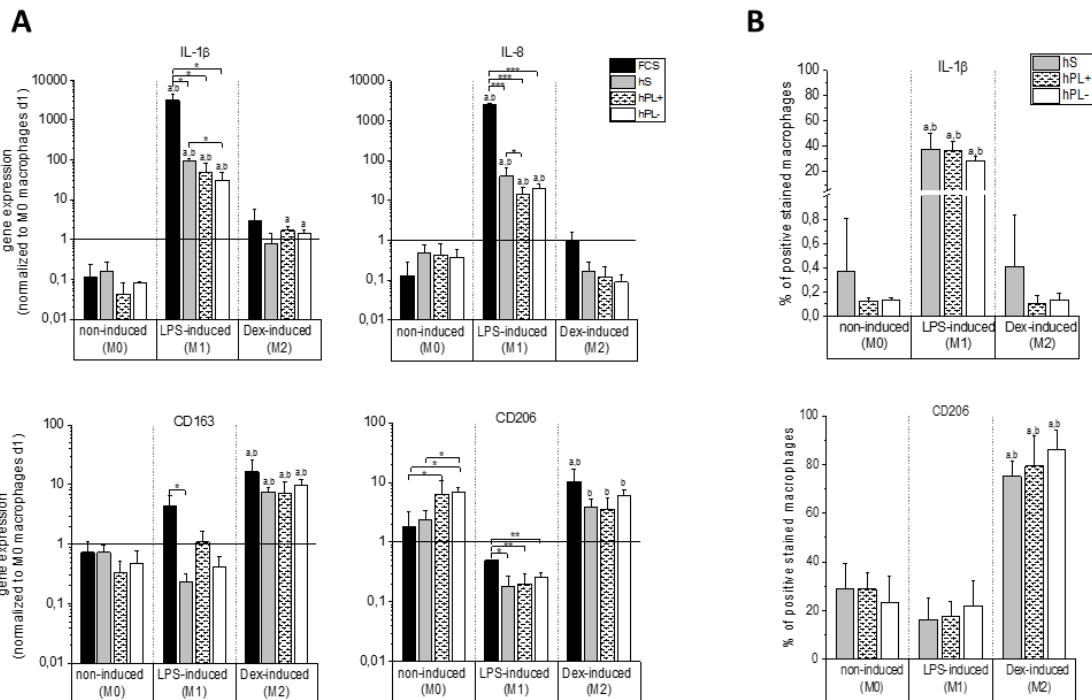
Figure 21. Gene and protein expression of spontaneously (M0) and induced (M1/M2) differentiated macrophages after seven days. *A: Gene expression was analyzed by qPCR. Independent of culture conditions, spontaneous as well as induced differentiation, was observed. The M1 markers IL-1β and IL-8 were downregulated in the non-induced (M0) as well as Dex-induced (M2) macrophages and highly upregulated in LPS-induced (M1) ones. The M2 markers CD163 and CD206 were more highly expressed in M2 macrophages, compared to M0 and M1. Spontaneous differentiation (M0) differed from the reference sample (monocytes/macrophages on day 1) in all four media (mean ± SD, n = 3). B: Polarization into M0/M1/M2 macrophages determined via protein analysis using flow cytometry. M1 macrophages reflected a 40 % higher IL-1β expression compared to M0 and M2. In contrast, M2 macrophages markedly showed a 60 % higher protein expression of CD206 in comparison to M0 and M1 macrophages (mean ± SD, n = 3). *p <0.05; **p < 0.01, ***p < 0.001; [a]p < 0.05 vs non-induced (M0), same serum supplement; [b]p < 0.05 between LPS-induced (M1)/Dex-induced (M2), same serum supplement.*
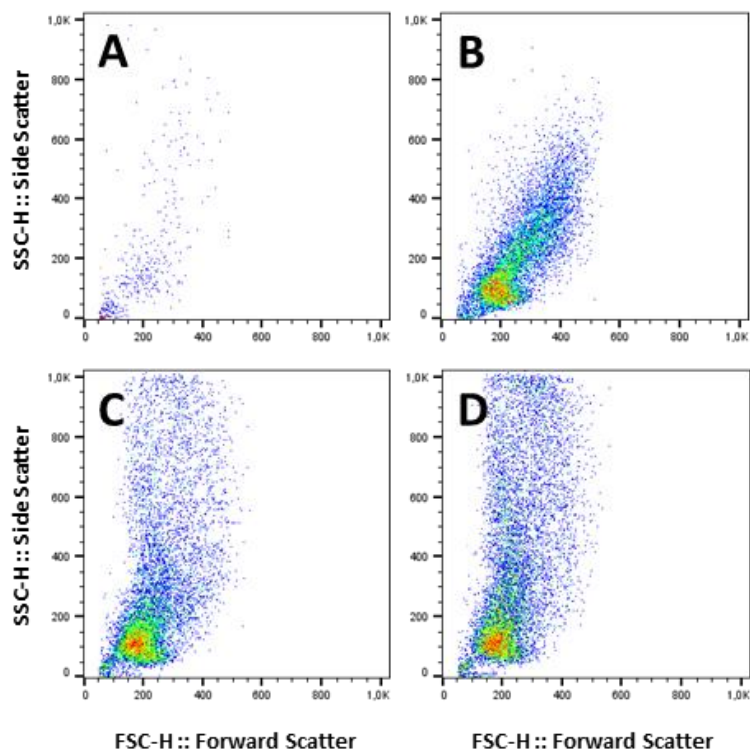
Figure 22. Flow cytometric scatter plots of macrophages cultivated for seven days in different sera.
Forward versus side scatter (FSC vs. SSC) gating was performed to identify macrophages based on size and granularity. Because of the lack of macrophages in medium supplemented with FCS (A) flow cytometric analysis was not possible. In medium with hS (B) as well as hPL+/- heparin (C/D), enough cells for reliable results were present.

4.3.1.3.   Cytokine release profile of non-induced (M0) macrophages

The cytokine release tested for 12 inflammatory cyto- and chemokines detected four markers (pro-inflammatory: IL-1β, IL-8, IL-6; anti-inflammatory: IL-10) with expression values above the detection limit of the assay (Figure 23). Thereby, the expression profile of each cytokine varied for different serum supplementations. The release of IL-1β was downregulated in macrophages cultivated in medium with FCS, compared to those cultivated in medium with hS and hPL +/- heparin. The highest expression of IL-6 was observed in the hPL + heparin group, whereas the lowest level was detectable in FCS. IL-8 was highly expressed in all tested culture conditions. The anti-inflammatory-related cytokine IL-10 was generally released at lower levels with the highest values for macrophages in media with hPL + heparin.
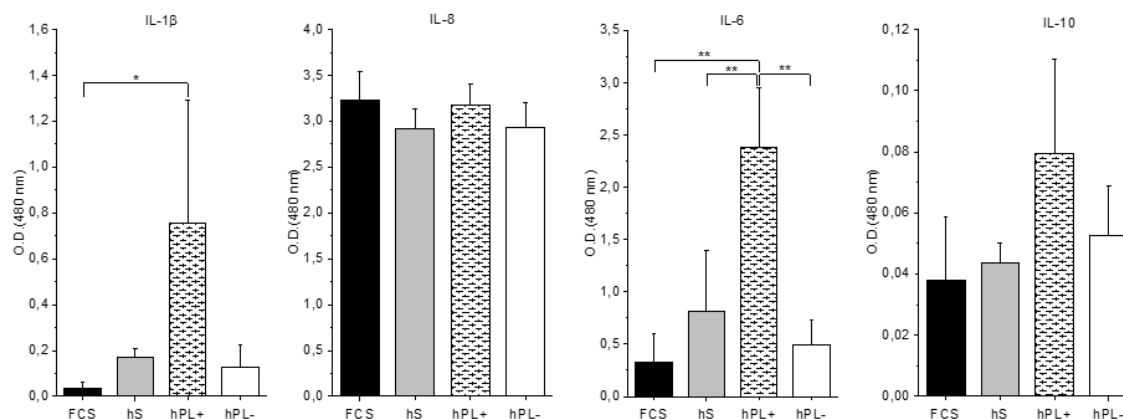
Figure 23. Cytokine release profiles of spontaneously differentiated macrophages after seven days of culture. *Cytokine release of IL-1β, IL-6, IL-8, and IL-10 was detected in supernatants of macrophages cultivated in medium with hS, FCS, and hPL +/- heparin using a commercially available ELISA kit. Relative protein amounts are given by arbitrary units of optical density at 450 nm and show varying release profiles for different serum supplementations (mean ± SD, n = 3). *p <0.05; **p < 0.01*

4.3.2. Co-culture experiments with monocyte-derived M0 macrophages and hMSCs

4.3.2.1. Phenotype of direct co-culture and quantification of macrophage amount

For the visualization of the phenotype of both cell types in direct co-culture, macrophages were stained with a green- and hMSCs with an orange-fluorescent non-transferable live cell tracker and imaged via inverted fluorescence microscopy after 72 h of co-cultivation (Figure 24 A). The cultivation in medium with hS led to an accumulation of hMSCs, whereas macrophage adhesion in medium with FCS was reduced. In medium supplemented with hPL +/- heparin instead, macrophages and hMSCs were successfully co-cultivated for the whole culture period of 72 h without any loss of normal cell behavior. The percentage of CD45-positive macrophages under the different culture conditions was determined (Figure 24 B). In co-cultures with hS, almost only macrophages and a small number of hMSC (3 %) were detected. In media with FCS in contrast, only 26 % macrophages were determined and hence outnumbered by more than 74 % of hMSCs. After 72 h of co-cultivation in media with hPL +/- heparin, 60 % of CD45-positive macrophages indicated 40 % of hMSCs.

By the examination of the hMSCs phenotype in mono-cultures with RPMI-1640 medium supplemented with different sera (Figure 25), it could be observed, that over the cultivation period of 3 days, hPL+/- supplementation maintained the typical spindle-shaped, fibroblast-like phenotype of hMSCs as observed under standard cultivation with

FCS. In contrast, hS supplementation resulted in low cell numbers and star-shaped morphology.
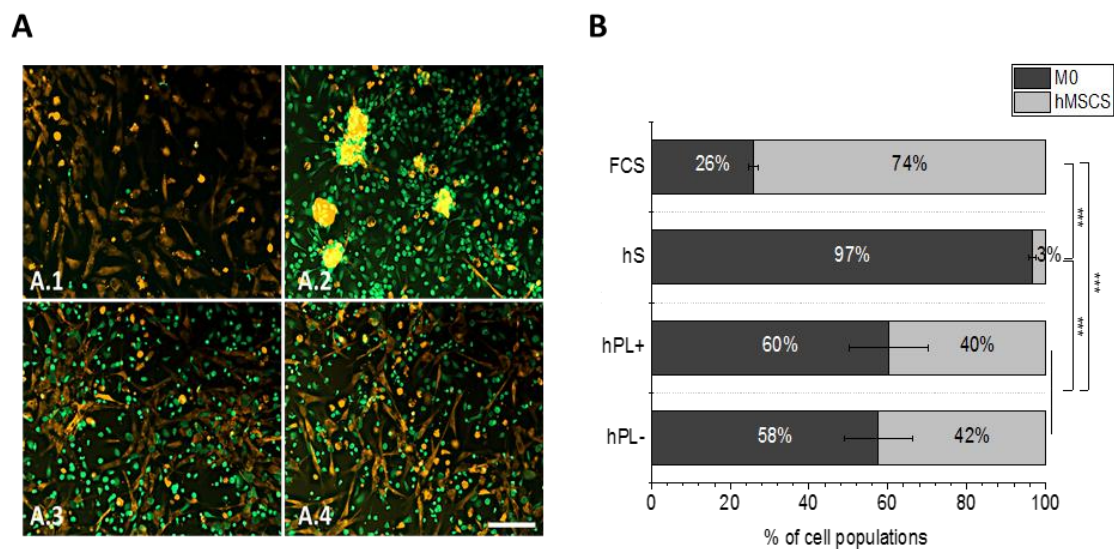
Figure 24. Phenotype and proportion of cell populations in the co-culture of M0 macrophages and hMSCs. *The phenotypes of macrophages (green) and hMSCs (orange) were investigated under different culture conditions (A). In medium with FCS (A.1), only very few macrophages adhered, and in medium with hS (A.2) hMSCs aggregated. In cell cultures with hPL + (A.3) /- (A.4) heparin, both, macrophages and hMSCs, displayed cell type-specific phenotypes corresponding to their morphology in mono-cultures with the respective standard serum. The percentage of macrophages in co-cultures measured via flow cytometric analysis of CD45 expression (B) confirmed the microscopic observations (mean ± SD, n=4). Scale bar = 200 μm. ***p < 0.001.*
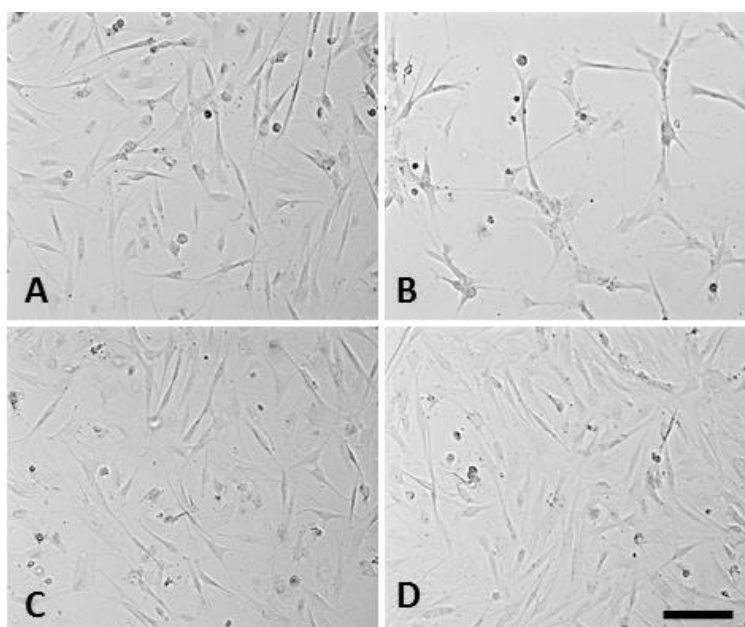
Figure 25. Phenotype of hMSCs in medium supplemented with different sera after 3 days of cultivation. *Via microscopy, differences in phenotype were observed after cultivation in medium supplemented with FCS (A), hS (B), and hPL +/- heparin (C/D). In media with FCS, the conventionally used serum, and hPL+/- hMSCs had a similar, spindle-shaped phenotype while those in hS displayed a different, star-shaped morphology. Scale bar = 100 μm*

4.3.2.2. Gene expression profile of M0 macrophages after co-cultivation with hMSCs

The gene expression profile of macrophages co-cultured for up to 72 h with hMSCs in direct contact was analyzed by qPCR after separation via a leukocyte-specific anti-CD45 magnetic bead system (Figure 26). Under different culture-conditions (hS, FCS, hPL +/- heparin), highly significant differences were detected. In macrophages cultivated in medium with FCS, IL-1β, IL-8, CD163, and CD206 were upregulated compared to the reference sample (mono-cultivated macrophages (M0)) as well as to macrophages cultivated in medium with other serum types. After 72 h, these macrophages showed a significant increase of CD206 and a decrease of CD163.
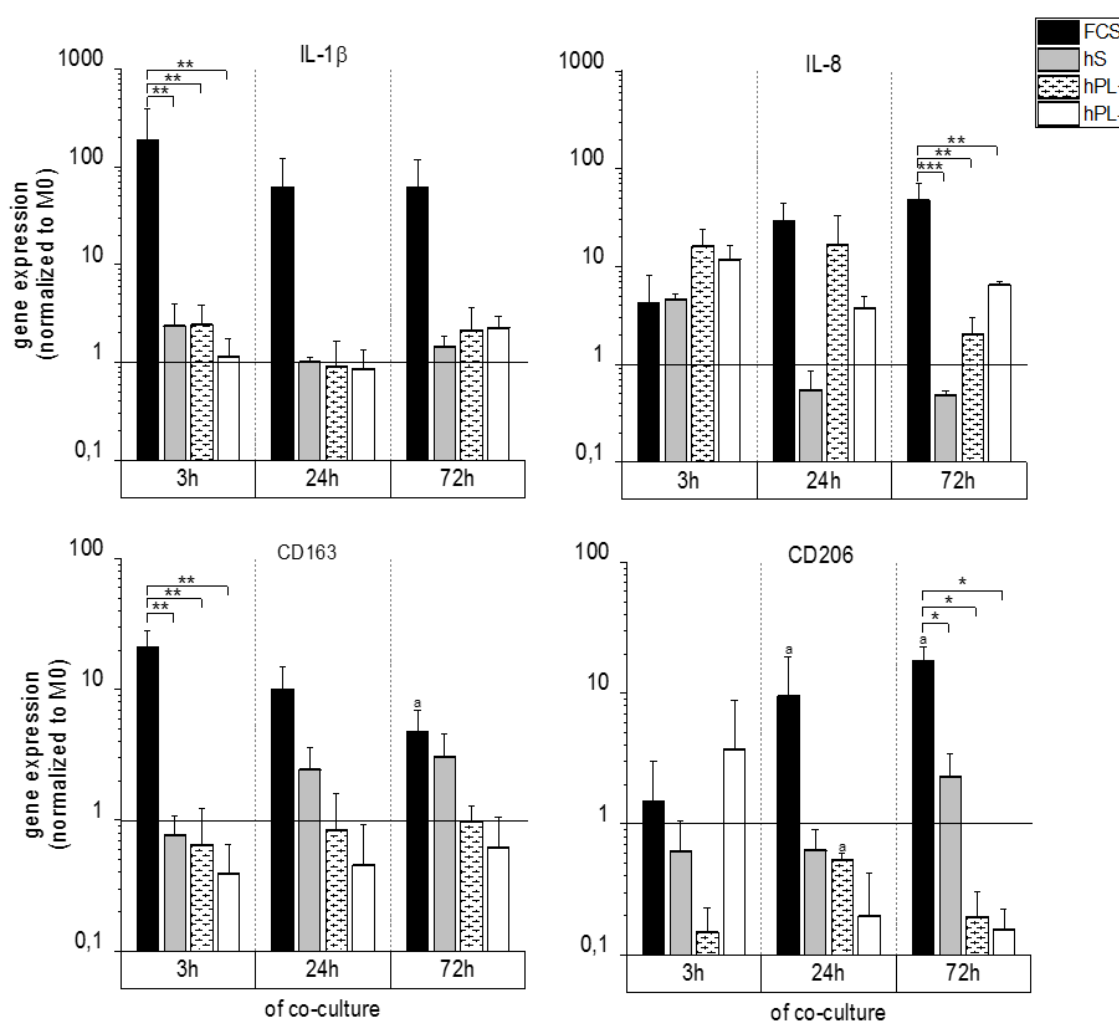
Figure 26. Gene expression profile of M0 macrophages after co-cultivation with hMSCs. The gene expression of the M1 markers IL-1β and IL-8, as well as the M2 markers CD163 and CD206, was analyzed for CD45-positive macrophages after 3 h, 24 h and 72 h of co-cultivation by qPCR. For the different culture conditions (medium supplemented with hS/FCS/hPL+/-), expression levels are depicted with normalization to RPS27A and M0 macrophages (mean ± SD, n = 3). *p <0.05; **p < 0.01; ***p < 0.001; ᵃp < 0.05 vs 3 h, same serum supplement.

During three days of co-cultivation, macrophages in hS displayed a decreased expression of the M1 markers IL-1β and IL-8 as well as an increase of the M2 markers CD163 and CD206. Co-cultivated macrophages in medium with hPL +/- heparin changed their expression pattern over the culture time with a minor upregulation of IL-1β and IL-8 and a downregulation of CD206 compared to the reference sample. Comparing the use of hPL with or without heparin, no significant difference was observed.

4.3.2.3. Phagocytic activity of macrophages after co-cultivation with hMSCs

The phagocytic activity of macrophages in mono- and co-cultures was measured over a period of 72 h via flow cytometry for phagocytosed green-fluorescent latex beads and CD45 marker staining to discriminate macrophages from hMSCs (Figure 27). After 3 h of co-cultivation with hMSCs, macrophages had a phagocytic rate similar to that of mono-cultured cells in all different culture media (supplemented with hS/FCS/hPL +/- heparin). After 24 h and 72 h, the phagocytic activity of co-cultured macrophages increased compared to mono-cultures in medium with FCS and hPL. Only for co-cultured macrophages in medium with hS, phagocytosis was not enhanced, and the mono-cultured ones even showed a higher uptake of beads. Cells cultured with FCS showed the highest uptake (up to 70 % of green fluorescent cells) at all time points. After 72 h in the hPL-supplemented medium, an effect of heparin was detected with a higher phagocytic uptake in the absence of heparin.
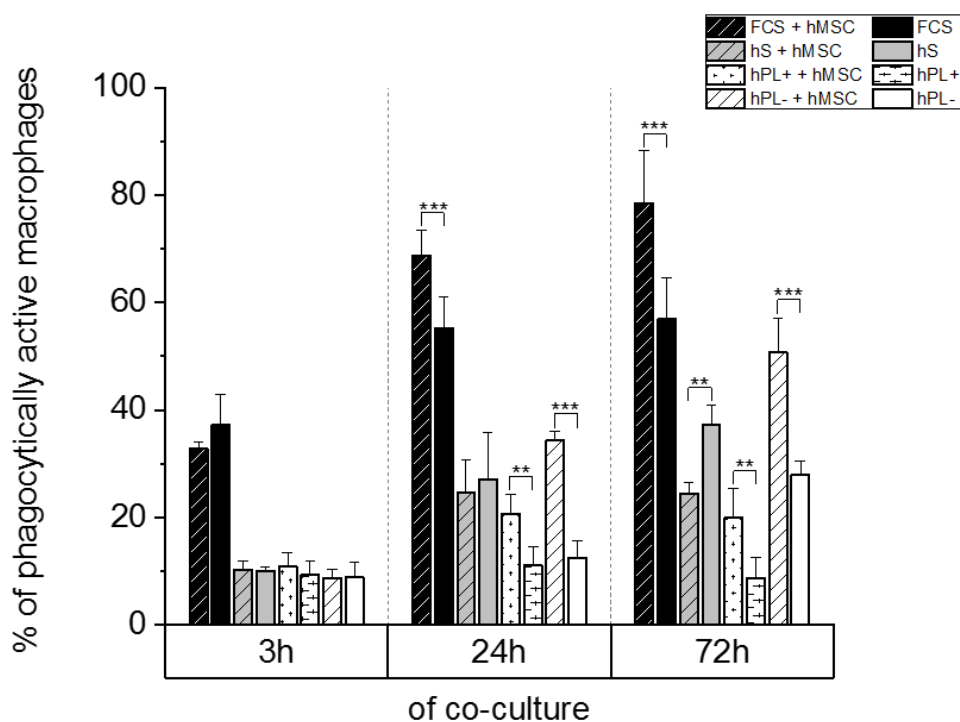
Figure 27. Phagocytic activity of M0 macrophages mono- and co-cultured with hMSCs. *The phagocytic activity of CD45-positive macrophages under different culture conditions (medium with hS/FCS/hPL + and - heparin) was measured via flow cytometry for the uptake of fluorescent beads after 3 h, 24 h, and 72 h. In medium with FCS and hPL, the phagocytosis rate of co-cultured cells exceeded that of the mono-cultured ones. Contrarily, in medium with hS, mono-cultured macrophages even exhibited a higher bead uptake than those in co-culture (mean ± SD, n = 3).* $**p < 0.01$; $***p < 0.001$

4.4. Discussion

In the present study, it could be demonstrated that human platelet lysate (hPL) is suitable as a serum supplement for monocyte-derived macrophage cultivation, comparable to human serum (hS) and preferable to fetal calf serum (FCS) as media supplements. The macrophage phenotype (Figure 19 A) was conserved in medium with hS and hPL and resembled that of spontaneously differentiated M0 macrophages. In accordance with literature, macrophages were characterized by an elongated as well as roundish shape of approximately 20 μm cell diameter, suggesting a spontaneously differentiated phenotype [84]. In contrast, in medium with FCS, macrophages were larger in diameter (up to 50 μm), but fewer numbers of cells adhered. The latter corresponded to low DNA retrieval from these samples (Figure 19 B). After seven days, the same level of DNA amounts was measured in cell cultures with hS and hPL, while for the supplementation with FCS, only half of the previously detected amount was determined. The observation of a DNA increase over time did not arise from cellular amplification since monocyte-derived macrophages are not able to proliferate *in vitro*. Rather the lack of media changes within the seven-day period analyzed here allowed for more and more still non-adherent macrophages settling down and therefore being included in the analysis. Moreover, the cell viability indirectly analyzed via the detection of the apoptotic cell marker 7AAD (Figure 20), was not affected significantly by any of the used culture conditions. The macrophage population included only a small apoptotic cell proportion of approximately 5-7 %. Since the DNA amount and hence the cell numbers did not decrease over time, the loss of dead cells that might have had detached from the culture plate surface was excluded and thus considered the low apoptotic value reliable.

Macrophages are highly heterogenic cells and differentiate upon stimulation by various factors. Their differentiation capacity into the two subtypes M1 and M2, induced by lipopolysaccharides and dexamethasone, respectively, was checked during cultivation with the different serum supplements and yielded the expected subtype characteristics on the gene (Figure 21 A) and protein (Figure 21 B) level. In accordance with the literature [57, 222], the M1-induced macrophages upregulated the M1 markers IL-1β and IL-8 and downregulated the M2 markers CD163 and CD206 while M2-induced macrophages showed the reversed expression pattern. Moreover, the ability of macrophages to differentiate spontaneously into the M0 type by environmental factors is important to investigate. This study proved that all four culture conditions applied

maintained this ability. However, differences in the expression profile on day seven, compared to the reference sample of day one, were observed. While hS and hPL supplementation revealed a similar outcome, both are different from the results obtained upon FCS supplementation. This might be explained by the higher similarity of hS and hPL being both human materials, but also the less effective adherence of macrophages in FCS might play a role.

A range of cytokines, which confer instructions and mediate communication among immune cells, plays a central role in the involvement of macrophages in immunity [33]. Hence, the effects of the different serum types on the cytokine release of spontaneously differentiated macrophages (Figure 23) were analyzed. Macrophages in media with hS and hPL without the addition of heparin had a similar cytokine release profile. Additionally, macrophages in medium containing FCS showed no significant differences to the other serum types without heparin. Only macrophages cultivated with hPL plus heparin released significantly higher amounts of the cytokines IL-1β and IL-6 into the cell culture media. It was assumed that heparin has a stimulating effect on the cytokine release of macrophages. This is in accordance with previous studies that have already described this effect [17].

To further evaluate the effects of hPL on hMSCs, also their phenotype (Figure 25) and their differentiation potential in media with either 10 % FCS or 5 % hPL including 2 U/ml heparin (hPL+) was analyzed on the protein level via Western blot analyses (data not shown, see dissertation of co-worker Maximilian Ries and supplement of Tylek et al. (Sci. Reports, 2019). Over the cultivation period of 3 days, hPL+/- supplementation maintained the typical spindle-shaped fibroblast-like phenotype of hMSCs as observed under standard cultivation with FCS. The results of this study suggest that hPL+ efficiently allows for osteogenesis of hMSCs, as has also been reported in literature [249]. Whereas heparin seems to be dispensable within the hPL-supplemented cultivation of macrophages, it is still needed as supplementation in the differentiation media for MSCs to prevent media gelation. Unlike the studies mentioned above, hMSCs employed in this thesis were all expanded in FCS-supplemented medium, which excluded the enrichment of different hMSC subpopulations by different sera prior to the initiation of differentiation.

Besides the mono-cultivation of macrophages and hMSCs, the influence of the different serum supplements on the co-culture with hMSCs putting the main attention to macrophages was investigated. The evaluation of the macrophage and hMSC phenotypes

within the co-cultures (Figure 24 A) lead to the conclusion that hPL was the best option since the phenotypes of both cell types corresponded to that of their respective standard culture medium. In contrast, the other media created disadvantages for one or the other cell type. In particular, the cultivation in medium with hS led to the aggregation of hMSCs, and media with FCS only allowed for the adhesion of few macrophages to the well plate, as already observed for mono-cultures. Accordingly, after 72h of co-cultivation in medium with hPL, 60 % macrophages, and hence 40 % hMSCs were present (Figure 24 B). In medium with hS, nearly no hMSCs were detectable, and in medium with FCS, the macrophage proportion was reduced to 26 %. Since hMSCs in the samples with hS supplementation were not able to adhere properly and instead formed cell aggregates (Figure 24 A.1), these cells were possibly lost during the sample preparation. Macrophages and hMSCs were cultivated together with a starting ratio of 1 hMSCs to 4 macrophages. Over 72 h of co-cultivation in media with hPL +/- heparin, this ratio shifted to 1 hMSCs to 1.5 macrophages. Thus, hMSCs were able to proliferate during this time.

The gene expression profiles of macrophages caused by co-cultivation led to different phenotypes depending on the culture conditions (Figure 26). As expected, reduced numbers of hMSCs in hS and low cell density of macrophages in FCS affected the gene expression. In hS medium, macrophages developed an M2-like phenotype over the culture period with increased CD206 and CD163, as well as decreased IL-1b and IL-8 expression, compared to the M0 macrophages. In medium containing FCS, no tendency to M1 or M2 phenotype could be detected. Both M1 (IL-1β, IL8) and M2 (CD163 and CD206) markers showed higher expression than in the reference samples. Throughout the experiment, there was a significant increase in the CD206 expression and a decrease of CD163. When cultivated with hPL and thus in a balanced co-culture, macrophages showed increased IL- 8 and decreased CD206 expression and, therefore, rather an M1-like type. The recognition of foreign cells could explain this. Foreign bodies always trigger an inflammatory immune response [250]. Since throughout the co-cultivation, hardly any hMSCs are present in medium with hS, and likewise, most of the macrophages were absent in FCS. Therefore, some differences in the expression patterns were expected. When compared to serum types, significant differences were found only in relation to FCS. It was hypothesized that this is due to the significantly decreased macrophage population in the medium with FCS. It might be necessary for the cells to express higher levels of the marker in order to share the information and cell responses on hMSCs with neighboring cells.

Phagocytosis of pathogens or foreign bodies is one of the main characteristics of macrophages. It is known that hMSCs can enhance the phagocytic activity in co-culture systems [128, 213]. Regarding this phenomenon, the phagocytic activity of macrophages in co-culture was compared to those in mono-culture (Figure 27). Co-cultures in medium with FCS and hPL yielded a higher phagocytic rate than mono-cultures. Contrarily, co-cultured macrophages in medium with hS showed a lower phagocytosis rate than mono-cultured ones. Hence, the presence of hMSCs in media preserving this cell type (i.e., media with FCS and hPL) supports and ameliorates bead uptake, which is in accordance with the known ability of hMSCs to enhance phagocytosis.

Co-cultures of different cell types are essential for a better understanding of cellular interactions *in vitro*. However, their establishment is often difficult because each cell type is usually cultivated under different conditions [117]. Thus, co-cultivation is commonly a compromise to preserve the most important cell properties of both cell types. Experiments performed in media supplemented with hPL (without the use of heparin) showed that both macrophages and hMSCs have comparable phenotypes to their standard cultivation sera. Furthermore, both cell types retain their properties to differentiate spontaneously (macrophages) as well as induced (macrophages, hMSCs). In the direct co-culture, macrophages and hMSCs were cultivated together without disadvantages, i.e., the maintenance of hMSCs could be shown, and the enhancement of phagocytosis by macrophages was preserved. Neither cultivation with hS nor FCS could achieve this totally.

In all experiments performed here, the need for heparin during the culture of macrophages with hPL was tested. Neither cell shape, gene expression, nor phagocytic activity showed a significant difference between hPL with or without heparin. However, significant differences in the cytokine profile could be detected in medium containing heparin compared to all other sera. Furthermore, despite the omission of heparin in hPL-samples, no gelation of the medium was visible as had contradictorily been described in previous studies [16]. Hence, this suggests that the expression of heparan sulfate proteoglycans by monocytes and macrophages themselves, which has been described before [251], was sufficient to act as an anticoagulant factor as exogenous heparin [252]. Therefore, avoiding additional heparin during macrophage culture is recommended, mainly because of higher amounts of released pro-inflammatory cytokines IL-1β and IL-6 and other possible stimulation side effects on macrophages [17, 248]. Moreover, hMSCs

in co-cultures might be influenced by higher anticoagulant concentrations, resulting in impaired cellular proliferation and reduced colony-forming units [16].

Conclusion

This study demonstrates that hPL, in particular without adding heparin, can efficiently replace hS for the *in vitro* culture of human macrophages without any restrictions. In co-culture experiments of primary human macrophages and hMSC, apparent negative effects of FCS as a culture supplement were shown. Using hPL as best performing serum supplement, it was able to define a co-culture system for human macrophages and hMSCs without the need for heparin in the culture medium. These results envision that this system will be of great value for research questions that imply the co-culture of macrophage and hMSCs, with biomaterial assessment under culture conditions that more closely mimic the early phase of the innate immune response after implantation as one important example.

4.5. Experimental section

4.5.1. Cell culture

All Experiments were performed with the approval of the Local Ethics Committee of the University of Wuerzburg. Buffy coats were obtained from the Bavarian Red Cross with written informed consent of each blood donor.

Monocytes were isolated from human blood-derived buffy coats (Blood donor service, German Red Cross, Wiesentheid (D)) of healthy donors. Peripheral blood mononuclear cells were collected by density gradient centrifugation with Pancoll (Density: 1,077 g/l; Pan-Biotech, Aidenbach (D)). Monocytes were then isolated via negative selection (Pan Monocyte Isolation Kit, Miltenyi Biotec, Gladbach (D)) and cultivated up to seven days in macrophage culture medium (RPMI-1640, GlutaMAX^{TM} (Thermo Fischer Scientific, Waltham (USA)) with either 10 % of human serum (hS, pooled serum of 6 healthy donors), 10 % fetal calf serum (FCS, Thermo Fisher Scientific, Waltham (USA)) or 10 % of human platelet lysate (hPL, PL Bioscience, Aachen (D)) with (+) or without (-) addition of 2 units/ml of heparin (PL Bioscience, Aachen (D)) and 1 % Penicillin-Streptomycin (Pen-Strep; 5,000 U/ml) (Thermo Fisher Scientific, Waltham (USA)) in non-treated 12-well plates (Corning, Corning (USA)) in a humidified atmosphere at 37 °C and 5 % CO_2 without any medium change. Monocytes differentiated spontaneously, i.e., without supplemented differentiation factors, into macrophages within this time (M0 macrophages).

For the induced differentiation of monocytes into M1 and M2 type macrophages, respectively, 1 µg/ml lipopolysaccharides (Sigma-Aldrich, Munich (D), M1) and 10^{-7} M dexamethasone (Sigma-Aldrich, Munich (D), M2) were used.

Human mesenchymal stromal cells (hMSCs) from trabecular bone were isolated from the femoral heads of patients undergoing total hip arthroplasty and selected via plastic adherence [220]. All experiments were approved by the Local Ethics Committee of the University of Wuerzburg with the written informed consent of each donor patient. They were routinely tested for their differentiation potential along the adipose-, chondrogenic- and osteogenic lineage. Obtained hMSCs were cultured in DMEM F-12 GlutaMAX^{TM} (Thermo Fisher Scientific, Waltham (USA)) with 10 % FCS, 1 % Pen-Strep and 50 µg/ml L-ascorbic-acid-2-phosphate (Sigma Aldrich, Munich (D)) in 175 cm^2 cell culture flasks (Greiner Bio-One, Kremsmuenster (D)). Medium was changed every three to four days.

Cell passaging was performed at 90 % confluence. For all experiments, undifferentiated hMSCs in passage 2 were used.

4.5.2. Co-culture experiments

For co-culture experiments, monocytes/macrophages were cultivated four days on suspension plates (Sarstedt, Nümbrecht (D)). After that time, hMSCs in a ratio of one (hMSCs) to four (macrophages) in passage 2 were added onto the monocytes/macrophages in fresh macrophage culture medium. Co-culture studies were performed for up to three days. For gene expression analysis, macrophages were separated after co-cultivation via magnetic CD45 MicroBeads (Miltenyi Biotec, Bergisch Gladbach (D)) according to the manufacturer's protocol.

4.5.3. Inverted light and fluorescence microscopy

The cell shape of macrophages was monitored via inverted light microscopy. For the discrimination of both cell types in the co-culture, cells were stained with 50 nM non-transferable CellTracker™ fluorescent dyes (Thermo Fisher, Invitrogen) (macrophages: green CMFDA; hMSCs: orange CMRA). Specimens were analyzed via fluorescence microscopy (Axio Observer, Zeiss, Oberkochen (D), equipped with epifluorescence optics and an XY camera).

4.5.4. Determination of DNA amount

To determine the DNA amount and thereby the cell adhesion of macrophages, the Quant-iT™ PicoGreen® dsDNA Reagent and Kit (Thermo Fisher Scientific, Waltham (USA)) was used per the manufacturer's manual. In short, macrophages were cultivated in a 24-well plate in 1 ml macrophage culture medium in a humidified atmosphere at 37 °C and 5 % CO_2. After one, three and seven days, cells were washed once with PBS- and lyzed in 1 ml 1 % Triton X-100 in PBS- for 1 h at 4 °C. The standard curve was prepared as described in the manual. The samples were excited at 485 nm, and the fluorescence emission intensity was measured at 538 nm on a plate reader (Tecan, Männedorf (CH)).

4.5.5. Gene expression analysis

Total cellular RNA of macrophages was isolated using PeqGold Trifast™ (VWR, Darmstadt (D)) per the manufacturer's protocol. Afterward, cDNA was generated with

the High-Capacity cDNA Reverse Transcription Kit (Thermo Fisher Scientific, Waltham (USA)) according to the manufacturer's manual. The mRNA levels of macrophages were analyzed via quantitative Real-Time PCR (qPCR) (StepOnePlus; Thermo Fisher Scientific, Waltham (USA)) with "Sybr Select" Mastermix (Thermo Fisher Scientific, Waltham (USA)). For the amplification of the mRNA, each 10 µl qPCR reaction comprised 5 ng of cDNA and 200 nM primer sequences (Biomers, Ulm (D)) (Table 3). For each cDNA sample, the threshold cycle (Ct) value of each target sequence was subtracted from the Ct value of the housekeeping mRNA RPS27a, to derive ΔCt. The RQ values were calculated by the $2^{-\Delta\Delta Ct}$ method. A control group of macrophages was used for normalization.

Table 3. Primer sequences

Name	Sequence 5' → 3'	Annealing temperature [°C]	Fragment size [bp]
RPS27A*			141
Forward	5'-TCGTGGTGGTGCTAAGAAAA-3'	61	
Reverse	5'-TCTCGACGAAGGCGACTAAT-3'		
IL-8			113
Forward	5'-CATACTCCAAACCTTTCCACCC-3'	61	
Reverse	5'-CTCTGCACCCAGTTTTCCTTG-3'		
IL-1β			120
Forward	5'-GACCTGAGCACCTTCTTTCCC-3'	61	
Reverse	5'-GCACATAAGCCTCGTTATCCC-3'		
CD163			85
Forward	5'-GTGCCTGTTTTGTCACCAGTTC-3'	61	
Reverse	5'-TTACACACCGTTCCCCACTCC-3'		
CD206			156
Forward	5'-TCCAAACGCCTTCATTTGCC-3'	61	
Reverse	5'-GCTTTTCGTGCCTCTTGCC-3'		

*housekeeping gene

4.5.6. Flow cytometry

The surface proteins CD45 and CD206, as well as the intracellular protein IL-1β, were quantified via flow cytometric analysis on a FACSCalibur™ device (BD Bioscience, Heidelberg (D)). For this, cultured macrophages were scraped off the well bottom and incubated with specific antibodies and the corresponding non-immune isotype control, respectively, according to the manufacturer's protocol (Table 4). For the staining of intracellular IL-1β, samples were prepared with the "InsideStain Kit" (Miltenyi Biotec, Bergisch Gladbach (D)). After centrifugation at 300 x g for 10 min, the supernatant was discarded, and the pellets were resuspended with 500 µl FC-buffer (phosphate-buffered

saline (PBS), pH 7.2, 0.5 % bovine serum albumin (BSA), 2 mM EDTA). Data was analyzed with the Software "FlowJo" (FlowJo LLC, Ashland (USA)). Appropriate cell gating excluded dead cells and cell debris.

Table 4. Antibodies for flow cytometry

Antibody against	Isotype	Fluorescence dye	company
CD206, human	Mouse IgG1	FITC	Biolegend, San Diego (USA)
CD45, human	Recombinant human IgG1	FITC	Miltenyi Biotec, Bergisch Gladbach (D)
IL-1β, human	Mouse IgG1	APC	Biolegend

4.5.7. Cytokine quantification via Multi-Analyte ELISArray

Cytokine release of spontaneously differentiated macrophages was tested via the Multi-Analyte ELISArray Kit (Qiagen, Hilden (D)) after seven days of cultivation. The production of IL-1α, IL-1β, IL-2, IL-4, IL-6, IL-8, IL-10, IL-12, IL-17A, IFN-γ, TNF-α and GM-CSF was analyzed in supernatants according to the manufacturer's protocol. The absorbance was measured on a plate reader (Tecan, Männedorf (CH)) at 450 nm, corrected with the absorbance at the reference wavelength of 570 nm.

4.5.8. Phagocytosis assay

The phagocytic activity of macrophages was analyzed using 2 μm green fluorescence-labeled latex beads (Sigma-Aldrich, Munich (D)). The beads were opsonized in pooled human serum for 30 min prior to addition to the macrophage culture in a ratio of 10 beads per seeded cell and incubated in a humidified atmosphere for 2 h at 37 °C and 5 % CO_2. Cells were washed three times with serum-free macrophage culture medium to remove non-phagocytosed beads.

Bead uptake was analyzed via flow cytometry. Therefore, macrophages were scraped off the well plate, transferred into suitable 5 ml tubes (Sarstedt, Nümbrecht (D)), and centrifuged (300 x g, 5 min, 4 °C). The supernatant containing free-floating beads was discarded, whereas the pellet was resuspended in 500 μl of FC-buffer, and the number of positive cells was quantified. For the discrimination of cell types in co-culture studies with hMSCs, cells were stained against leukocyte-specific CD45 (Milteny Biotec; labeled with APC) according to the manufacturer's instruction. Double-positive cells were determined as bead-containing macrophages.

4.5.9.   Statistics

Statistica (StatSoft, Tulsa, USA) was used for statistical analyses. The statistical significance of qPCR data was determined by a two-sample t-test. For all other data, a two-way analysis of variance (ANOVA) was performed. Results were considered to be significantly different at a p-value below 0.05.

Chapter 5

Operating Procedures for an *in vitro* Co-Culture System of human Macrophages and hMSCs to Assess the Immunomodulation and the Regeneration Potential of Fiber-based Scaffolds

Chapter 5 is written in the style of a methodological manuscript. This chapter was thoroughly written by the author of this thesis Tina Tylek, who conceived the research, performed all experiments and data evaluation.

5.1. Abstract

In vitro co-cultures of different primary human cell types are essential for the evaluation of different biomaterials under conditions that are closer to the human *in vivo* situation. In the context of the innate immune response, the co-culture of macrophages and mesenchymal stromal cells (MSCs) can be of particular interest. Both are present and involved in tissue regeneration and inflammatory reactions and play crucial roles in the immediate inflammatory reactions and the onset of regenerative processes, thus reflecting the decisive early phase of biomaterial contact with the host. Due to the complexity of co-cultures in indirect or direct conditions on biomaterials, however, mostly mono-cultures are performed. Therefore, protocols have to be established to allow for the co-cultivation of relevant cell types and to analyze step-by-step the phenotypical and molecular changes of co-cultures provoked by distinct material properties of biomaterials.

Here, setups for the direct and indirect co-cultures of macrophages and human MSCs (hMSCs) on fiber-based scaffolds have been established. In addition, protocols for the evaluation of phenotypical as well as molecular changes have been developed and proven for functionality. Differences in macrophage responses cultivated with or without hMSCs and on scaffolds versus plastic surfaces were detected, and therefore, a meaningful impact of the biological and physical environment was determined.

5.2. Introduction

The immune response to foreign bodies is a major issue in designing new biomaterials. Thereby, the host response is characterized by the involvement of many immune and tissue cells, such as neutrophils, monocytes/macrophages, fibroblasts or mesenchymal stromal cells (MSCs) [2, 3]. Especially the reactions of macrophages, key players of the innate immune response, is often examined to get hints of the host response to biomaterials.

Macrophages are highly plastic cells, which can, upon various stimuli, differentiate into several subtypes. Roughly, they can be divided into the pro-inflammatory, classically activated M1 and the anti-inflammatory, alternatively activated M2 type. M1-differentiated macrophages are characterized by the production of pro-inflammatory related cytokines, such as IL-1α, IL-1β, IL-6, TNF-α, IL-8, IL-12, IL-13, as well as by a low secretion of the anti-inflammatory cytokine IL-10 [57]. Characteristics of M1 macrophages are the phagocytosis of pathogens and the production of reactive oxygen species (ROS) [66]. Therefore, M1 macrophages have a strong anti-microbicidal and anti-tumoral activity. M1 type macrophages are known to impair tissue regeneration and wound healing. To balance this, M2 type macrophages are induced by a regulative mechanism [67]. The M2 macrophages can be divided into additional subtypes, each with different stimuli, expression patterns, and functionalities, as M2a [68], M2b [74] or M2c [69, 76]. M2 macrophages release anti-inflammatory cytokines such as IL-10 and are characterized by the expression of scavenger (CD163) as well as mannose receptors (CD206) [54]. While the M2a and M2b subgroups fulfill immune regulatory functions, the M2c subset is crucial for tissue remodeling and the suppression of inflammatory immune responses by the secretion of TGF-β1 and IL-10 [52, 53].

Interactions with other cell types also stimulate macrophages to exert a different phenotype, such as neutrophils, fibroblasts or MSCs. MSCs are spindle-shaped, plastic-adherent cells, which can be isolated from various tissues, such as bone marrow, adipose tissue, dental pulp or umbilical cord blood and are characterized as multipotent stem cells by their potential to differentiate into various cell types, like adipocytes, chondrocytes, and osteoblast [86, 87]. Furthermore, MSCs are known to interact with cells of the immune system, including macrophages, on several levels either directly or by soluble factors [93]. As a result of the interaction with MSCs, macrophages adapt an M2-like phenotype, secreting less TNF-α and higher amounts of IL-10 and CCL18, and further

show an increased phagocytic activity [104]. Moreover, macrophages show an increased expression of the surface markers CD163 and CD206, however, the release of pro-inflammatory cytokines such as IL-6 is also increased [105].

To mimic and examine *in vivo* processes in more detail, *in vitro* experiments should be of higher complexity than mono-cultures can achieve it. For this reason, the establishment and analysis of co-cultures comprised of two or more cell types has gained some attention over the last years. Co-culture systems can differ depending on the number of cell populations, the similarity between these cell populations, the degree of separation, and the duration of the co-cultivation [117]. Also, in the field of biomaterial research and the assessment of the host response, a co-culture can be beneficial. Therefore, several co-cultures, such as of macrophages and fibroblasts [253-255] or macrophages and other leukocytes [256, 257], have been established. In the context of macrophages and MSCs, the investigation of their crosstalk has so far either included MSCs as part of the therapy itself (cell therapies or implanted together with biomaterials) or relied on endogenously derived MSCs, which migrate to the site of injury or implantation during the healing process [5].

Here, a protocol for the assessment, on molecular and visual levels, of the macrophage response to biomaterials in co-culture with hMSCs, mimicking the influence of endogenously derived cells after implantation of biomaterials was established. By this, a more exact forecast of the reactions to specifically designed biomaterials will be possible.

5.3. Protocols

NOTE: All protocols using human donor materials must first be reviewed and approved by the local ethics committee.

NOTE: Working conditions must ensure the highest degree of sterility.
Equipment must be sterilized before use and stored in 70 % ethanol when not in use. All solutions and reagents that come into contact with tissues or cells must be sterile.

NOTE: All culture incubations should be performed in a 37 °C, 5 % CO_2 incubator with 95 % relative humidity. As soon as prepared, cultures must be maintained in this type of incubator.

NOTE: All chemicals were purchased from Merck (Darmstadt, Germany) unless otherwise stated.

5.3.1. Basic Protocol 1: Indirect co-culture of macrophages and human mesenchymal stromal cells to examine the effects of fiber-based scaffolds

The setup of an indirect co-culture of human macrophages and hMSCs has been established to analyze the effects of hMSCs' soluble factors on macrophages. By culturing macrophages and hMSCs either on scaffolds or on plastic well plates, responses due to the properties of the materials can be examined and, therefore, set into a more *in vivo*-related context. All necessary arrangements for conditioned media experiments, including essential controls, are shown in Figure 28.

The main steps of preparing the co-culture are shown in Table 5. Prior to co-culture experiments, both human monocytes (4 days prior) (see supporting protocol 1) and hMSCs (1-2 weeks prior) (see supporting protocol 2) have to be isolated. As a source for human monocytes, peripheral blood and for hMSCs trabecular bone from femoral heads (of patients undergoing hip arthroplasty) are used. By culturing cells on scaffolds, responses specific to biomaterial properties can be examined.

For preparing conditioned media, one day before starting the co-culture, 1 ml macrophage culture media (see recipe) has to be added to hMSCs and collected after 24 h. The collected media has to be filtered to avoid cell cross-contamination and subsequently transferred onto macrophages.
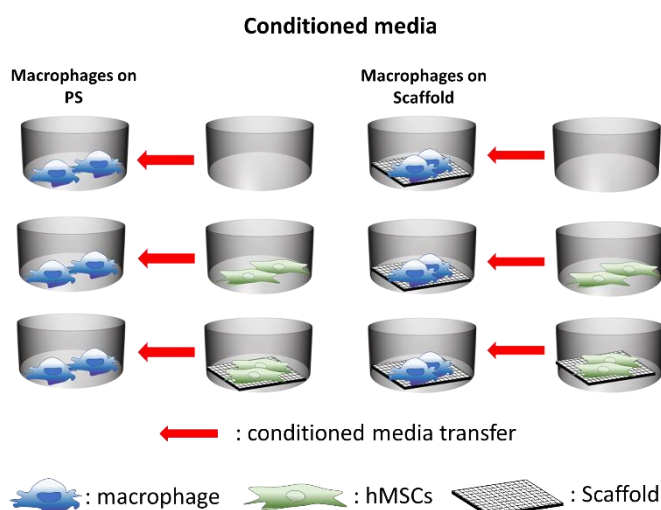
Figure 28. Setup for conditioned media experiments. On the left: conditioned media transfer to macrophages cultivated on plastic surfaces, on the right: conditioned media transfer to macrophages cultivated on scaffolds. The first row shows the transfer of control macrophage media after 24 h incubation in a blank well. The middle row shows the transfer of conditioned media from hMSCs cultivated on plastic surfaces. The third row shows the transfer of conditioned media from hMSCs cultivated on scaffolds.

Chapter 5

Materials

- sterilized and pretreated fiber-based scaffolds (see supporting protocol 3) seeded with primary human monocytes (see supporting protocol 1)

- sterilized and pretreated fiber-based scaffolds (see supporting protocol 3) seeded with hMSCs up to passage 2 (see supporting protocol 2)

- non-treated 24-well plates seeded with primary human monocytes (see supporting protocol 1)

- tissue culture-treated 24-well plates seeded with hMSCs up to passage 2 (see supporting protocol 2)

- macrophage culture medium (see recipe)

Table 5. Preparation of conditioned media

Day	Action
-X (7-14 days prior d0)	Prepare hMSCs cultures (see supporting protocol 2)
-1	Passage and seed hMSCs on scaffolds or wells (see supporting protocol 2)
0	Isolate and seed human monocytes on scaffolds or wells (see supporting protocol 1)
3	Add fresh macrophage culture medium to hMSCs
4	Transfer conditioned media to macrophages and start co-culture

Setup of indirect co-culture

1. On the day conditioned media has to be prepared (see Table 5), transfer hMSC-containing scaffolds in a new well plate, and add exactly 1 ml fresh macrophage media to each scaffold.

2. Remove media from hMSCs cultivated in well plates and add exactly 1 ml of fresh macrophage media.

3. One day later (day of co-culture start), collect media of hMSCs, and pass it through a 0.2 µm sterile filter to avoid cell contamination.

4. Remove media from macrophages (on scaffolds and well plates) and add either 1 ml hMSC-conditioned media or 1 ml macrophage culture media incubated in a blank well as control.

5. Incubate cells at 37 °C, 5 % CO_2, and 95 % relative humidity until sample collection (3 h, 24 h, and 72 h).

5.3.2. Basic Protocol 2: Direct co-culture of macrophages and hMSCs to examine effects of fiber-based scaffolds

In contrast to indirect co-culture, via direct co-culture cell-cell interactions can be examined. The co-culture setup is shown in Figure 29. As a control, macrophages are cultivated in mono-cultures. The main steps of preparing the co-culture are shown in Table 6. The isolation of both cell types (see supporting protocol 1 and 2) takes place as previously mentioned (see basic protocol 1).

After 4 days of monocyte/macrophage cultivation, hMSCs from mono-cultures are passaged, resuspended in macrophage medium, and seeded onto the monocytes/macrophages. For the duration of the co-culture, both cell types are cultivated together.

The direct co-culture on plastic has to be performed on surfaces that are suitable for both cell types. Under normal culture conditions, for human macrophages, non-treated well plates and for hMSCs tissue-culture treated well plates are used. In preliminary studies, suspension plates (Sarstedt, Nümbrecht) were identified as an appropriate candidate for direct co-culture experiments.
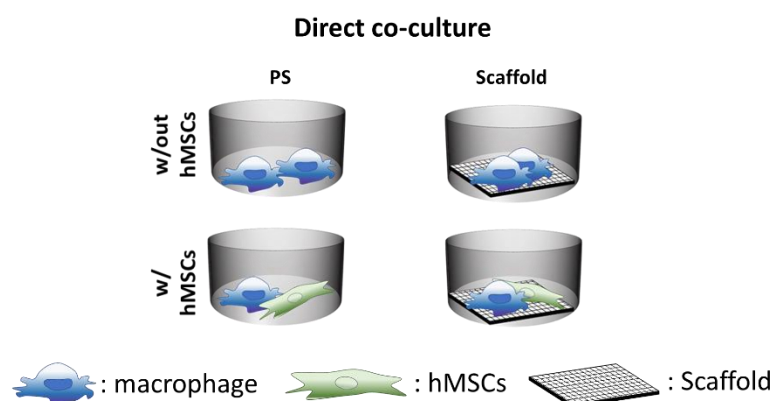
Figure 29. Setup for direct co-culture. On the left: cell culture on plastic surfaces, on the right: cell culture on scaffolds. The upper row shows the mono-culture of macrophages. The lower row shows the co-culture of macrophages and hMSCs.

Materials

- sterilized and pre-treated fiber-based scaffolds (see supporting protocol 3) seeded with primary human monocytes (see supporting protocol 1)

- non-treated 24-well plates seeded with primary human monocytes (see supporting protocol 1)
- tissue culture-treated 24-well plates seeded with hMSCs up to passage 2 (see supporting protocol 2)
- macrophage culture medium (see recipe)

Table 6. Preparations for direct co-culture

Day	Action
-X (7-14 days prior d0)	Prepare hMSCs cultures (see supporting protocol 2)
0	Isolate and seed human monocytes on scaffolds or wells (see supporting protocol 1)
4	Passage and seed confluent hMSCs (see supporting protocol 2) on macrophage-containing scaffolds or wells and start co-culture

Setup of direct co-culture

1. On the day co-culture is started (see Table 6), transfer macrophage-containing scaffolds in a new well plate and add 1 ml fresh macrophage culture media.
2. Remove media from macrophages on well plates and add 1 ml fresh macrophage culture media.
3. Passage hMSCs and seed either 1.25×10^5 cells onto the respective macrophage-containing scaffolds or on top of the macrophages in well plates.
4. Incubate the cells at 37 °C, 5 % CO_2, and 95 % relative humidity until sample collection (3 h, 24 h, and 72 h).

5.3.3. Basic Protocol 3: Examination of co-culture phenotype via fluorescent microscopy and scanning electron microscopy.

To examine cellular interactions and cell phenotypes, microscopic techniques can be advantageous. Thereby, different methods suit different applications and examination aims. By live cell staining, e.g., staining with fluorescent cell trackers (see supporting protocol 4), different cell types can be tracked in mono- or co-cultures over a certain period. Thus, cell interactions and changes in phenotypes can be investigated in the same sample. Benefits of SEM (see supporting protocol 5) are the high resolution of cellular structures and the possibility to investigate the cell-material interactions in detail.

However, a clear discrimination of macrophages and hMSCs is not possible. By Immunofluorescent staining (see supporting protocol 6) under consideration of suitable antibodies, such as CD45, it can be distinguished between macrophages (CD45+) and hMSCs (CD45-). Furthermore, macrophage polarization (see Table 4) can be analyzed. For SEM and immunofluorescent staining, cells have to be fixed prior to the staining, while cell tracker staining can be conducted with viable cells.

Material and Devices

- Macrophages and hMSCs in direct co-culture stained with different non-transferable cell tracker dyes (see supporting protocol 4)
- Fixed macrophages and hMSCs after direct co-culture prepared for scanning electron microscopy (see supporting protocol 5)
- Fixed and antibody-labeled macrophages after direct and indirect co-culture (see supporting protocol 6)
- Inverted fluorescence microscope (here: Axio Observer, Zeiss equipped with epifluorescence optics and an MRm camera; Zeiss, Oberkochen, Germany)
- Scanning electron microscope (here: Crossbeam 340 scanning electron microscope; Zeiss, Oberkochen, Germany)

Examination of co-culture phenotype

1. Analyze co-culture interactions of cell tracker-stained cells via fluorescence microscopy after 3 h, 24 h, and 72 h of co-cultivation.
2. By the use of cell tracker, live cell imaging is possible for at least 72 h.
3. Fix co-culture samples after 3 h, 24 h, and 72 h. After dehydration and sputtering, examine the co-culture phenotype by SEM.
4. Capture images of antibody-labeled macrophages in direct and indirect co-culture after 24 h and 72 h via fluorescence microscopy.

   If not under analysis, keep stained samples in the dark to avoid bleaching of fluorescent signals.

5.3.4. Basic Protocol 4: Analysis of macrophage response at the molecular level

For highly plastic cells, such as macrophages, the molecular response needs to be examined to predict polarization effects depending on cell-cell and cell-material interactions.

Gene expression analysis and changes in cytokine release allow for the determination of cell polarization. Examples of reliable markers and cytokines are stated in Table 7, Table 8 and Table 9.

One major issue of the direct co-culture protocol is the strong cell adhesion onto the scaffolds and the concomitant failure of cell detachment from these scaffolds after cultivation. Thus, a separation of both cell types after co-cultivation is not feasible. Therefore, gene expression analyses and cytokine studies of direct co-cultures always reflect a gene expression/cytokine release mixture of both cell types.

Material and Devices

- Transcribed cDNA (see supporting protocol 7)
- QPCR device (here: StepOnePlus; Thermo Fisher Scientific, Waltham, USA)
- QPCR Software for analysis (here: StepOne Plus v.2.3; Thermo Fisher Scientific, Waltham, USA)
- Cell culture supernatant (see supporting protocol 8)
- ELISA array kits (here: Single-Analyte ELISArray Kits; Qiagen, Hilden, Germany)
- Cell lysate (see supporting protocol 8)
- Kit for DNA quantification (here: Quant-iT™ PicoGreen® dsDNA Reagent and Kit; Thermo Fisher Scientific, Waltham, USA)
- Plate reader (here: Tecan, Männedorf, Switzerland)

Determination of gene expression changes

1. Measure gene expression changes of transcribed cDNA using a qPCR device and under consideration of the appropriate house-keeping genes and controls.
2. Analyze gene expression using the ddCt method

Qiagen and Thermo Scientific have particularly helpful online manuals and background information on RT-PCR basics that can be found here: https://www.qiagen.com/us/resources/molecular-biology-methods/pcr/ and https://www.thermofisher.com/us/en/home/life-science/pcr/real-time-pcr/

Examination of cytokine release

1. Quantify the DNA amount using a DNA Assay (here: Quant-iT™ PicoGreen®) according to manufacturer's protocol and measure the fluorescent signal using a plate reader at the appropriate excitation, here: 480 nm and emission: 520 nm.
2. Perform ELISA Assay in accordance to the instructions of the kit used, e.g., Single-Analyte ELISArray Kit, Qiagen ….

   Measure the absorbance using a plate reader at 450 nm with wavelength correction at 570 nm and determine the amount of released cytokine in the different samples under consideration of the measured DNA amount.

5.3.5. Supporting Protocol 1: Monocyte isolation and cultivation

Monocytes were isolated from peripheral blood. Firstly, all mononuclear cells from peripheral blood (PBMCs) were obtained from buffy coats using density gradient centrifugation. Subsequently, in order to prevent polarization effects by the isolation (magnet labeling by positive isolation or cell-cell contact by plastic adherence), negative selection was used to separate monocytes from PBMCs. By the negative selection, all PBMCs except for monocytes get labeled with magnetic antibodies and are thus retained in a suitable column, while non-labeled monocytes can pass this column and are collected with the flow through. Buffy coats with a volume of approximately 35 ml (processed from a 500 ml whole blood donation) obtain approx. 6 x 10^7 monocytes. Monocytes were then cultured either on non-treated plastic well plates or on scaffolds in macrophage culture medium (see recipe) without adding differentiation factors. By adherence to surfaces, monocytes start to differentiate spontaneously into macrophages. Due to the completed differentiation after seven days, the cultivation period of monocytes/macrophages did not exceed this time. If not mentioned otherwise, no media exchange took place during this time.

Chapter 5

Materials

- Buffy coat (commercially available; here: Blood donor service, Bavarian Red Cross, Wiesentheid, Germany)

- Dulbecco's PBS without calcium and magnesium (Thermo Fisher Scientific, Waltham, USA)

- Pancoll or another separating solution for density gradient centrifugation with equivalent properties (Density: 1.077 g l^{-1}; Pan-Biotech, Aidenbach, Germany)

- Negative selection kit for human monocytes (here: Pan Monocyte Isolation Kit, Miltenyi Biotec, Gladbach, Germany)

- Macrophage culture medium (see recipe)

- Sterilized and pretreated fiber-based scaffolds (see supporting protocol 3)

- Non-treated 24-well plates (here: Corning Costar)

- Tissue culture-treated 24-well plates (here: Nunc, Thermo Fischer Scientific, Waltham, USA)

Isolation of peripheral blood mononuclear cells (PBMC) from buffy coats

1. Four days before going to start the co-culture experiments, perform the isolation of peripheral blood mononuclear cells (PBMC) from buffy coats by density gradient centrifugation

   A buffy coat contains approximately 30 ml of peripheral blood.

2. To obtain PBMCs, put 22.5 ml of Pancoll into each of two conical 50 ml centrifuge tubes and carefully overlay with 30 ml of peripheral blood diluted 1:1 with PBS without disturbing the interface.

3. Subsequently, centrifuge the tubes at 350 x *g* for 40 min at room temperature without break.

4. Gently collect the PBMCs at the interface between the Pancoll and the plasma layer by aspiration with a Pasteur pipette and transfer them into a new 50 ml conical tube.

5. Wash PBMCs at least three times by adding 50 ml of PBS each time prior to centrifugation at 250 x *g*, 200 x *g*, and 150 x *g*, respectively, for 10 min each.

   By decreasing the centrifugation speed, platelet contamination can be reduced.

Isolation of human monocytes from PBMCs

6. Count the obtained PBMCs and subsequently isolate monocytes via negative selection according to the manufacturer's protocol.

By negative selection, all PBMCs except for monocytes get labeled with a magnetic bead-containing antibody and can be separated via a suitable magnetic column.

Cultivation of human monocytes

7. Count the obtained monocytes and prepare cell suspensions in macrophage culture medium. For cell seeding on scaffolds, add 50 µl of a 1.5 x 10^7 cell/ml suspension dropwise onto the 1 cm^2 sized scaffolds, and incubate them for 30 min at 37 °C and 5 % CO_2. Subsequently, add 1 ml of macrophage culture medium. For cell seeding in 24-well plates, add 1 ml of a 1 x 10^7 cell/ml suspension into each well.

8. Incubate monocytes at 37 °C in a humidified atmosphere containing 5 % CO_2. If not stated otherwise, do not change media over the seven-day culture period.

By the adherence on surfaces, monocytes start to differentiate spontaneously into macrophages.

5.3.6. Supporting Protocol 2: Human mesenchymal stromal cell (hMSC) isolation and cultivation

For these protocols the used hMSCs are isolated from human bone marrow. For this purpose, trabecular bone from femoral heads of patients undergoing hip arthroplasty was collected, and cells were isolated. After isolation, up to 1.2 x 10^{10} cells can be obtained (depending on the quality and quantity of the provided donor material). After reaching 90 % confluency (which lasts up to two weeks), each T175 flask contains approximately 3-5 x 10^6 hMSCs. They are characterized by their adherence to plastic, their differentiation into osteoblasts, chondrocytes or adipocytes, and their lack of expression of the leukocyte marker CD45. Within the protocols described here, hMSCs are used in an undifferentiated state. For the duration of co-culture experiments, hMSCs were cultivated in macrophage culture medium. In previous experiments (see Chapter 4), it has been proven that the viability and proliferation is maintained without any restrictions during the applied three-day co-culture period.

Materials

- Femoral heads (of patients undergoing hip arthroplasty)
- DMEM F-12 GlutaMAX^{TM} (here: Thermo Fischer Scientific, Waltham, USA)
- Dulbecco's PBS without calcium and magnesium (Thermo Fischer Scientific, Waltham, USA)

- Trypsin-ethylenediaminetetraacetic acid (EDTA) solution (0.25 %) (Thermo Fischer Scientific, Waltham, USA)
- Tissue culture-treated T175 flasks (here: Nunc, Thermo Fischer Scientific, Waltham, USA)
- Suspension 24-well plates (Sarstedt, Nümbrecht; Germany)
- hMSCs growth medium (see recipe)

Isolation of hMSCs

1. Transfer the trabecular bone of femoral heads into conical 50 ml centrifuge tubes (a maximum volume of 15 ml per tube)

2. Fill these tubes with DMEM F-12 GlutaMAX^{TM} medium (without supplements) to 35 ml and vortex them. Allow the trabecular bone to sediment and transfer the cell-containing supernatant to another, fresh tube. Repeat this step 3-4 times.

3. Centrifuge the tubes at 300 x g for 5 min at room temperature.

4. Discard the supernatant and resuspend the cell pellet. Subsequently, pass the suspension trough a 70 µm cell strainer.

5. Count the resulting cells and seed each 8 x 10^8 cells into a tissue culture-treated T175 flask in 30 ml hMSCs growth medium.

6. 2 - 4 days after isolation, wash adherent cells three times with PBS and add new media. Change media every 3 - 4 days until confluency.

   Adherent cells are considered to be hMSCs.

7. After 90 % confluency is reached, passage hMSCs.

   For co-culture experiments, hMSCs were used up to passage 2.

Passaging of hMSCs

8. For passaging, wash the cells in the T175 flask with PBS, discard it, and add to each flask 3 ml of Trypsin-ethylenediaminetetraacetic acid (EDTA) solution. Incubate the cells at 37 °C in a humidified atmosphere containing 5 % CO_2 for 5 min. Subsequently, add 7 ml hMSCs growth medium to stop the enzymatic reaction.

9. Collect the cells in a 15 ml tube, centrifuge at 300 x g for 5 min, and resuspend the cell pellet in the desired fresh medium.

Cultivation of hMSCs

10. For the cultivation on scaffolds, place the scaffolds into non-treated well plates. Add 500 µl cell suspension of 2.5 x 10^5 cells/ml in macrophage culture medium onto

the scaffolds and incubate overnight at 37 °C in a humidified atmosphere containing 5 % CO_2.

11. For the cultivation in well plates, seed 1.25 x 10^5 hMSCs in 1 ml into a 24-well suspension plate and cultivate the cells at 37 °C in a humidified atmosphere containing 5 % CO_2.

12. On the next day, add 500 µl macrophage medium to each cell-containing scaffold and incubate until needed.

5.3.7. Supporting Protocol 3: Scaffold preparation

Melt electrowritten fiber-based poly(ε-caprolactone) (PCL) scaffolds, as described previously (Chapter 2), were used in these protocols as representative biomaterials. However, the protocol can easily be applied to other fiber-based scaffolds and by slight adaptions to other materials and scaffold types. For cell culture, scaffolds should be sterilized by incubation in 70 % (v/v) ethanol for 30 min and subsequently washed with PBS. On the day of cell seeding, scaffolds are pre-incubated in serum-free macrophage culture medium at 37 °C to pre-warm the scaffolds and to remove remaining PBS. A pre-incubation in PBS might impede cell adherence.

To increase the attachment preference of the cells to the scaffolds, use well plates on which cells show low attachment under standard culture conditions, i.e., tissue culture-treated well plates for macrophages and non-treated well plates for hMSCs.

Materials

- Scaffolds (here: fiber-based PCL scaffolds, 1 cm²; suitable for 24-well plates)
- 70 % (v/v) Ethanol (here: Merck, Darmstadt, Germany)
- Dulbecco's PBS without calcium and magnesium (Thermo Fischer Scientific, Waltham, USA)
- Serum-free RPMI-1640 (GlutaMAX^{TM}, Thermo Fischer Scientific, Waltham, USA)
- 24-well plates (tissue culture-treated and non-treated, described above)

Scaffold sterilization

1. For sterilization, incubate scaffolds for 30 min in 70 % ethanol and subsequently wash them twice with PBS$^-$ for at least 30 min.

2.   Until the day of use, store the scaffolds in PBS at 4 °C.

Scaffold pretreatment

3.   On the day of cell seeding, remove PBS, place the scaffolds into a suitable well plate, and incubate them in serum-free RPMI-1640 at 37 °C, 5 % CO_2.

> *For macrophage cultivation on scaffolds, use tissue culture-treated well plates, for hMSC cultivation on scaffolds use non-treated well plates.*

5.3.8. Supporting Protocol 4: Cell tracker staining

For live cell imaging of the direct co-culture and to distinguish between macrophages and hMSCs, both cell types can be stained with non-transferable cell tracker in green and orange, respectively. Firstly, suitable staining solutions have been established to ensure optimal fluorescence intensities for a culture period of three days. Thus, macrophages were stained with higher dye concentrations as hMSCs. Before starting co-culture experiments, both cell types were stained and afterward washed extensively to avoid cross staining. Subsequently, cell interactions of the same samples could be examined for 72 h.

Materials

- Non-transferable cell tracker (Invitrogen, Thermo Fischer Scientific, Waltham, USA)
- Serum-free RPMI-1640 medium (GlutaMAX^{TM}, Thermo Fischer Scientific, Waltham, USA)
- sterilized and pretreated fiber-based scaffolds (see supporting protocol 3) seeded with primary human monocytes/macrophages (see supporting protocol 1)
- non-treated 24-well plates seeded with primary human monocytes (see supporting protocol 1)
- Dulbecco's PBS without calcium and magnesium (Thermo Fischer Scientific, Waltham, USA)

Note: Perform non-transferable cell tracker staining prior to starting the co-culture experiments.

Preparation of working solutions

1. Prepare a working solution of both cell trackers used (here, macrophages are going to be stained in green and hMSCs in orange). Resuspend each vial in 10 μl DMSO. The working solution used for macrophage staining contains 1 μl of cell tracker dye mixed with 1 ml supplement-free macrophage medium. The working solution used for hMSCs staining contains 0.5 μl of cell tracker dye mixed with 1 ml serum-free macrophage culture medium. Prewarm working solutions at 37 °C.

Cell staining

2. Remove media from macrophages, add 500 μl staining solution per 24-well, and incubate cells for 30 min at 37 °C, 5 % CO_2.

3. Stain hMSCs prior to passaging directly in the T175 flask using 3 ml of staining solution.

4. Subsequently, wash cells at least twice with PBS. Add fresh macrophage culture media to macrophages and passage hMSCs to seed them onto macrophages.

    Cells stained with cell tracker remain their fluorescence approximately for 3 days.

5. Analyze the co-culture interactions via fluorescence microscopy.

5.3.9. Supporting Protocol 5: Sample preperation for scanning electron microscopy

To investigate cell-cell and cell-material interactions, samples were prepared for SEM. Therefore, samples must be incubated with 6 % glutaraldehyde, which ensures proper fixation and maintains most of the fragile cellular structures. Subsequently, samples are dehydrated using an ascending ethanol series and hexamethyldisilane. The dehydration process described here has been attuned to PCL fiber-based scaffolds. When other biomaterials are used, it must be ensured that ethanol is not a solvent of them. To avoid electric charges within the SEM device, samples are coated with a 2 nm platinum layer.

Materials

- Scaffolds containing human macrophages and hMSCs in direct co-culture (basic protocol 2)
- Scaffolds containing human macrophages (supporting protocol 1)

- Dulbecco's PBS without calcium and magnesium (Thermo Fischer Scientific, Waltham, USA)
- Ethanol (100 %, 90 %, 70 % (v/v))
- 6 % glutaraldehyde (see recipe)
- Hexamethyldisilane
- SEM stubs
- Sputter coater (platinum) (here: Leica EM ACE600 sputtering unit (Leica Microsystems, Wetzlar, Germany)

Note: This SEM sample preparation protocol is suitable for PCL scaffolds as well as other polymeric scaffolds not being soluble in ethanol.

1. At the time points of interest, wash the samples twice with PBS and fix them by incubation in 6 % glutaraldehyde for 15 min on ice.
2. Wash samples twice in PBS for 10 min on ice.
3. Subsequently, dehydrate specimens at RT in ascending ethanol concentrations (each twice for 10 min: 70 %, 90 %, and 100 %) and incubate them for 2 × 15 min in hexamethyldisilane.
4. Air dry samples and mount them onto stubs
5. Afterward, coat samples with 2 nm platinum. Examine cellular phenotypes via scanning electron microscopy.

5.3.10.   Supporting Protocol 6: Immunofluorescence staining

Immunofluorescent staining is performed to both visualize the macrophage/co-culture phenotype and to examine the expression of cell surface markers (see Table 7). As several cell surface markers might be expressed on both macrophages and hMSCs, the additional use of a CD45 antibody allows for the discrimination and identification of macrophages. CD45 is a specific leukocyte marker, which is absent on hMSCs but expressed by macrophages. As negative controls, suitable non-immune IgGs must be used to ensure the specificity of the staining. After staining, mount samples on glass slides. Thereby, it is essential to ensure that the scaffolds are mounted as free as possible from air bubbles

and then appropriately sealed with coverslips. If necessary, seal with clear nail polish to avoid dehydration and hence, the loss of fluorescent signals of the sample.

Materials

- Scaffolds or well plates containing human macrophages and hMSCs in direct co-culture (basic protocol 2)
- Scaffolds or well plates containing human macrophages (supporting protocol 1)
- Dulbecco's PBS without calcium and magnesium (Thermo Fischer Scientific, Waltham, USA)
- 4 % formaldehyde (in PBS, pH 7.4)
- Bovine serum albumin
- Primary antibodies (here: CD163 (#TA506380, OriGene, Rockville, USA; 1:100) and CD45 (#ab64693, Abcam, Cambridge, UK; 1:400))
- IgG controls (here: rabbit IgG (#VEC-I-1000, Biozol, Eching, Germany; 1:1000), mouse IgG (#VEC-I-2000, Biozol, Eching, Germany; 1:400)
- Secondary antibodies (here: fluorescence-labeled secondary antibodies (Cy^{TM}2-conjugated AffiniPure Goat Anti-Rabbit or Cy^{TM}3-conjugated AffiniPure Goat Anti-Mouse (Jackson ImmunoResearch; Dianova, Hamburg, Germany)
- Humidity chamber
- Mounting medium with DAPI (here: Immunoselect Antifading Mounting Medium with DAPI (Dianova, Hamburg, Germany))
- Glass slides
- Coverslips
- Clear nail polish

Table 7. Examples of macrophage protein markers for immunofluorescent staining

general	M1	M2
CD45	IL-1β	CD163
CD14	TNF-α	CD206
	CCR7	IL-10

1. Wash samples at the time points of interest with PBS and fix them using 4% formaldehyde over night at 4 °C.

2. Subsequently, wash samples twice with PBS for 10 min at RT and block them by adding 2 % bovine serum albumin in PBS for 30 min at RT.

3. Apply suitable primary antibodies, like anti-CD45, anti-CD163, and anti-CD206, as well as the corresponding IgG controls for 2 h in a humidity chamber.

   For direct co-cultures, the parallel staining of CD45, along with the staining of the surface marker of interest, is needed to distinguish between macrophages and hMSCs.

4. Subsequently, wash samples twice with PBS for 5 min each and apply suitable fluorescence-labeled secondary antibodies for 30 min at RT in a humidified chamber in the dark.

5. Wash and mount samples, e.g., with Immunoselect Antifading Mounting Medium with DAPI on glass slides and seal them with coverslips.

   DAPI is used to counterstain nuclei.

6. Capture images via fluorescence microscopy and maintain stained samples in the dark to avoid bleaching of fluorescent signals.

5.3.11.   Supporting Protocol 7: Preparations of quantitative polymerase chain reactions

Gene expression analysis by qPCR is a quantitative method to obtain first results of macrophage polarization changes. Prior to performing qPCR reactions, RNA needs to be extracted and transcribed into cDNA. The use of a phenol-based reagent (Trifast™) for RNA extraction enables the dissolution of the whole scaffold and thus avoids the loss of cell material. When using other biomaterials, it should be checked beforehand, if these were also soluble in phenol or if other methods were more promising. Isolated RNA is reverse transcribed into cDNA by using suitable kits. Here, it should be considered to transcribe enough cDNA for all related experiments to avoid technical differences. In this protocol, for each qPCR reaction, 5 ng cDNA is used.

Materials

- Scaffolds containing human macrophages and hMSCs in direct co-culture (see basic protocol 2)
- Scaffolds containing human macrophages (see basic protocol 1)
- Phenol-based extraction solution (here: TriFast™ (VWR, Darmstadt, Germany))
- 1.5 ml reaction tubes
- Chloroform
- Isopropanol

- 70 % Ethanol (v/v)

- DEPC Water (see recipe)

- cDNA kit (here: High-Capacity cDNA Reverse Transcription Kit (Thermo Fisher Scientific, Waltham, USA)

- Sybr^{TM} Green reagent (here: SYBR™ Select Master Mix; Thermo Fisher Scientific, Waltham, USA)

- Forward and reverse primers (200 nM) (see Table 8 for suitable markers) (here: see Table 2, Biomers, Ulm, Germany)

- 96-well plates suitable for the qPCR device used (here: Thermo Fisher Scientific, Waltham, USA)

- qPCR plate seals (here: Thermo Fisher Scientific, Waltham, USA)

Table 8. Examples of gene expression markers of macrophage types and housekeeping genes

Housekeeping	M1	M2
RPS27a	IL-1β	CD163
GAPDH	TNF-α	CD206
	IL-8	IL-10
	IL-6	CCL22

RNA extraction

1. At the time points of interest, remove media from all samples and transfer cell-containing scaffolds into a new well plate.

   By placing the scaffolds into a new well plate, the RNA of any cells undesirably adherent to the well plate itself can be excluded from further analyses.

2. Add 400 µl of Trifast^{TM} to each sample in a chemical fume hood, lyse RNA via vigorous micro-pipetting and transfer it to a 1.5 ml tube. Samples can be stored in TriFast^{TM} at −80 °C until RNA extraction will be continued.

   The use of TriFast^{TM} ensures the complete dissolution of PCL.

3. Frozen samples need to be defrosted at room temperature for 5 min, and the tubes might be briefly vortexed or inverted to ensure complete thawing.

4. Add 80 µl chloroform per 400 µl of Trifast^{TM} Reagent used above. Cover the sample tightly, shake vigorously by hand for 15 s, and incubate for 10 min at RT.

5. Centrifuge the resulting mixture at 12,000 × *g* for 15 min at RT.

6. The phase separation should be visible, with the aqueous (clear) phase forming the top layer, a white/pale interphase, and the organic (pink) phase forming the bottom layer.

7. Transfer the maximum amount of the top, clear, aqueous phase, without disrupting the interphase, to a fresh 1.5 ml tube.

8. Add 500 µl of isopropanol to the clear phase and mix it by inverting. Incubate tubes for 10 min on ice.

9. Centrifuge the mixture at 12,000 × g for 10 min at 4 °C.

10. Discard the supernatant and wash the pellet twice by adding 1 ml 70 % ethanol, vortexing and centrifugation at 12,000 × g for 10 min at 4 °C.

11. Air-dry the pellet and dissolve it with at least 11 µl DEPC water.

12. Quantify the RNA amounts using spectroscopy and confirm the purity by measuring the absorbance at 230 nm, 260 nm, and 280 nm.

cDNA transcription

13. Transcribe RNA into cDNA using appropriate cDNA transcriptions kits and according to the manufacturer's protocol.

Preparations of qPCR reactions

14. Prepare the master mix containing 5 µl Sybr™ Green reagent, 0.2 µl of both forward and reverse primer (200 nM each), and 3.6 µl DEPC water for each reaction.
    Prepare a master mix, as stated for the appropriate device and Sybr™ Green reagent instructions.

15. Transfer 9 µl of the master mix into each required well of a 96-well plate and add 1 µl of the respective cDNA per well. For the no-template controls, add 1 µl DEPC water.
    Perform reactions in technical triplicates.

16. Seal the plate, spin it briefly in a suitable centrifuge to remove any air bubbles and place it in the qPCR device. Follow the instructions of the device used.

5.3.12. Supporting Protocol 8: Preparations for cytokine release measurements

Cytokine release is a major response mechanism of macrophages. Therefore, the examination of the release into the cell culture supernatant is a promising method to quantify the protein expression.

Despite seeding equal amounts of cells onto scaffolds, a variable number of cells might not attach onto the scaffolds. Thus, the quantification of the cell amounts (here via DNA

content) is needed to allow for the normalization of cytokine release data. Prior to performing a complete ELISA array, appropriate dilutions of the culture media supernatants have to be evaluated. The absorbance of the dilutions should be located in the concurrently determined exponential phase of the standard curve.

Materials

- Scaffolds or well plates containing human macrophages and hMSCs in direct co-culture (see basic protocol 2)
- Scaffolds or well plates containing human macrophages containing (see basic protocol 1)
- Dulbecco's PBS without calcium and magnesium (here: Thermo Fisher Scientific, Waltham, USA)
- Triton X-100
- ELISA array kits (here: Single-Analyte ELISArray Kits, Qiagen, Hilden, Germany)
- Kit for DNA quantification (here: Quant-iT™ PicoGreen® dsDNA Reagent and Kit; Thermo Fisher Scientific, Waltham, USA)
- Plate reader (here: Tecan, Männedorf, Switzerland)

Table 9. Examples of cytokines of different macrophage types

M1	M2
IL-1β	IL-10
TNF-α	TGF-β1
IL-8	IL1-Ra
IL-6	

Sample collection

1. At the time points of interest, collect cell culture supernatants in 1.5 ml tubes for direct use or store them at -20 °C in appropriate aliquots for later use.

Cell lysis for DNA amount determination

2. Lyse the cells by adding 400 µl of 0.1 % Triton X-100 in PBS to each sample and incubate for 1 h at 4 °C. Transfer the lysates into 1.5 ml tubes and store them at -20 °C until DNA quantification.

3. Quantify the DNA amount using a DNA assay according to the manufacturer's protocol.

ELISA preparations

4. Prior to performing a complete ELISA assay, examine the appropriate sample dilutions of the collected culture medium supernatant (Table 6). Dilute samples with the appropriate buffer included in the kit.

Table 10. Sample dilutions for ELISA arrays. One part of the cell culture supernatant is diluted with the stated amount of sample dilution buffer (included in the kit).

Cytokine / Culture condition	IL-8	IL-6
fresh culture media	1:100	1:10
hMSC-conditioned media	1:100	1:100
direct co-culture	1:100	1:100

5. Follow the instructions of the ELISA Kit.

    Perform reactions, at least in technical duplicates.

6. Prepare a suitable working space for washing steps.

    Use absorbent pads and lab tissues.

7. Measure the absorbance using a plate reader. Recipes

5.3.13. Recipes

Macrophage culture medium

- RPMI-1640 medium, GlutaMAX^{TM} (Thermo Fischer Scientific, Waltham, USA)
- 10 % (v/v) platelet lysate (PL Bioscience, Aachen, Germany)
- 100 IU/ml penicillin/100 µg/ml streptomycin (Thermo Fischer Scientific, Waltham, USA)

hMSCs growth medium

- DMEM F-12 GlutaMAX^{TM} (Thermo Fischer Scientific, Waltham, USA)
- 10 % (v/v) FCS (Thermo Fischer Scientific, Waltham, USA)
- 100 IU/ml penicillin/100 µg/ml streptomycin (Thermo Fischer Scientific, Waltham, USA)
- 50 µg/ml L-Ascorbic acid 2-phosphate

DEPC water

- Solution of 1 ml DEPC in 1 L H_2O l [0.1 % DEPC v/v]
- Stir solution overnight at RT and autoclave subsequently

6 % glutaraldehyde

- 24 % glutaraldehyde
- Dulbecco's PBS (Thermo Fischer Scientific, Waltham, USA)

5.4. Representative results

Representative results display macrophages and hMSCs in indirect and direct co-culture on well plates or PCL fiber-based scaffolds with a pore size of 60 μm.

Staining of both macrophages and hMSCs with green and orange cell trackers, respectively, showed the distribution of both cell types in direct co-culture on scaffolds (Figure 30 A). After 72 h an increase of orange-stained hMSCs in the direct co-culture was observed, compared to the co-culture after 24 h. Both cell types show a relatively equal distribution within the scaffolds. Via scanning electron microscopy, cell-cell and cell-material interactions could be observed in high resolution (Figure 30 B). While elongated cells in macrophage mono-cultures on scaffolds were <1 μm thin, on the scaffolds of direct co-cultures, thicker cellular extensions with a diameter up to >1 μm were visible as well. The red fluorescent staining of cells in conditioned media (Figure 30 C.1, C.2) and in direct co-culture (Figure 30 C.3) reflects the expression of CD163 after 24 h. In conditioned media experiments, macrophages were only labeled against CD163, however, after direct co-cultivation, cells were additionally stained against CD45 in green to distinguish them from hMSCs. The counterstaining of the nuclei with DAPI led to the observation that not all macrophages expressed CD163. Moreover, in direct co-culture, also CD45-negative cells (without green fluorescence) showed an expression of CD163. For indirect co-culture experiments, macrophages were either incubated with conditioned cell culture media from hMSCs cultivated on polystyrene (PS) or on PCL-scaffolds (Figure 30 C.1 and C.2, respectively).
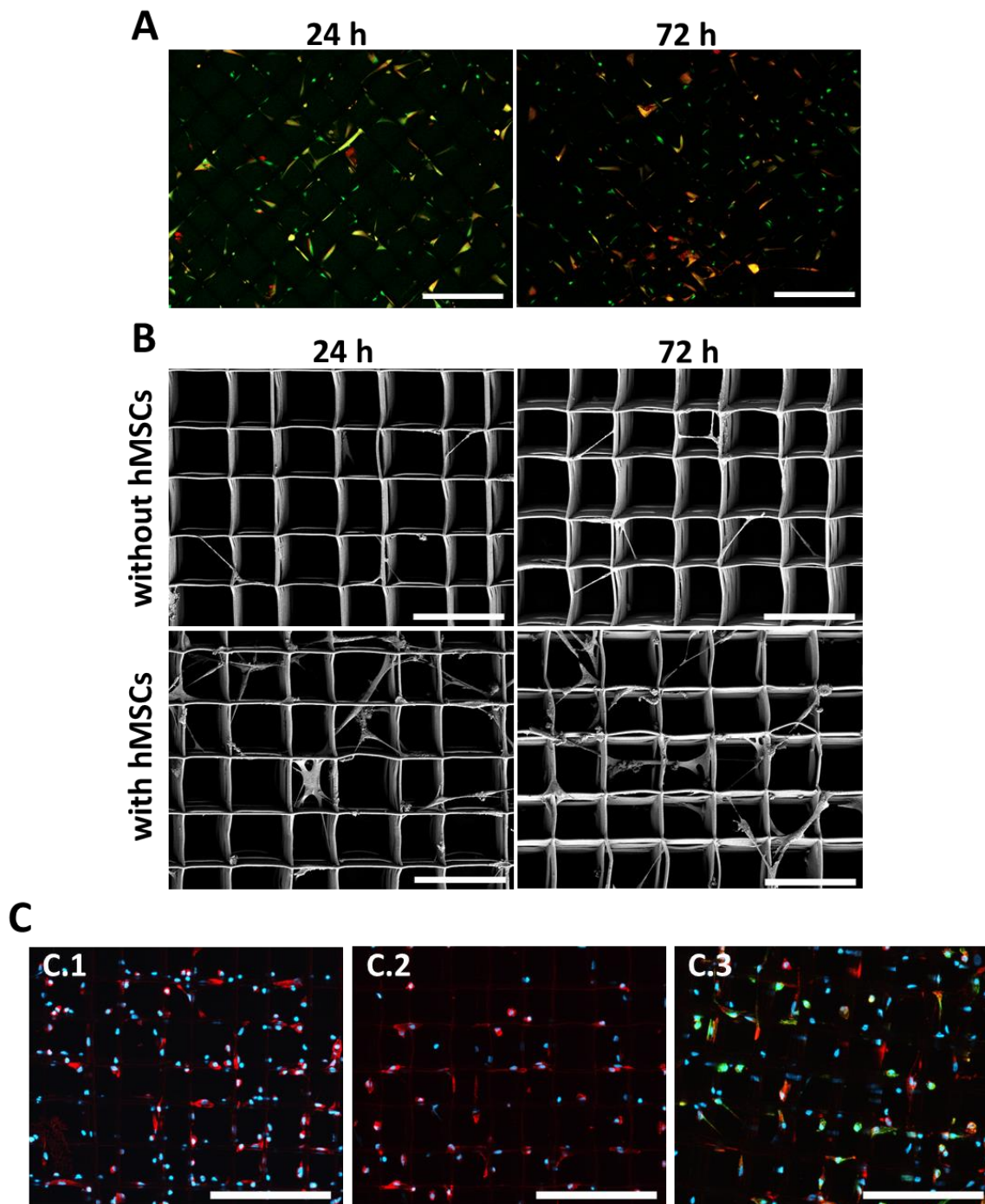
Figure 30. Representative images of the examination of co-culture phenotype via fluorescence microscopy and scanning electron microscopy (basic protocol 3). *(A) Live cell staining of macrophages and hMSCs in direct co-culture with non-transferable cell tracker in green and orange, respectively. (B) Scanning electron microscopy of macrophages in mono- and direct co-culture with hMSCs on PCL scaffolds. (C) Immunofluorescent staining of macrophages on scaffolds in conditioned media of hMSCs on polystyrene (PS) (C.1) and scaffolds (C.2), respectively, as well as of direct co-culture (C.3). A red fluorescence staining indicates CD163 expression. Cells in direct co-culture were additionally stained against CD45 in green. Counterstaining of nuclei was performed with DAPI. Scale bar = 200 µm (A, C); 100 µm (B).*
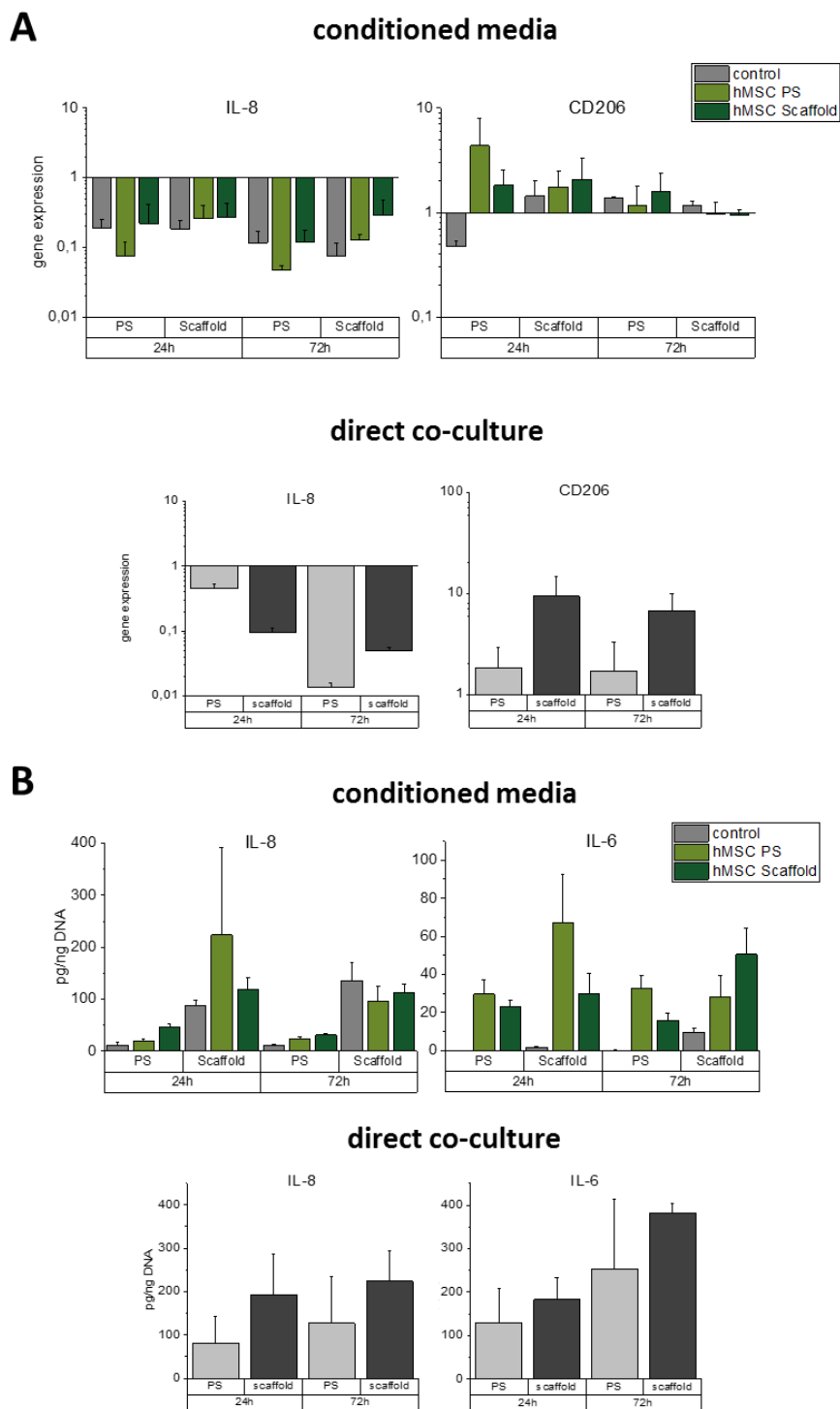
Figure 31. Representative results of the analysis of macrophage response at the molecular level (basic protocol 4). (A) Gene expression of IL-8 and CD206 was determined by qPCR after the indirect and direct co-culture of macrophages and hMSCs on PS or scaffolds. Gene expression was normalized to the housekeeping gene (RPS27a) and to macrophages cultured for 3 h in the control medium. (B) The cytokine release of IL-8 and IL-6 was measured using supernatants of indirect and direct co-culture of macrophages and hMSCs on PS or scaffolds. The amounts of released cytokines were normalized to the DNA content of the corresponding sample. (n = 2) As a blank control, the macrophage culture medium was used.

On the molecular basis, differences in macrophages' response to hMSCs were detectable. The gene expression of IL-8 and CD206, as representative markers for the M1 and M2 macrophage type, respectively, reflected changes depending on the cultivation in conditioned media or in direct co-culture as well as depending on the cultivation on PS or on scaffolds (Figure 31 A). The gene expression data were normalized to the expression levels of macrophages in the control medium after 3 h on the respective material. While in conditioned media, CD206 was more highly expressed on PS than on scaffolds, in direct co-culture, its expression was increased after cultivation on scaffolds. Furthermore, in conditioned media, the impact of hMSCs increased the gene expression of IL-8, especially when they were previously cultured on scaffolds. The lowest gene expression of IL-8 was observed after cultivation in conditioned media and in direct co-culture on PS when compared to the cultivation on scaffolds. In accordance, the cytokine release of IL-8 was higher when macrophages were cultivated on scaffolds (Figure 31 B). Moreover, the release of IL-6 was noticeably higher when macrophages were cultivated with hMSC-conditioned media, compared to those cultivated in fresh macrophage culture medium. When both cell types were cultured on scaffolds (indirect and direct co-culture), the release increased over the culture period.

5.5. Discussion

When new biomaterials are designed, the macrophage response to them is often investigated to get an insight into later *in vivo* processes. The common aim is to create biomaterials with immunomodulatory functions, which improve healing. However, macrophages are not the only cell type in this complex system. Amongst others, adult multipotent mesenchymal stromal cells interact with macrophages in wound healing processes. Therefore, the co-culture of both cell types and the examination of their interplay is a growing research field. However, on biomaterials, the co-culture and, therefore, the interaction of both cell types, and in particular, the consideration of endogenously derived mesenchymal stromal cells (MSCs), is mostly undiscovered. One reason for this might be the relatively complex and elaborate composition of the culture conditions. A defined medium with platelet lysate as serum supplement has been described above (see **Chapter 4**) as an optimal culture medium for both cell types during the intended cultivation period. Based on this, protocols/operating procedures for the cultivation of macrophages and human MSCs (hMSCs) in indirect, i.e., conditioned media-based, and in direct co-culture, on fiber-based melt electrowritten scaffolds have been established.

Furthermore, to analyze the co-culture outcome, detailed operating procedures that allow for the examination of co-culture phenotypes by microscopic techniques and the investigation of macrophage/co-culture expression changes at the molecular level have been developed or adapted. Previously established protocols had only focused on the indirect co-culture on poly styrene (PS) [258] or on the mono-culture of macrophages on biomaterials [259]. Moreover, the establishment of methods for analyses of co-culture setups has mainly been neglected so far. The improvement and the functionality of the microscopic and molecular examination techniques for co-cultures and macrophage phenotypes regarding changes in their morphology and cell activity has been proven by the representative results of basic protocols 3 and 4.

By cell tracker staining and SEM, differences in phenotypes over the culture period as well as by co-culture compared to mono-cultured macrophages were observed. Immunofluorescent imaging showed the importance of double-staining against the leukocyte-specific surface marker CD45 [260] in direct co-cultures: In addition to CD45-positive macrophages, CD45-negative hMSCs also presented CD163 on their surface. This is in accordance with the broad surface marker spectrum of MSCs [261]. At the molecular

level, hMSCs and the scaffolds themselves, as well as in combination, had an impact on macrophages compared to macrophages cultivated under control conditions. The single-factor impact of scaffolds or hMSCs on macrophages has been shown above (**Chapter 2 and 4**). Therefore, the combination of both protocols/procedures promises to be a useful tool to examine processes of the innate immune response in a more *in vivo* reflecting way. Hitherto, only a few studies considered the co-culture of macrophages and MSCs on biomaterials in the context of understanding macrophage responses to newly designed materials and endogenously derived MSCs [235]. In those studies, differences by co-cultivation and material were detected. However, only indirect co-culture experiments and gene expression analyses were performed, and thus, only slight insights into the complex system could be gained. For meaningful statements, further investigation methods are indispensable. In particular, released cytokines should be investigated, since macrophages communicate with other cells in their environment via this mechanism [33].

So far, the established protocols/procedures for direct co-culture comprise one major issue for the examination of single cell type responses: the lack of a technique to separate the different cell types after co-cultivation on the scaffolds. Further experiments should, therefore, focus on the establishment of such detachment protocols/procedures. Thereby, emerging issues are the strong cell attachment to the scaffolds and the fast polarization switch of macrophages due to changes in their environment, such as too long enzymatic incubation or physical and mechanical stress. Thus, an optimal method should be as gentle and as fast as possible.

In conclusion, procedures for the co-culture of human macrophages and hMSCs on fiber-based scaffolds have been successfully established. From now on, they can be used to investigate the influence of various biomaterials differing in material and/or shape on this co-culture system, and hence, they can give a more reliable *in vitro*-prediction of the immunomodulatory properties of the respective biomaterial.

# Chapter 6

Concluding Discussion and Further Perspectives

Concluding Discussion and Further Perspectives

A co-culture system of human macrophages and human mesenchymal stromal cells (hMSCs) for the assessment of the immune response to biomaterials has been successfully established and applied to melt electrowritten (MEW) fiber-based scaffolds. Thereby, an indirect system via conditioned media, as well as a direct co-culture setup, has been proven to be functional.

Prior to performing co-culture experiments in general and on biomaterials, macrophage mono-culture experiments were conducted on MEW fiber-based scaffolds. For this purpose, scaffolds varying in pore geometry and pore size were produced by a co-worker (Carina Blum), and the corresponding macrophage response was examined. Depending on the pore geometry, differences in gene expression of macrophages were observed. Different scaffold geometries and pore sizes have already been reported to influence the polarization of macrophages [13, 163]. The design rationale for the MEW- poly(ε-caprolactone) (PCL) scaffolds used in this thesis was therefore based on these previous observations that porous scaffolds cast en -bloc with a pore size of approximately 40 μm led to the polarization into the pro-healing, M2-like macrophage-type [13, 189]. However, these scaffolds were limited regarding their manufacturing capabilities of different pore geometries and the restricted examination of cellular behavior and morphologies within the scaffolds. In contrast, the most promising MEW scaffolds, based on the gene expression results and the spontaneous polarization of macrophages towards the M2 type, had a box-shaped geometry of 40 μm pore sizes with a fiber diameter of approximately 2 μm. In contrast to former studies, the within this thesis used setup enabled the tracking of the cellular behavior and of the cell-material interactions at any cultivation time point. By additionally using scaffolds with pore sizes from 100 μm to 40 μm, changes in gene expression and cell morphology were detected and suggested an elongation-driven polarization effect towards the M2 type. Here, smaller pores led to an increased elongation behavior and further promoted the macrophage polarization into the pro-healing type (Figure 8; Figure 32).
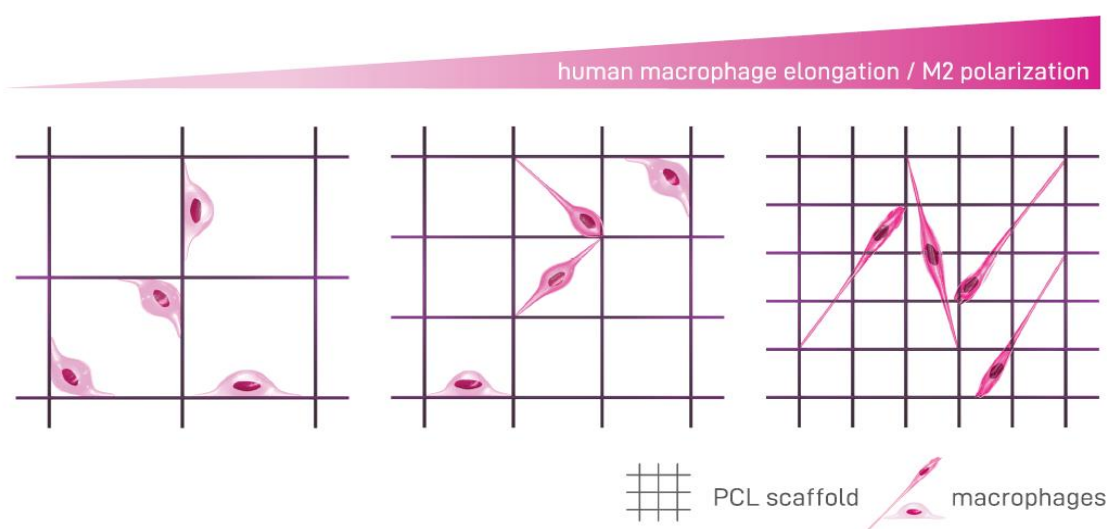
Figure 32. Simplified scheme of macrophage elongation on MEW-PCL fiber-based scaffolds. *While on bigger pores, more roundish macrophages occur, smaller pores lead to an enhanced macrophage elongation and thereby promote M2 polarization.*

Furthermore, when murine macrophages were triggered into an elongated phenotype on 2D micro-structured surfaces [165, 166], the expression and release of M2-related markers and cytokines were increased. Thus, within this thesis, the suggested effect of the cell morphology on macrophage polarization has been further assessed for human macrophages in 3D environments. In addition, the use of scaffolds with decreasing pore sizes provided an explanation for the increased M2 polarization of murine macrophages by culturing on pHEMA sphere template scaffolds with uniform and homogeneously distributed pores around 40 μm in studies of Bryers *et al.* (2012) [13] and Sussman *et al.* (2014) [189].

The results of this thesis suggest that the spontaneous differentiation of macrophages in 3D environments may depend on the triggered cellular morphology. Subsequent experiments should focus on whether this effect is material- or geometry-dependent by assessing the polarization of macrophages to various forms and topographies of biomaterials that could trigger the induction of macrophage elongation.

To achieve a functional co-culture system, several approaches were undertaken. At first, cell-to-cell communication modes in indirect and direct co-culture were identified and have already been published. Here, up to the date of publishing, it has been proven for the first time that during the interaction of macrophages and hMSCs, mitochondria can be transferred from both human macrophages to hMSCs and vice versa and not only from MSCs to macrophages, as it was shown in previous studies [213, 217]. In indirect co-culture, extracellular vesicles (EVs) have been recognized as mediators of communication.

The possibility to transmit mitochondria or other cell organelles by EVs has already been shown in previous studies [262, 263]. In addition, in this work as well as in other studies, tunneling nanotubes (TNTs) have been identified as cellular communication pathways due to the presence of mitochondria within these inter-cellular connections [128, 214]. If mitochondria are transferred from one cell type to another, it can be assumed that also other organelles, proteins or intracellular compartments can pass through the TNTs, and thus, both cell types can properly interact with and respond to each other. This is imperative for a functional co-culture, and particularly for the study of the impact of hMSCs on the macrophage response.

Moreover, an optimized culture medium is mandatory for a co-culture of two or more cell types. Accordingly, within this thesis, several culture media and serum supplements for the cultivation of macrophages and hMSCs were tested. As standard culture medium for human macrophages, RPMI-1640 GlutaMAX^{TM} media supplemented with human serum (hS) is used, while for hMSCs DMEM F-12 GlutaMAX^{TM} media supplemented with 10 % fetal calf serum (FCS) is widely applied. When culturing in RPMI-1640 GlutaMAX^{TM} as culture medium, on suspension plates, as plastic surface and without further differentiation factor, it was observed that neither hS nor FCS are suitable for the other cell type. While in hS an aggregation of hMSCs was detected, in FCS nearly no macrophages adhered (Figure 24). Therefore, the successful culture of either hMSCs in hS [264, 265] or macrophages in FCS [266, 267] described in previous studies may be due to a different culture surface, like tissue culture-treated plastic, or the supplementation with further differentiation factors, such as M-CSF or GM-CSF. Moreover, previously described co-cultures were mostly performed under indirect conditions [102, 268] or for a maximum duration of 24 h [269]. Thus, it could be that the effects of an unadjusted serum supplementation were not recognized. However, by using human platelet lysate (hPL) instead, an optimal serum supplement for both cell types for a more extended co-culture period has been identified within the present thesis. Previous studies have appreciated the potential of PL for the cultivation of MSCs. Thereby compared to FCS-containing media, increased proliferation rates [241] and a similar ability to differentiate into osteoblasts, chondrocytes or adipocytes [15] were observed. In this thesis, the additional potential of hPL as serum supplement for macrophages has been proven with a similar differentiation potential and phenotypical outcome as in hS. Thus, these findings laid the foundation to test for the capability of hPL as serum supplement for the co-culture of both cell types, which has then been confirmed by the maintenance of the phenotypes

as well as the distribution of both cell populations. Furthermore, hMSCs known for their immunomodulating properties that accelerate phagocytic activity of macrophages retained this function in hPL. The positive effect of hPL on both cell types might arise from the cellular interplay of macrophages, hMSCs, and platelets *in vivo* during tissue regeneration processes (Figure 33).
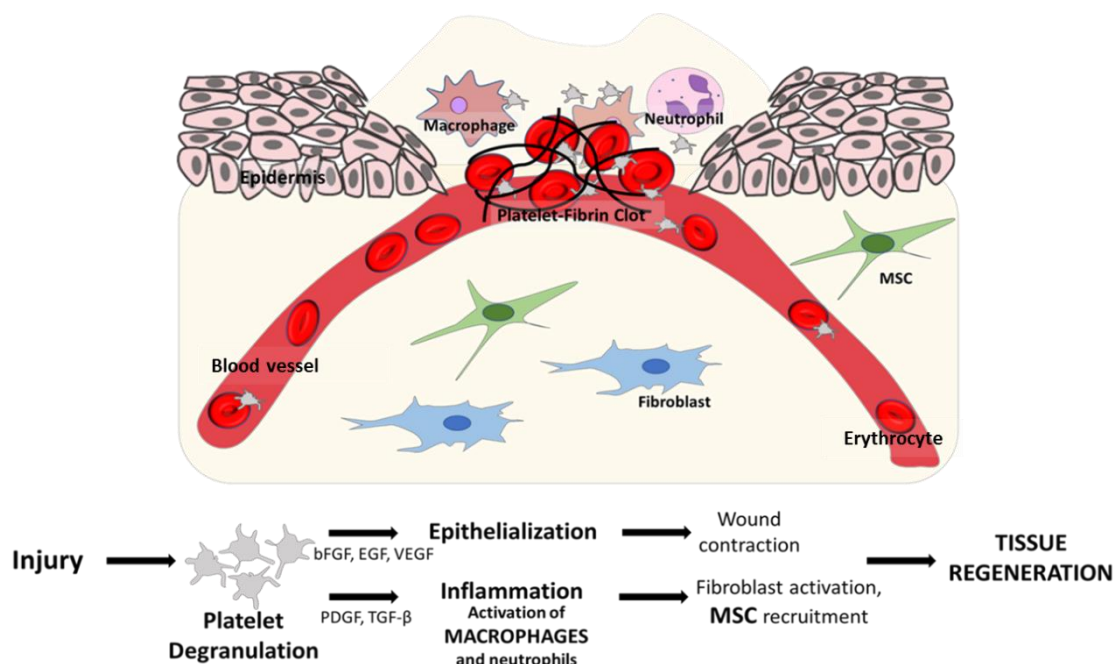
Figure 33. Interplay of platelets, macrophages and MSCs in tissue regeneration. *Redrawn and simplified from reference [14].*

After an injury, circulating platelets from the bloodstream degranulate at the wound site and form together with fibrin a platelet-fibrin clot [270]. Thereby, platelets release various growth factors, which are present in PL as well [14]. These growth factors can on the one side induce the epithelialization of the damaged blood vessels and on the other side induce an inflammation process, mainly determined by monocytes and macrophages [271]. Subsequently, endogenously derived MCSs and fibroblasts are recruited by factors released from macrophages to rebuild the tissue [26]. The course of events within the co-culture that has been established in the present thesis follows a similar order as described for the *in vivo* situation. Accordingly, monocytes were isolated and cultivated for 4 days, as by this time they differentiated via adherence into macrophages. Subsequently, hMSCs were seeded onto the macrophages to analyze the corresponding macrophage response. Moreover, hPL as culture medium supplement closely mimics those *in vivo* events occurring after biomaterial implantation and during

the following regeneration phase that are related to the presence of platelets at the wound site.

In order to examine the macrophage response to biomaterials in a more *in vivo*-related manner, a co-culture setup for the indirect and direct co-cultivation of human macrophages and hMSCs on biomaterials has been established. In the *in vivo* foreign body reaction (Figure 4), numerous cell types are involved, and they specifically interact upon contact with different materials or particles. Although, the co-cultivation of macrophages and hMSCs displays only a small part of this system, the reliability of data generated from these co-cultures likely outperforms the findings obtained from mono-cultures. For this thesis, fiber-based PCL scaffolds with a pore size of 60 µm were chosen on the one hand to prevent excessive monolayer formation of hMSCs occurring on the top surface of scaffolds with smaller pores (detected by Kathrin Knorr in the department, so far unpublished data), which might prevent the proper interaction with macrophages inside the scaffold. On the other hand, bigger pore sizes would be disadvantageous due to the decrease of macrophage M2 polarization. After having established the setup for the co-cultivation on scaffolds, several operating procedures for the examination and analysis of the co-culture phenotype and the macrophage response after co-cultivation have been developed and proven reliable. Until now, only a few studies analyzed the macrophage response after co-cultivation with hMSCs in the context of biomaterial use [235]. The relative high complexity compared to macrophage mono-cultures on materials [272-275] might hinder these strongly needed investigations. To the best of my knowledge, only one operating procedure for macrophage mono-cultivation on biomaterials [259] and one set up for the co-cultivation of macrophages and hMSCs on plastic well plates [258] have been published so far. From now on, the protocols established within the present thesis set the stage for an easier study design and thus will hopefully increase the number of investigations into co-cultures to expand the knowledge in this research area.

Direct follow-up studies to this thesis should examine the macrophage response in co-culture on promising scaffolds, like the MEW-PCL fiber-based scaffolds with 40 µm pore size or on further scaffolds with different geometries and/or topographies causing the macrophage elongation. In addition, the protocols should be further adapted to other kinds of biomaterials, such as cement or hydrogels, to expand the application possibilities for a better assessment of biomaterials in terms of the immune response prior to engrafting.

One issue that should be addressed is the separation of both cell types after co-cultivation on scaffolds. While after cultivation on plastic well plates, both cell types can be easily separated by scraping and subsequent magnetic labeling and isolation [85], on scaffolds, in particular macrophages, adhere strongly and can hardly be detached. Thus, single-cell type analyses are not possible and results of the gene expression and cytokine release display always a mixture of the whole co-culture. Therefore, a suitable separation protocol could improve the examination of single cell type responses. Despite the issue mentioned above with the detachment and separation of different cell types from the scaffolds, *in vivo* cytokines, which are released into the environment, are usually derived from a mixture of different cell types. Thus, in a non-separated co-culture, the overall increase of anti-inflammatory and the decrease of pro-inflammatory genes and cytokines can be considered to resemble a positive effect triggered by the biomaterial properly.

In conclusion, within this thesis, a functional co-culture system of macrophages and hMSCs on biomaterials has been established for an improved assessment of the immune response, compared to the use of macrophage mono-cultures. The functionality has been demonstrated by cell-cell communication, equal distribution of both cell types in the co-culture, and molecular changes in macrophages after co-cultivation on scaffolds. Furthermore, a new design criterion for biomaterials, which focuses on the modulation of human macrophage morphology, has been identified to improve the M2-like polarization of macrophages, which correlated with the adaptation of an elongated macrophage phenotype.

Chapter 7

Summary/Zusammenfassung

7.1. Summary

The outcome of the innate immune response to biomaterials mainly determines whether the material will be incorporated in the body to fulfill its desired function or, when it gets encapsulated, will be rejected in the worst case. Macrophages are key players in this process, and their polarization state with either pro- (M1), anti-inflammatory (M2), or intermediate characteristics is crucial for deciding on the biomaterial's fate. While a transient initial pro-inflammatory state is helpful, a prolonged inflammation deteriorates the proper healing and subsequent regeneration. Therefore, biomaterial-based polarization may aid in driving macrophages in the desired direction. However, the *in vivo* process is highly complex, and a mono-culture of macrophages *in vitro* displays only one part of the cellular system, but, to this date, there is a lack of established co-cultures to assess the immune response to biomaterials. Thus, this thesis aimed to establish a functional co-culture system of human macrophages and human mesenchymal stromal cells (hMSCs) to improve the assessment of the immune response to biomaterials *in vitro.* Together with macrophages, hMSCs are involved in tissue regeneration and inflammatory reactions and can modulate the immune response. In particular, endogenously derived hMSCs considerably contribute to the successful engrafting of biomaterials. This thesis focused on poly(ε-caprolactone) (PCL) fiber-based scaffolds produced by the technique of melt electrowriting (MEW) as biomaterial constructs. Via this fabrication technique, uniform, precisely ordered scaffolds varying in geometry and pore size have been created in-house.

To determine the impact of scaffold geometries and pore sizes on macrophages, mono-cultures incubated on scaffolds were conducted. As a pre-requisite to achieve a functional co-culture system on scaffolds, setups for direct and indirect systems in 2D have initially been established. These setups were analyzed for the capability of cell-cell communication. In parallel, a co-culture medium suitable for both cell types was defined, prior to the establishment of a step-by-step procedure for the co-cultivation of human macrophages and hMSCs on fiber-based scaffolds.

Regarding the scaffold morphologies tested within this thesis to improve M2-like polarization, box-shaped scaffolds outperformed triangular-, round- or disordered-shaped ones. Upon further investigation of scaffolds with box-shaped pores and precise inter-fiber spacing from 100 μm down to only 40 μm, decreasing pore sizes facilitated primary

human macrophage elongation accompanied by their differentiation towards the M2 type, which was most pronounced for the smallest pore size of 40 μm. To the best of my knowledge, this was the first time that the elongation of human macrophages in a 3D environment has been correlated to their M2-like polarization. Thus, these results may set the stage for the design, the assessment, and the selection of new biomaterials, which can positively affect the tissue regeneration.

The cell communication of both cell types, detected via mitochondria exchange in direct and indirect co-cultures systems, took place in both directions, i.e., from hMSCs to macrophages and vice versa. Thereby, in direct co-culture, tunneling nanotubes enabled the transfer from one cell type to the respective other, while in indirect co-culture, a non-directional transfer through extracellular vesicles (EVs) released into the medium seemed likely. Moreover, the phagocytic activity of macrophages after 2D co-cultivation and hence immunomodulation by hMSCs increased with the highest phagocytic rate after 48 h being most pronounced in direct co-cultivation.

As the commonly used serum supplements for macrophages and hMSCs, i.e., human serum (hS) and fetal calf serum (FCS), respectively, failed to support the respective other cell type during prolonged cultivation, these sera were replaced by human platelet lysate (hPL), which has been proven to be the optimal supplement for the co-cultivation of human macrophages with hMSCs within this thesis. Thereby, the phenotype of both cell types, the distribution of both cell populations, the phagocytic activity of macrophages, and the gene expression profiles were maintained and comparable to the respective standard mono-culture conditions. This was even true when hPL was applied without the anticoagulant heparin in all cultures with macrophages, and therefore, heparin was omitted for further experiments comprising hPL and macrophages.

Accordingly, a step-by-step operating procedure for the co-cultivation on fiber-based scaffolds has been established comprising the setup for 3D cultivation as well as the description of methods for the analysis of phenotypical and molecular changes upon contact with the biomaterial. The evaluation of the macrophage response depending on the cultivation with or without hMSCs and either on scaffolds or on plastic surfaces has been successfully achieved and confirmed the functionality of the suggested procedures.

In conclusion, the functional co-culture system of human macrophages and hMSCs established here can now be employed to assess biomaterials in terms of the immune response in a more *in vivo*-related way. Moreover, specifically designed scaffolds used within the present thesis showed auspicious design criteria positively influencing the macrophage polarization towards the anti-inflammatory, pro-healing type and might be adaptable to other biomaterials in future approaches.

Hence, follow-up experiments should focus on the evaluation of the co-culture outcome on promising scaffolds, and the suggested operating procedures should be adjusted to further kinds of biomaterials, such as cements or hydrogels.

7.2. Zusammenfassung

Der Verlauf der angeborene Immunantwort auf Biomaterialien bestimmt maßgebend, ob das Material vom Körper angenommen wird, um so seine gewünschte Funktion zu erfüllen, oder ob es zur Einkapselung und im schlimmsten Fall zur Abstoßung kommt. Makrophagen spielen in diesem Prozess eine Schlüsselrolle, und ihr Polarisationszustand, entweder pro (M1), antiinflammatorisch (M2) oder ein dazwischenliegender Subtyp, ist dabei von entscheidender Bedeutung. Während ein vorübergehender proinflammatorischer Anfangszustand hilfreich ist, verschlechtert eine anhaltende Entzündung eine zeitnahe Heilung und die anschließende Regeneration. Daher könnte eine durch Biomaterialien beeinflusste Polarisation hilfreich sein, um die Makrophagen in die gewünschte Richtung zu lenken. Die *in vivo* Reaktion ist jedoch äußerst komplex und die Kultivierung von Makrophagen *in vitro* stellt nur einen Teil des Prozesses dar. An etablierten Co-Kultursystem zur Untersuchung der immunmodulierenden Eigenschaften von Biomaterialien mangelt es jedoch. Daher war es Ziel dieser Arbeit ein funktionelles Co-Kultursystem von humanen Makrophagen und humanen mesenchymalen Stromazellen (hMSCs) zu etablieren um die *in vitro* Bewertung der Immunantwort nach Kontakt mit Biomaterialien zu verbessern. Von Interesse sind hMSCs hierbei, da sie zusammen mit Makrophagen an der Geweberegeneration und an Entzündungsreaktionen beteiligt sind. Zudem weisen MSCs immunmodulierende Eigenschaften in Hinblick auf Makrophagen auf und sind aktiv am Verlauf der Fremdkörperreaktion nach der Transplantation von Biomaterial beteiligt. Im Rahmen dieser Arbeit wurden Poly(ε-caprolactone) (PCL)-Scaffolds auf Faserbasis als Biomaterialkonstrukte verwendet, welche mit der Technik des Melt Electrowriting (MEW) hergestellt wurden. Mit dieser Technik kann sowohl die Form der Scaffolds als auch die Porengröße variiert werden.

Um Unterschiede der Scaffoldgeometrien und Porengrößen in Hinblick auf die Makrophagenreaktion zu untersuchen, wurden zunächst Versuche mit Makrophagen-Monokulturen durchgeführt. Zur Etablierung eines funktionellen Co-Kultursystem, wurde zu Beginn ein Aufbau für ein direktes und indirektes System in 2D erstellt. Dieser Aufbau wurde anschließend auf die Möglichkeit der Zell-Zell-Kommunikation darin analysiert. Weiterhin wurde ein, für beide Zelltypen, geeignetes Kulturmedium definiert, gefolgt von der Etablierung eines Protokoll für die Co-Kultivierung beider Zelltypen auf faserbasierten Scaffolds.

Im Bezug zu dieser Arbeit wurden Scaffolds mit unterschiedlicher Geometrie mittels der Technik des Melt Electrowriting hergestellt um die Veränderung der Makrophagenpolarisation zu untersuchen. Dabei zeigte sich eine verstärkte M2-Polarisation auf Scaffolds mit einer kastenförmigen Morphologie, verglichen mit dreieckigen, runden oder ungeordnet-strukturierten Scaffolds. Die weitere Untersuchung von Scaffolds mit kastenförmigen Poren und präzisen Faserabständen von 100 μm bis zu 40 μm zeigte das kleinere Porengrößen die Elongation primärer menschlicher Makrophagen förderten. Begleitet wurde die verstärkte Elongation mit einer gesteigerten Polarisation in Richtung des M2 Typs. Dieser Effekt war nach Kultivierung von Makrophagen auf Scaffolds mit 40 μm Poren am stärksten ausgeprägt. Im Rahmen dieser Arbeit konnte damit erstmals eine länglichen Morphologie humaner Makrophagen mit einer Polarisierung in den M2 Typ korreliert werden. Diese Ergebnisse könnten daher für das Design neuer Biomaterialien, welche sich positiv auf die Geweberegeneration auswirken sollen, von Bedeutung sein.

Die Zellkommunikation beider Zelltypen, welche über Mitochondrienaustausch im direkten und indirekten Co-Kultur-System nachgewiesen wurde, fand sowohl ausgehend von Makrophagen als auch von hMSCs statt. Dabei ermöglichten „Tunneling Nanotubes" in der direkten Co-Kultur den Transfer von Mitochondrien von einem Zelltyp zum jeweils anderen, während in der indirekter Co-Kultur ein ungerichteter Transfer durch in das Medium freigesetzte extrazelluläre Vesikel (EVs) stattfand. Darüber hinaus wurde die phagozytotische Aktivität von Makrophagen nach Co-Kultivierung untersucht, um die immunmodulatorischen Eigenschaften von hMSCs nachzuweisen, wobei die höchste phagozytotische Aktivität nach 48 stündiger Co-Kultivierung festgestellt wurde.

Da die üblicherweise verwendeten Serumzusätze für Makrophagen (humanes Serum (hS)) und hMSCs (fötales Kälberserum (FCS)) bei längerer Kultivierung den jeweils anderen Zelltyp nicht unterstützen konnten, wurden diese Seren durch humanes Thrombozytenlysat (hPL) ersetzt. Dieses erwies sich im Rahmen dieser Arbeit als optimale Ergänzung für die gemeinsame Kultivierung beider Zelltypen in der Co-Kultur. Dabei wurden der Phänotyp und die Populationsverteilung beider Zelltypen, sowie die phagozytotische Aktivität und die Veränderung des Genexpressionsprofils von Makrophagen untersucht und mit den jeweiligen Standard-Monokulturbedingungen

verglichen. Des Weiteren konnte gezeigt werde, dass eine Zugabe von Heparin in Zellkulturen mit Makrophagen und hPL nicht nötig ist. Daher wurde auf den Zusatz von Heparin für alle weitere Experimente, die hPL und Makrophagen umfassten, verzichtet.

Im letzten Teil der Arbeit wurde ein Protokoll für die Co-Kultivierung auf MEW Scaffolds erstellt. Neben der Etablierung eines Setups für die 3D-Kultivierung wurden sowohl Protokolle zur Bewertung phänotypischer als auch molekularer Veränderungen entwickelt. Durch Feststellung von Unterschieden in der Makrophagenreaktion in Abhängigkeit zu der Kultivierung mit / ohne hMSCs und entweder auf Scaffolds oder Plastik-Kulturschalen konnte die Funktionalität der Protokolle nachgewiesen werden.

Mit dem in dieser Arbeit etabliertem funktionellen Co-Kultursystem von humanen Makrophagen und hMSCs können zukünftig Biomaterialien mit einem stärkeren *in vivo* - Bezug in Hinblick auf die Immunantwort bewertet werden. Darüber hinaus deuten Ergebnisse auf speziell konstruierte MEW-Scaffolds ein vielversprechendes Designkriterium für neu entwickelte Biomaterialien an, wobei die Polarisation der Makrophagen in Richtung des entzündungshemmenden, heilungsfördernden Typens durch eine gesteuerte Morphologieänderung beeinflusst werden kann.

An diese Arbeit anschließende Experimente sollten sich auf die Untersuchung vielversprechender Scaffolds mittels Co-Kultivierung sowie auf die Anpassung der etablierten Protokolle an andere Biomaterialgruppen, wie beispielsweiße für Zemente oder Hydrogele, konzentrieren.

References

[1] G. Zhou, T. Groth, Host Responses to Biomaterials and Anti-Inflammatory Design—a Brief Review, *Macromolecular Bioscience* **18**, 1800112 (2018).

[2] E. Mariani, G. Lisignoli, R.M. Borzi, L. Pulsatelli, Biomaterials: Foreign Bodies or Tuners for the Immune Response?, *International Journal of Molecular Sciences* **20**, (2019).

[3] J.M. Anderson, A. Rodriguez, D.T. Chang, Foreign body reaction to biomaterials, *Seminars in Immunology* **20**, 86-100 (2008).

[4] A. Mantovani, S.K. Biswas, M.R. Galdiero, A. Sica, M. Locati, Macrophage plasticity and polarization in tissue repair and remodelling, *The Journal of Pathology* **229**, 176-85 (2013).

[5] R. Sridharan, A.R. Cameron, D.J. Kelly, C.J. Kearney, F.J. O'Brien, Biomaterial based modulation of macrophage polarization: a review and suggested design principles, *Materials Today* **18**, 313-325 (2015).

[6] B.N. Brown, B.D. Ratner, S.B. Goodman, S. Amar, S.F. Badylak, Macrophage polarization: an opportunity for improved outcomes in biomaterials and regenerative medicine, *Biomaterials* **33**, 3792-802 (2012).

[7] R.S. Waterman, S.L. Tomchuck, S.L. Henkle, A.M. Betancourt, A New Mesenchymal Stem Cell (MSC) Paradigm: Polarization into a Pro-Inflammatory MSC1 or an Immunosuppressive MSC2 Phenotype, *PLoS One* **5**, e10088 (2010).

[8] K. Le Blanc, D. Mougiakakos, Multipotent mesenchymal stromal cells and the innate immune system, *Nature Reviews Immunology* **12**, 383-96 (2012).

[9] K. Le Blanc, L.C. Davies, Mesenchymal stromal cells and the innate immune response, *Immunology Letters* **168**, 140-6 (2015).

[10] P.D. Dalton, Melt electrowriting with additive manufacturing principles, *Current Opinion in Biomedical Engineering* **2**, 49-57 (2017).

[11] A. Youssef, S.J. Hollister, P.D. Dalton, Additive manufacturing of polymer melts for implantable medical devices and scaffolds, *Biofabrication* **9**, 012002 (2017).

[12] G. Hochleitner, A. Youssef, A. Hrynevich, N. Haigh Jodie, T. Jungst, J. Groll, D. Dalton Paul, Fibre pulsing during melt electrospinning writing, *BioNanoMaterials* **17**, 159 (2016).

[13] J.D. Bryers, C.M. Giachelli, B.D. Ratner, Engineering biomaterials to integrate and heal: the biocompatibility paradigm shifts, *Biotechnology and Bioengineering* **109**, 1898-911 (2012).

[14] T. Burnouf, D. Strunk, M.B.C. Koh, K. Schallmoser, Human platelet lysate: Replacing fetal bovine serum as a gold standard for human cell propagation?, *Biomaterials* **76**, 371-387 (2016).

[15] K. Bieback, Platelet Lysate as Replacement for Fetal Bovine Serum in Mesenchymal Stromal Cell Cultures, *Transfusion Medicine and Hemotherapy* **40**, 326-335 (2013).

[16] H. Hemeda, J. Kalz, G. Walenda, M. Lohmann, W. Wagner, Heparin concentration is critical for cell culture with human platelet lysate, *Cytotherapy* **15**, 1174-1181 (2013).

[17] V. Bruno, J. Svensson-Arvelund, M. Rubér, G. Berg, E. Piccione, M.C. Jenmalm, J. Ernerudh, Effects of low molecular weight heparin on the polarization and cytokine profile of macrophages and T helper cells in vitro, *Scientific Reports* **8**, 4166-4166 (2018).

[18] S.A. Eming, T. Krieg, J.M. Davidson, Inflammation in Wound Repair: Molecular and Cellular Mechanisms, *Journal of Investigative Dermatology* **127**, 514-525 (2007).

References

[19] A.M.D. Herskowitz, D.T.P.M.D. Mangano, Inflammatory Cascade: A Final Common Pathway for Perioperative Injury?, *Anesthesiology: The Journal of the American Society of Anesthesiologists* **85**, 957-960 (1996).

[20] L. Chen, H. Deng, H. Cui, J. Fang, Z. Zuo, J. Deng, Y. Li, X. Wang, L. Zhao, Inflammatory responses and inflammation-associated diseases in organs, *Oncotarget* **9**, 7204-7218 (2017).

[21] G. Han, R. Ceilley, Chronic Wound Healing: A Review of Current Management and Treatments, *Advances in therapy* **34**, 599-610 (2017).

[22] J. Parkin, B. Cohen, An overview of the immune system, *Lancet* **357**, 1777-89 (2001).

[23] D. Artis, J. Tschopp, Innate immunity, *Current Opinion in Immunolgy* **22**, 1-3 (2010).

[24] F.A. Bonilla, H.C. Oettgen, Adaptive immunity, *Journal of Allergy and Clinical Immunology* **125**, S33-40 (2010).

[25] S.A. Eming, P. Martin, M. Tomic-Canic, Wound repair and regeneration: mechanisms, signaling, and translation, *Science translational medicine* **6**, 265-265 (2014).

[26] P. Krzyszczyk, R. Schloss, A. Palmer, F. Berthiaume, The Role of Macrophages in Acute and Chronic Wound Healing and Interventions to Promote Pro-wound Healing Phenotypes, *Frontiers in physiology* **9**, 419 (2018).

[27] F. Geissmann, M.G. Manz, S. Jung, M.H. Sieweke, M. Merad, K. Ley, Development of monocytes, macrophages, and dendritic cells, *Science* **327**, 656-61 (2010).

[28] D. Hirayama, T. Iida, H. Nakase, The Phagocytic Function of Macrophage-Enforcing Innate Immunity and Tissue Homeostasis, *International Journal of Molecular Sciences* **19**, (2017).

[29] F. Merien, A Journey with Elie Metchnikoff: From Innate Cell Mechanisms in Infectious Diseases to Quantum Biology, *Frontiers in Public Health* **4**, 125 (2016).

[30] A. Sica, A. Mantovani, Macrophage plasticity and polarization: *in vivo* veritas, *Journal of Clinical Investigation* **122**, 787-95 (2012).

[31] S. Gordon, F.O. Martinez, Alternative activation of macrophages: mechanism and functions, *Immunity* **32**, 593-604 (2010).

[32] K.W. Yoon, Dead cell phagocytosis and innate immune checkpoint, *BMB Reports* **50**, 496-503 (2017).

[33] G. Arango Duque, A. Descoteaux, Macrophage cytokines: involvement in immunity and infectious diseases, *Frontiers in immunology* **5**, 491-491 (2014).

[34] S.K. Biswas, A. Mantovani, Macrophage plasticity and interaction with lymphocyte subsets: cancer as a paradigm, *Nature Immunology* **11**, 889-96 (2010).

[35] L. Martinez-Pomares, S. Gordon, Antigen presentation the macrophage way, *Cell* **131**, 641-3 (2007).

[36] P. Italiani, D. Boraschi, Development and Functional Differentiation of Tissue-Resident Versus Monocyte-Derived Macrophages in Inflammatory Reactions, *Results and Problems in Cell Differentiation* **62**, 23-43 (2017).

[37] Q. Lahmar, J. Keirsse, D. Laoui, K. Movahedi, E. Van Overmeire, J.A. Van Ginderachter, Tissue-resident versus monocyte-derived macrophages in the tumor microenvironment, *Biochimica et Biophysica Acta* **1865**, 23-34 (2016).

[38] L. Honold, M. Nahrendorf, Resident and Monocyte-Derived Macrophages in Cardiovascular Disease, *Circulation Research* **122**, 113-127 (2018).

[39] L.C. Davies, P.R. Taylor, Tissue-resident macrophages: then and now, *Immunology* **144**, 541-8 (2015).

[40] Y. Zhao, W. Zou, J. Du, Y. Zhao, The origins and homeostasis of monocytes and tissue-resident macrophages in physiological situation, *Journal of Cellular Physiology* **233**, 6425-6439 (2018).

[41] Q. Li, B.A. Barres, Microglia and macrophages in brain homeostasis and disease, *Nature Reviews Immunology* **18**, 225-242 (2018).

[42] B. Allard, A. Panariti, J.G. Martin, Alveolar Macrophages in the Resolution of Inflammation, Tissue Repair, and Tolerance to Infection, *Frontiers in immunology* **9**, 1777 (2018).

[43] L.J. Dixon, M. Barnes, H. Tang, M.T. Pritchard, L.E. Nagy, Kupffer cells in the liver, *Comprehensive Physiology* **3**, 785-97 (2013).

[44] H. Borges da Silva, R. Fonseca, R.M. Pereira, A. Cassado Ados, J.M. Alvarez, M.R. D'Imperio Lima, Splenic Macrophage Subsets and Their Function during Blood-Borne Infections, *Frontiers in immunology* **6**, 480 (2015).

[45] L. Chorro, A. Sarde, M. Li, K.J. Woollard, P. Chambon, B. Malissen, A. Kissenpfennig, J.B. Barbaroux, R. Groves, F. Geissmann, Langerhans cell (LC) proliferation mediates neonatal development, homeostasis, and inflammation-associated expansion of the epidermal LC network, *Journal of Experimental Medicine* **206**, 3089-100 (2009).

[46] K. Kierdorf, M. Prinz, F. Geissmann, E. Gomez Perdiguero, Development and function of tissue resident macrophages in mice, *Seminars in Immunology* **27**, 369-78 (2015).

[47] S. Watanabe, M. Alexander, A.V. Misharin, G.R.S. Budinger, The role of macrophages in the resolution of inflammation, *Journal of Clinical Investigation* **130**, 2619-2628 (2019).

[48] J. Yang, L. Zhang, C. Yu, X.-F. Yang, H. Wang, Monocyte and macrophage differentiation: circulation inflammatory monocyte as biomarker for inflammatory diseases, *Biomarker research* **2**, 1-1 (2014).

[49] J. Chen, M. Li, C. Yang, X. Yin, K. Duan, J. Wang, B. Feng, Macrophage phenotype switch by sequential action of immunomodulatory cytokines from hydrogel layers on titania nanotubes, *Colloids and Surfaces B: Biointerfaces* **163**, 336-345 (2018).

[50] J.L. Pace, S.W. Russell, R.D. Schreiber, A. Altman, D.H. Katz, Macrophage activation: priming activity from a T-cell hybridoma is attributable to interferon-gamma, *PNAS* **80**, 3782-6 (1983).

[51] C.F. Nathan, H.W. Murray, M.E. Wiebe, B.Y. Rubin, Identification of interferon-gamma as the lymphokine that activates human macrophage oxidative metabolism and antimicrobial activity, *Journal of Experimental Medicine* **158**, 670-89 (1983).

[52] A.G. Doyle, G. Herbein, L.J. Montaner, A.J. Minty, D. Caput, P. Ferrara, S. Gordon, Interleukin-13 alters the activation state of murine macrophages in vitro: comparison with interleukin-4 and interferon-gamma, *European Journal of Immunology* **24**, 1441-5 (1994).

[53] M. Stein, S. Keshav, N. Harris, S. Gordon, Interleukin 4 potently enhances murine macrophage mannose receptor activity: a marker of alternative immunologic macrophage activation, *Journal of Experimental Medicine* **176**, 287-92 (1992).

[54] A. Classen, J. Lloberas, A. Celada, Macrophage activation: classical versus alternative, *Methods in Molecular Biology* **531**, 29-43 (2009).

[55] M.H. Manjili, X.Y. Wang, S. Abrams, Evolution of Our Understanding of Myeloid Regulatory Cells: From MDSCs to Mregs, *Frontiers in immunology* **5**, 303 (2014).

[56] B.D. Fleming, D.M. Mosser, Regulatory macrophages: setting the threshold for therapy, *European Journal of Immunology* **41**, 2498-502 (2011).

[57] F.O. Martinez, S. Gordon, The M1 and M2 paradigm of macrophage activation: time for reassessment, *F1000Prime Reports* **6**, 13 (2014).

[58] A. Saradna, D.C. Do, S. Kumar, Q.L. Fu, P. Gao, Macrophage polarization and allergic asthma, *Translational Research* **191**, 1-14 (2018).

References

[59] J. Angsana, J. Chen, L. Liu, C.A. Haller, E.L. Chaikof, Efferocytosis as a regulator of macrophage chemokine receptor expression and polarization, *European Journal of Immunology* **46**, 1592-1599 (2016).

[60] G.S. Selders, A.E. Fetz, M.Z. Radic, G.L. Bowlin, An overview of the role of neutrophils in innate immunity, inflammation and host-biomaterial integration, *Regenerative Biomaterials* **4**, 55-68 (2017).

[61] X. Hu, L.B. Ivashkiv, Cross-regulation of signaling pathways by interferon-gamma: implications for immune responses and autoimmune diseases, *Immunity* **31**, 539-50 (2009).

[62] S.J. Waddell, S.J. Popper, K.H. Rubins, M.J. Griffiths, P.O. Brown, M. Levin, D.A. Relman, Dissecting interferon-induced transcriptional programs in human peripheral blood cells, *PLoS One* **5**, e9753 (2010).

[63] F.O. Martinez, S. Gordon, M. Locati, A. Mantovani, Transcriptional profiling of the human monocyte-to-macrophage differentiation and polarization: new molecules and patterns of gene expression, *Journal of Immunology* **177**, 7303-11 (2006).

[64] X. Wu, W. Xu, X. Feng, Y. He, X. Liu, Y. Gao, S. Yang, Z. Shao, C. Yang, Z. Ye, TNF-a mediated inflammatory macrophage polarization contributes to the pathogenesis of steroid-induced osteonecrosis in mice, *International Journal of Immunopathology and Pharmacology* **28**, 351-61 (2015).

[65] D.C. Lacey, A. Achuthan, A.J. Fleetwood, H. Dinh, J. Roiniotis, G.M. Scholz, M.W. Chang, S.K. Beckman, A.D. Cook, J.A. Hamilton, Defining GM-CSF- and macrophage-CSF-dependent macrophage responses by in vitro models, *Journal of Immunology* **188**, 5752-65 (2012).

[66] H.Y. Tan, N. Wang, S. Li, M. Hong, X. Wang, Y. Feng, The Reactive Oxygen Species in Macrophage Polarization: Reflecting Its Dual Role in Progression and Treatment of Human Diseases, *Oxidative Medicine and Cellular Longevity* **2016**, 2795090 (2016).

[67] N. Wang, H. Liang, K. Zen, Molecular mechanisms that influence the macrophage m1-m2 polarization balance, *Frontiers in immunology* **5**, 614-614 (2014).

[68] F.O. Martinez, L. Helming, R. Milde, A. Varin, B.N. Melgert, C. Draijer, B. Thomas, M. Fabbri, A. Crawshaw, L.P. Ho, N.H. Ten Hacken, V. Cobos Jimenez, N.A. Kootstra, J. Hamann, D.R. Greaves, M. Locati, A. Mantovani, S. Gordon, Genetic programs expressed in resting and IL-4 alternatively activated mouse and human macrophages: similarities and differences, *Blood* **121**, e57-69 (2013).

[69] F.O. Martinez, A. Sica, A. Mantovani, M. Locati, Macrophage activation and polarization, *Frontiers in Bioscience* **13**, 453-61 (2008).

[70] D.A. Chistiakov, Y.V. Bobryshev, N.G. Nikiforov, N.V. Elizova, I.A. Sobenin, A.N. Orekhov, Macrophage phenotypic plasticity in atherosclerosis: The associated features and the peculiarities of the expression of inflammatory genes, *International Journal of Cardiology* **184**, 436-45 (2015).

[71] A. Mantovani, M. Locati, A. Vecchi, S. Sozzani, P. Allavena, Decoy receptors: a strategy to regulate inflammatory cytokines and chemokines, *Trends in Immunology* **22**, 328-36 (2001).

[72] M. Hesse, M. Modolell, A.C. La Flamme, M. Schito, J.M. Fuentes, A.W. Cheever, E.J. Pearce, T.A. Wynn, Differential regulation of nitric oxide synthase-2 and arginase-1 by type 1/type 2 cytokines in vivo: granulomatous pathology is shaped by the pattern of L-arginine metabolism, *Journal of Immunology* **167**, 6533-44 (2001).

[73] M. Modolell, I.M. Corraliza, F. Link, G. Soler, K. Eichmann, Reciprocal regulation of the nitric oxide synthase/arginase balance in mouse bone marrow-derived macrophages by TH1 and TH2 cytokines, *European Journal of Immunology* **25**, 1101-4 (1995).

[74] C.F. Anderson, D.M. Mosser, A novel phenotype for an activated macrophage: the type 2 activated macrophage, *Journal of Leukocyte Biology* **72**, 101-6 (2002).

[75] C.F. Anderson, D.M. Mosser, Cutting edge: biasing immune responses by directing antigen to macrophage Fc gamma receptors, *Journal of Immunology* **168**, 3697-701 (2002).

[76] A.F. Valledor, M. Ricote, Nuclear receptor signaling in macrophages, *Biochemical Pharmacology* **67**, 201-12 (2004).

[77] A. Shapouri-Moghaddam, S. Mohammadian, H. Vazini, M. Taghadosi, S.A. Esmaeili, F. Mardani, B. Seifi, A. Mohammadi, J.T. Afshari, A. Sahebkar, Macrophage plasticity, polarization, and function in health and disease, *Journal of Cellular Physiology* **233**, 6425-6440 (2018).

[78] G. Zizzo, B.A. Hilliard, M. Monestier, P.L. Cohen, Efficient clearance of early apoptotic cells by human macrophages requires M2c polarization and MerTK induction, *Journal of Immunology* **189**, 3508-20 (2012).

[79] Q. Wang, H. Ni, L. Lan, X. Wei, R. Xiang, Y. Wang, Fra-1 protooncogene regulates IL-6 expression in macrophages and promotes the generation of M2d macrophages, *Cell Research* **20**, 701-12 (2010).

[80] A. Mantovani, S. Sozzani, M. Locati, P. Allavena, A. Sica, Macrophage polarization: tumor-associated macrophages as a paradigm for polarized M2 mononuclear phagocytes, *Trends in Immunology* **23**, 549-55 (2002).

[81] A. Mantovani, P. Allavena, A. Sica, Tumour-associated macrophages as a prototypic type II polarised phagocyte population: role in tumour progression, *European Journal of Cancer* **40**, 1660-7 (2004).

[82] J. Condeelis, J.W. Pollard, Macrophages: obligate partners for tumor cell migration, invasion, and metastasis, *Cell* **124**, 263-6 (2006).

[83] C.J. Ferrante, G. Pinhal-Enfield, G. Elson, B.N. Cronstein, G. Hasko, S. Outram, S.J. Leibovich, The adenosine-dependent angiogenic switch of macrophages to an M2-like phenotype is independent of interleukin-4 receptor alpha (IL-4Ralpha) signaling, *Inflammation* **36**, 921-31 (2013).

[84] S. Eligini, M. Crisci, E. Bono, P. Songia, E. Tremoli, G.I. Colombo, S. Colli, Human monocyte-derived macrophages spontaneously differentiated in vitro show distinct phenotypes, *Journal of Cellular Physiology* **228**, 1464-1472 (2013).

[85] T. Tylek, T. Schilling, K. Schlegelmilch, M. Ries, M. Rudert, F. Jakob, J. Groll, Platelet lysate outperforms FCS and human serum for co-culture of primary human macrophages and hMSCs, *Scientific Reports* **9**, 3533 (2019).

[86] A. Keating, Mesenchymal stromal cells, *Current Opinion in Hematology* **13**, 419-25 (2006).

[87] E.M. Horwitz, A. Keating, Nonhematopoietic mesenchymal stem cells: what are they?, *Cytotherapy* **2**, 387-8 (2000).

[88] E.M. Horwitz, K. Le Blanc, M. Dominici, I. Mueller, I. Slaper-Cortenbach, F.C. Marini, R.J. Deans, D.S. Krause, A. Keating, T. International Society for Cellular, Clarification of the nomenclature for MSC: The International Society for Cellular Therapy position statement, *Cytotherapy* **7**, 393-5 (2005).

[89] F.J. Lv, R.S. Tuan, K.M. Cheung, V.Y. Leung, Concise review: the surface markers and identity of human mesenchymal stem cells, *Stem Cells* **32**, 1408-19 (2014).

[90] U. Noth, L. Rackwitz, A. Heymer, M. Weber, B. Baumann, A. Steinert, N. Schutze, F. Jakob, J. Eulert, Chondrogenic differentiation of human mesenchymal stem cells in collagen type I hydrogels, *Journal of Biomedical Materials Research Part A* **83**, 626-35 (2007).

[91] Y.A. Romanov, A.N. Darevskaya, N.V. Merzlikina, L.B. Buravkova, Mesenchymal stem cells from human bone marrow and adipose tissue: isolation, characterization, and differentiation potentialities, *Bulletin of Experimental Biology and Medicine* **140**, 138-43 (2005).

References

[92] K. Baghaei, S.M. Hashemi, S. Tokhanbigli, A. Asadi Rad, H. Assadzadeh-Aghdaei, A. Sharifian, M.R. Zali, Isolation, differentiation, and characterization of mesenchymal stem cells from human bone marrow, *Gastroenterology and Hepatology from Bed to Bench* **10**, 208-213 (2017).

[93] M.J. Hoogduijn, Are mesenchymal stromal cells immune cells?, *Arthritis research & therapy* **17**, 88-88 (2015).

[94] K. Le Blanc, C. Tammik, K. Rosendahl, E. Zetterberg, O. Ringden, HLA expression and immunologic properties of differentiated and undifferentiated mesenchymal stem cells, *Experimental Hematology* **31**, 890-6 (2003).

[95] M.E. Bernardo, W.E. Fibbe, Mesenchymal stromal cells: sensors and switchers of inflammation, *Cell Stem Cell* **13**, 392-402 (2013).

[96] V. Ulivi, R. Tasso, R. Cancedda, F. Descalzi, Mesenchymal stem cell paracrine activity is modulated by platelet lysate: induction of an inflammatory response and secretion of factors maintaining macrophages in a proinflammatory phenotype, *Stem Cells and Development* **23**, 1858-69 (2014).

[97] J.M. Brown, K. Nemeth, N.M. Kushnir-Sukhov, D.D. Metcalfe, E. Mezey, Bone marrow stromal cells inhibit mast cell function via a COX2-dependent mechanism, *Clinical & Experimental Allergy* **41**, 526-34 (2011).

[98] L. Chen, E.E. Tredget, P.Y. Wu, Y. Wu, Paracrine factors of mesenchymal stem cells recruit macrophages and endothelial lineage cells and enhance wound healing, *PLoS One* **3**, e1886 (2008).

[99] G.M. Spaggiari, A. Capobianco, S. Becchetti, M.C. Mingari, L. Moretta, Mesenchymal stem cell-natural killer cell interactions: evidence that activated NK cells are capable of killing MSCs, whereas MSCs can inhibit IL-2-induced NK-cell proliferation, *Blood* **107**, 1484 (2006).

[100] E. R. Andreeva, L. Buravkova, The Role of Interplay of Mesenchymal Stromal Cells and Macrophages in Physiological and Reparative Tissue Remodeling, (2018).

[101] K. Anton, D. Banerjee, J. Glod, Macrophage-associated mesenchymal stem cells assume an activated, migratory, pro-inflammatory phenotype with increased IL-6 and CXCL10 secretion, *PLoS One* **7**, e35036 (2012).

[102] J. Kim, P. Hematti, Mesenchymal stem cell-educated macrophages: a novel type of alternatively activated macrophages, *Experimental Hematology* **37**, 1445-53 (2009).

[103] E. Eggenhofer, M.J. Hoogduijn, Mesenchymal stem cell-educated macrophages, *Transplantation Research* **1**, 12 (2012).

[104] F. Carty, B.P. Mahon, K. English, The influence of macrophages on mesenchymal stromal cell therapy: passive or aggressive agents?, *Clinical and Experimental Immunology* **188**, 1-11 (2017).

[105] J. Maggini, G. Mirkin, I. Bognanni, J. Holmberg, I.M. Piazzon, I. Nepomnaschy, H. Costa, C. Canones, S. Raiden, M. Vermeulen, J.R. Geffner, Mouse bone marrow-derived mesenchymal stromal cells turn activated macrophages into a regulatory-like profile, *PLoS One* **5**, e9252 (2010).

[106] L. Chiossone, R. Conte, G.M. Spaggiari, M. Serra, C. Romei, F. Bellora, F. Becchetti, A. Andaloro, L. Moretta, C. Bottino, Mesenchymal Stromal Cells Induce Peculiar Alternatively Activated Macrophages Capable of Dampening Both Innate and Adaptive Immune Responses, *Stem Cells* **34**, 1909-21 (2016).

[107] H. Choi, R.H. Lee, N. Bazhanov, J.Y. Oh, D.J. Prockop, Anti-inflammatory protein TSG-6 secreted by activated MSCs attenuates zymosan-induced mouse peritonitis by decreasing TLR2/NF-kappaB signaling in resident macrophages, *Blood* **118**, 330-8 (2011).

[108] C. Brown, C. McKee, S. Bakshi, K. Walker, E. Hakman, S. Halassy, D. Svinarich, R. Dodds, C.K. Govind, G.R. Chaudhry, Mesenchymal Stem Cells: Cell Therapy and Regeneration Potential, *Journal of Tissue Engineering and Regenerative Medicine*, (2019).

[109] B. Lukomska, L. Stanaszek, E. Zuba-Surma, P. Legosz, S. Sarzynska, K. Drela, Challenges and Controversies in Human Mesenchymal Stem Cell Therapy, *Stem Cells International* **2019**, 9628536 (2019).

[110] J.A. Ankrum, J.F. Ong, J.M. Karp, Mesenchymal stem cells: immune evasive, not immune privileged, *Nature Biotechnology* **32**, 252-60 (2014).

[111] E. Andreeva, P. Bobyleva, A. Gornostaeva, L. Buravkova, Interaction of multipotent mesenchymal stromal and immune cells: Bidirectional effects, *Cytotherapy* **19**, 1152-1166 (2017).

[112] T.A. Wynn, Fibrotic disease and the T(H)1/T(H)2 paradigm, *Nature Reviews Immunology* **4**, 583-94 (2004).

[113] D.O. Freytes, J.W. Kang, I. Marcos-Campos, G. Vunjak-Novakovic, Macrophages modulate the viability and growth of human mesenchymal stem cells, *Journal of Cellular Biochemistry* **114**, 220-9 (2013).

[114] E. Chung, Y. Son, Crosstalk between mesenchymal stem cells and macrophages in tissue repair, *Tissue Engineering and Regenerative Medicine* **11**, 431-438 (2014).

[115] C. Shi, T. Jia, S. Mendez-Ferrer, T.M. Hohl, N.V. Serbina, L. Lipuma, I. Leiner, M.O. Li, P.S. Frenette, E.G. Pamer, Bone marrow mesenchymal stem and progenitor cells induce monocyte emigration in response to circulating toll-like receptor ligands, *Immunity* **34**, 590-601 (2011).

[116] E. Fennema, N. Rivron, J. Rouwkema, C. van Blitterswijk, J. de Boer, Spheroid culture as a tool for creating 3D complex tissues, *Trends in Biotechnology* **31**, 108-115 (2013).

[117] L. Goers, P. Freemont, K.M. Polizzi, Co-culture systems and technologies: taking synthetic biology to the next level, *Journal of the Royal Society. Interface* **11**, (2014).

[118] C. Moraes, G. Mehta, S.C. Lesher-Perez, S. Takayama, Organs-on-a-chip: a focus on compartmentalized microdevices, *Annals of Biomedical Engineering* **40**, 1211-27 (2012).

[119] Y. Tanouchi, R.P. Smith, L. You, Engineering microbial systems to explore ecological and evolutionary dynamics, *Current Opinion in Biotechnology* **23**, 791-7 (2012).

[120] S. Cottet, I. Corthesy-Theulaz, F. Spertini, B. Corthesy, Microaerophilic conditions permit to mimic in vitro events occurring during in vivo Helicobacter pylori infection and to identify Rho/Ras-associated proteins in cellular signaling, *Journal of Biological Chemistry* **277**, 33978-86 (2002).

[121] K. Hatherell, P.-O. Couraud, I.A. Romero, B. Weksler, G.J. Pilkington, Development of a three-dimensional, all-human in vitro model of the blood–brain barrier using mono-, co-, and tri-cultivation Transwell models, *Journal of Neuroscience Methods* **199**, 223-229 (2011).

[122] S.J. Bidarra, C.C. Barrias, M.A. Barbosa, R. Soares, J. Amedee, P.L. Granja, Phenotypic and proliferative modulation of human mesenchymal stem cells via crosstalk with endothelial cells, *Stem Cell Research* **7**, 186-97 (2011).

[123] K. McCoy-Simandle, S.J. Hanna, D. Cox, Exosomes and nanotubes: Control of immune cell communication, *The International Journal of Biochemistry & Cell Biology* **71**, 44-54 (2016).

[124] A. Coondoo, Cytokines in dermatology - a basic overview, *Indian Journal of Dermatology* **56**, 368-74 (2011).

[125] D.M. Davis, M.L. Dustin, What is the importance of the immunological synapse?, *Trends in Immunology* **25**, 323-7 (2004).

References

[126] J.C. Saez, V.M. Berthoud, M.C. Branes, A.D. Martinez, E.C. Beyer, Plasma membrane channels formed by connexins: their regulation and functions, *Physiological Reviews* **83**, 1359-400 (2003).

[127] E.R. Abels, X.O. Breakefield, Introduction to Extracellular Vesicles: Biogenesis, RNA Cargo Selection, Content, Release, and Uptake, *Cellular and Molecular Neurobiology* **36**, 301-12 (2016).

[128] T. Tylek, K. Schlegelmilch, A. Ewald, M. Rudert, F. Jakob, J. Groll, Cell communication modes and bidirectional mitochondrial exchange in direct and indirect macrophage/hMSC co-culture models, *BioNanoMaterials* **18**, (2017).

[129] K.P. Hough, J.L. Trevor, J.G. Strenkowski, Y. Wang, B.K. Chacko, S. Tousif, D. Chanda, C. Steele, V.B. Antony, T. Dokland, X. Ouyang, J. Zhang, S.R. Duncan, V.J. Thannickal, V.M. Darley-Usmar, J.S. Deshane, Exosomal transfer of mitochondria from airway myeloid-derived regulatory cells to T cells, *Redox Biology* **18**, 54-64 (2018).

[130] M.N. Islam, S.R. Das, M.T. Emin, M. Wei, L. Sun, K. Westphalen, D.J. Rowlands, S.K. Quadri, S. Bhattacharya, J. Bhattacharya, Mitochondrial transfer from bone-marrow-derived stromal cells to pulmonary alveoli protects against acute lung injury, *Nature Medicine* **18**, 759-65 (2012).

[131] F. Figeac, P.F. Lesault, O. Le Coz, T. Damy, R. Souktani, C. Trebeau, A. Schmitt, J. Ribot, R. Mounier, A. Guguin, C. Manier, M. Surenaud, L. Hittinger, J.L. Dubois-Rande, A.M. Rodriguez, Nanotubular crosstalk with distressed cardiomyocytes stimulates the paracrine repair function of mesenchymal stem cells, *Stem Cells* **32**, 216-30 (2014).

[132] B. Önfelt, S. Nedvetzki, R.K.P. Benninger, M.A. Purbhoo, S. Sowinski, A.N. Hume, M.C. Seabra, M.A.A. Neil, P.M.W. French, D.M. Davis, Structurally Distinct Membrane Nanotubes between Human Macrophages Support Long-Distance Vesicular Traffic or Surfing of Bacteria, *The Journal of Immunology* **177**, 8476-8483 (2006).

[133] H.-H. Gerdes, N.V. Bukoreshtliev, J.F.V. Barroso, Tunneling nanotubes: A new route for the exchange of components between animal cells, *FEBS Letters* **581**, 2194-2201 (2007).

[134] J. Ariazi, A. Benowitz, V. De Biasi, M.L. Den Boer, S. Cherqui, H. Cui, N. Douillet, E.A. Eugenin, D. Favre, S. Goodman, K. Gousset, D. Hanein, D.I. Israel, S. Kimura, R.B. Kirkpatrick, N. Kuhn, C. Jeong, E. Lou, R. Mailliard, S. Maio, G. Okafo, M. Osswald, J. Pasquier, R. Polak, G. Pradel, B. de Rooij, P. Schaeffer, V.A. Skeberdis, I.F. Smith, A. Tanveer, N. Volkmann, Z. Wu, C. Zurzolo, Tunneling Nanotubes and Gap Junctions-Their Role in Long-Range Intercellular Communication during Development, Health, and Disease Conditions, *Frontiers in molecular neuroscience* **10**, 333-333 (2017).

[135] A. Rustom, R. Saffrich, I. Markovic, P. Walther, H.H. Gerdes, Nanotubular highways for intercellular organelle transport, *Science* **303**, 1007-10 (2004).

[136] Z. Sheikh, P.J. Brooks, O. Barzilay, N. Fine, M. Glogauer, Macrophages, Foreign Body Giant Cells and Their Response to Implantable Biomaterials, *Materials* **8**, 5671-5701 (2015).

[137] A. Robert, J. Latour, Biomaterials: protein-surface interactions, (2008).

[138] M.D. Swartzlander, C.A. Barnes, A.K. Blakney, J.L. Kaar, T.R. Kyriakides, S.J. Bryant, Linking the foreign body response and protein adsorption to PEG-based hydrogels using proteomics, *Biomaterials* **41**, 26-36 (2015).

[139] T.H. Barker, A.J. Engler, The provisional matrix: setting the stage for tissue repair outcomes, *Matrix Biology* **60-61**, 1-4 (2017).

[140] S. Jhunjhunwala, S. Aresta-DaSilva, K. Tang, D. Alvarez, M.J. Webber, B.C. Tang, D.M. Lavin, O. Veiseh, J.C. Doloff, S. Bose, A. Vegas, M. Ma, G. Sahay, A. Chiu, A. Bader, E. Langan, S. Siebert, J. Li, D.L. Greiner, P.E. Newburger, U.H. von Andrian, R. Langer, D.G. Anderson, Neutrophil Responses to Sterile Implant Materials, *PLoS One* **10**, e0137550 (2015).

[141] B. Ode Boni, L. Lamboni, T. Souho, M. Gauthier, G. Yang, Immunomodulation and Cellular Response to Biomaterials: The Overriding Role of Neutrophils in Healing, (2019).

[142] H.F. Penaloza, P.A. Nieto, N. Munoz-Durango, F.J. Salazar-Echegarai, J. Torres, M.J. Parga, M. Alvarez-Lobos, C.A. Riedel, A.M. Kalergis, S.M. Bueno, Interleukin-10 plays a key role in the modulation of neutrophils recruitment and lung inflammation during infection by Streptococcus pneumoniae, *Immunology* **146**, 100-12 (2015).

[143] O. Soehnlein, S. Steffens, A. Hidalgo, C. Weber, Neutrophils as protagonists and targets in chronic inflammation, *Nature Reviews Immunology* **17**, 248 (2017).

[144] K.R. Martin, D. Ohayon, V. Witko-Sarsat, Promoting apoptosis of neutrophils and phagocytosis by macrophages: novel strategies in the resolution of inflammation, *Swiss Medical Weekly* **145**, w14056 (2015).

[145] M.C. Greenlee-Wacker, Clearance of apoptotic neutrophils and resolution of inflammation, *Immunological Reviews* **273**, 357-70 (2016).

[146] R.G. Ferreira, T.C. Matsui, A.M. Godin, L.F. Gomides, P.E.M. Pereira-Silva, I.D.G. Duarte, G.B. Menezes, M.M. Coelho, A. Klein, Neutrophil recruitment is inhibited by nicotinamide in experimental pleurisy in mice, *European Journal of Pharmacology* **685**, 198-204 (2012).

[147] S. Gordon, Phagocytosis: An Immunobiologic Process, *Immunity* **44**, 463-475 (2016).

[148] A. Haas, The phagosome: compartment with a license to kill, *Traffic* **8**, 311-30 (2007).

[149] R.F. Diegelmann, M.C. Evans, Wound healing: an overview of acute, fibrotic and delayed healing, *Frontiers in Bioscience* **9**, 283-9 (2004).

[150] B.D. Ratner, Reducing capsular thickness and enhancing angiogenesis around implant drug release systems, *Journal of Controlled Release* **78**, 211-8 (2002).

[151] T. Oviedo-Socarras, A.C. Vasconcelos, I.X. Barbosa, N.B. Pereira, P.P. Campos, S.P. Andrade, Diabetes alters inflammation, angiogenesis, and fibrogenesis in intraperitoneal implants in rats, *Microvascular Research* **93**, 23-9 (2014).

[152] N. Fujiwara, K. Kobayashi, Macrophages in inflammation, *Current Drug Targets - Inflammation & Allergy* **4**, 281-6 (2005).

[153] V. Ballotta, A. Driessen-Mol, C.V. Bouten, F.P. Baaijens, Strain-dependent modulation of macrophage polarization within scaffolds, *Biomaterials* **35**, 4919-28 (2014).

[154] A. McEvoy, M. Jeyam, G. Ferrier, C.E. Evans, J.G. Andrew, Synergistic effect of particles and cyclic pressure on cytokine production in human monocyte/macrophages: proposed role in periprosthetic osteolysis, *Bone* **30**, 171-7 (2002).

[155] A.J. Garcia, M.D. Vega, D. Boettiger, Modulation of cell proliferation and differentiation through substrate-dependent changes in fibronectin conformation, *Molecular Biology of the Cell* **10**, 785-98 (1999).

[156] J. Kajahn, S. Franz, E. Rueckert, I. Forstreuter, V. Hintze, S. Moeller, J.C. Simon, Artificial extracellular matrices composed of collagen I and high sulfated hyaluronan modulate monocyte to macrophage differentiation under conditions of sterile inflammation, *Biomatter* **2**, 226-36 (2012).

[157] B.N. Brown, R. Londono, S. Tottey, L. Zhang, K.A. Kukla, M.T. Wolf, K.A. Daly, J.E. Reing, S.F. Badylak, Macrophage phenotype as a predictor of constructive remodeling following the implantation of biologically derived surgical mesh materials, *Acta biomaterialia* **8**, 978-987 (2012).

[158] L. Huleihel, J.L. Dziki, J.G. Bartolacci, T. Rausch, M.E. Scarritt, M.C. Cramer, T. Vorobyov, S.T. LoPresti, I.T. Swineheart, L.J. White, B.N. Brown, S.F. Badylak, Macrophage phenotype in response to ECM bioscaffolds, *Seminars in Immunology* **29**, 2-13 (2017).

References

[159] H. Cheng, X. Fan, C. Wu, X. Wang, L.-J. Wang, X.J. Loh, Z. Li, Y.-L. Wu, Cyclodextrin-Based Star-Like Amphiphilic Cationic Polymer as a Potential Pharmaceutical Carrier in Macrophages, *Macromolecular Rapid Communications* **40**, 1800207 (2019).

[160] H. Sun, X. Wang, X. Hu, W. Yu, C. You, H. Hu, C. Han, Promotion of angiogenesis by sustained release of rhGM-CSF from heparinized collagen/chitosan scaffolds, *Journal of Biomedical Materials Research Part B: Applied Biomaterials* **100**, 788-98 (2012).

[161] C.L. Yang, Y.H. Sun, W.H. Yu, X.Z. Yin, J. Weng, B. Feng, Modulation of macrophage phenotype through controlled release of interleukin-4 from gelatine coatings on titanium surfaces, *European Cells & Materials* **36**, 15-29 (2018).

[162] V.S. Meli, P.K. Veerasubramanian, H. Atcha, Z. Reitz, T.L. Downing, W.F. Liu, Biophysical regulation of macrophages in health and disease, *Journal of Leukocyte Biology*, (2019).

[163] C.R. Almeida, T. Serra, M.I. Oliveira, J.A. Planell, M.A. Barbosa, M. Navarro, Impact of 3-D printed PLA- and chitosan-based scaffolds on human monocyte/macrophage responses: unraveling the effect of 3-D structures on inflammation, *Acta biomaterialia* **10**, 613-22 (2014).

[164] S. Chen, J.A. Jones, Y. Xu, H.Y. Low, J.M. Anderson, K.W. Leong, Characterization of topographical effects on macrophage behavior in a foreign body response model, *Biomaterials* **31**, 3479-91 (2010).

[165] F.Y. McWhorter, C.T. Davis, W.F. Liu, Physical and mechanical regulation of macrophage phenotype and function, *Cellular and Molecular Life Sciences* **72**, 1303-16 (2015).

[166] F.Y. McWhorter, T. Wang, P. Nguyen, T. Chung, W.F. Liu, Modulation of macrophage phenotype by cell shape, *PNAS* **110**, 17253-8 (2013).

[167] D.W. Hutmacher, P.D. Dalton, Melt Electrospinning, *Chemistry – An Asian Journal* **6**, 44-56 (2011).

[168] M.L. Muerza-Cascante, D. Haylock, D.W. Hutmacher, P.D. Dalton, Melt electrospinning and its technologization in tissue engineering, *Tissue Engineering Part B: Reviews* **21**, 187-202 (2015).

[169] R. McMaster, C. Hoefner, A. Hrynevich, C. Blum, M. Wiesner, K. Wittmann, T.R. Dargaville, P. Bauer-Kreisel, J. Groll, P.D. Dalton, T. Blunk, Tailored Melt Electrowritten Scaffolds for the Generation of Sheet-Like Tissue Constructs from Multicellular Spheroids, *Adv Healthc Mater*, 1801326 (2019).

[170] A. Hrynevich, B.S. Elci, J.N. Haigh, R. McMaster, A. Youssef, C. Blum, T. Blunk, G. Hochleitner, J. Groll, P.D. Dalton, Dimension-Based Design of Melt Electrowritten Scaffolds, *Small* **14**, 1800232 (2018).

[171] G. Hochleitner, T. Jungst, T.D. Brown, K. Hahn, C. Moseke, F. Jakob, P.D. Dalton, J. Groll, Additive manufacturing of scaffolds with sub-micron filaments via melt electrospinning writing, *Biofabrication* **7**, 035002 (2015).

[172] B.L. Farrugia, T.D. Brown, Z. Upton, D.W. Hutmacher, P.D. Dalton, T.R. Dargaville, Dermal fibroblast infiltration of poly(epsilon-caprolactone) scaffolds fabricated by melt electrospinning in a direct writing mode, *Biofabrication* **5**, 025001 (2013).

[173] T.D. Brown, F. Edin, N. Detta, A.D. Skelton, D.W. Hutmacher, P.D. Dalton, Melt electrospinning of poly(ε-caprolactone) scaffolds: Phenomenological observations associated with collection and direct writing, *Materials Science and Engineering: C* **45**, 698-708 (2014).

[174] A. Vishwakarma, N.S. Bhise, M.B. Evangelista, J. Rouwkema, M.R. Dokmeci, A.M. Ghaemmaghami, N.E. Vrana, A. Khademhosseini, Engineering Immunomodulatory Biomaterials To Tune the Inflammatory Response, *Trends in Biotechnology* **34**, 470-482 (2016).

[175] J.M. Anderson, Biological Responses to Materials, *Annual Review of Materials Research* **31**, 81-110 (2001).

[176] A. Mantovani, A. Sica, S. Sozzani, P. Allavena, A. Vecchi, M. Locati, The chemokine system in diverse forms of macrophage activation and polarization, *Trends in Immunology* **25**, 677-86 (2004).

[177] S. Recalcati, M. Locati, A. Marini, P. Santambrogio, F. Zaninotto, M. De Pizzol, L. Zammataro, D. Girelli, G. Cairo, Differential regulation of iron homeostasis during human macrophage polarized activation, *European Journal of Immunology* **40**, 824-35 (2010).

[178] T.J. Koh, L.A. DiPietro, Inflammation and wound healing: the role of the macrophage, *Expert Reviews in Molecular Medicine* **13**, e23 (2011).

[179] P. Italiani, D. Boraschi, From Monocytes to M1/M2 Macrophages: Phenotypical vs. Functional Differentiation, *Frontiers in immunology* **5**, 514 (2014).

[180] S. Gordon, Alternative activation of macrophages, *Nature Reviews Immunology* **3**, 23-35 (2003).

[181] L. Wistlich, J. Kums, A. Rossi, K.-H. Heffels, H. Wajant, J. Groll, Multimodal Bioactivation of Hydrophilic Electrospun Nanofibers Enables Simultaneous Tuning of Cell Adhesivity and Immunomodulatory Effects, *Advanced Functional Materials* **27**, 1702903 (2017).

[182] A. Toniolo, G.P. Fadini, S. Tedesco, R. Cappellari, E. Vegeto, A. Maggi, A. Avogaro, C. Bolego, A. Cignarella, Alternative activation of human macrophages is rescued by estrogen treatment in vitro and impaired by menopausal status, *The Journal of Clinical Endocrinology and Metabolism* **100**, E50-8 (2015).

[183] Y. Yang, N.S. Luo, R. Ying, Y. Xie, J.Y. Chen, X.Q. Wang, Z.J. Gu, J.T. Mai, W.H. Liu, M.X. Wu, Z.T. Chen, Y.B. Fang, H.F. Zhang, Z.Y. Zuo, J.F. Wang, Y.X. Chen, Macrophage-derived foam cells impair endothelial barrier function by inducing endothelial-mesenchymal transition via CCL-4, *International Journal of Molecular Medicine* **40**, 558-568 (2017).

[184] M. Bartneck, K.H. Heffels, Y. Pan, M. Bovi, G. Zwadlo-Klarwasser, J. Groll, Inducing healing-like human primary macrophage phenotypes by 3D hydrogel coated nanofibres, *Biomaterials* **33**, 4136-46 (2012).

[185] H. Cao, K. McHugh, S.Y. Chew, J.M. Anderson, The topographical effect of electrospun nanofibrous scaffolds on the in vivo and in vitro foreign body reaction, *Journal of Biomedical Materials Research Part A* **93**, 1151-9 (2010).

[186] F.M. Wunner, M.L. Wille, T.G. Noonan, O. Bas, P.D. Dalton, E.M. De-Juan-Pardo, D.W. Hutmacher, Melt Electrospinning Writing of Highly Ordered Large Volume Scaffold Architectures, *Advanced Materials* **30**, e1706570 (2018).

[187] C. Blum, K. Schlegelmilch, T. Schilling, A. Shridhar, M. Rudert, F. Jakob, P. Dalton, T. Blunk, L. Flynn, J. Groll, Extracellular matrix-modified fiber scaffolds as a pro-adipogenic mesenchymal stromal cell delivery platform, *ACS Biomaterials Science & Engineering*, (2019).

[188] T.D. Zaveri, J.S. Lewis, N.V. Dolgova, M.J. Clare-Salzler, B.G. Keselowsky, Integrin-directed modulation of macrophage responses to biomaterials, *Biomaterials* **35**, 3504-15 (2014).

[189] E.M. Sussman, M.C. Halpin, J. Muster, R.T. Moon, B.D. Ratner, Porous implants modulate healing and induce shifts in local macrophage polarization in the foreign body reaction, *Annals of Biomedical Engineering* **42**, 1508-16 (2014).

[190] N.R. Patel, M. Bole, C. Chen, C.C. Hardin, A.T. Kho, J. Mih, L. Deng, J. Butler, D. Tschumperlin, J.J. Fredberg, R. Krishnan, H. Koziel, Cell elasticity determines macrophage function, *PLoS One* **7**, e41024 (2012).

[191] N.E. Paul, C. Skazik, M. Harwardt, M. Bartneck, B. Denecke, D. Klee, J. Salber, G. Zwadlo-Klarwasser, Topographical control of human macrophages by a regularly microstructured polyvinylidene fluoride surface, *Biomaterials* **29**, 4056-64 (2008).

References

[192] P.C. Bota, A.M. Collie, P. Puolakkainen, R.B. Vernon, E.H. Sage, B.D. Ratner, P.S. Stayton, Biomaterial topography alters healing in vivo and monocyte/macrophage activation in vitro, *Journal of Biomedical Materials Research Part A* **95**, 649-57 (2010).

[193] F. Krombach, S. Münzing, A.M. Allmeling, J.T. Gerlach, J. Behr, M. Dörger, Cell size of alveolar macrophages: an interspecies comparison, *Environmental health perspectives* **105 Suppl 5**, 1261-1263 (1997).

[194] S. Bertlein, D. Hikimoto, G. Hochleitner, J. Hümmer, T. Jungst, M. Matsusaki, M. Akashi, J. Groll, Development of Endothelial Cell Networks in 3D Tissues by Combination of Melt Electrospinning Writing with Cell-Accumulation Technology, *Small* **14**, 1701521 (2018).

[195] E. Saino, M.L. Focarete, C. Gualandi, E. Emanuele, A.I. Cornaglia, M. Imbriani, L. Visai, Effect of electrospun fiber diameter and alignment on macrophage activation and secretion of proinflammatory cytokines and chemokines, *Biomacromolecules* **12**, 1900-11 (2011).

[196] R. Hixon Katherine, J. Dunn Andrew, R. Flores, A. Minden-Birkenmaier Benjamin, A.G. Kalaf Emily, P. Shornick Laurie, A. Sell Scott, Using Electrospun Scaffolds to Promote Macrophage Phenotypic Modulation and Support Wound Healing, *Electrospinning* **1**, 31 (2017).

[197] K.N. Couper, D.G. Blount, E.M. Riley, IL-10: the master regulator of immunity to infection, *Journal of Immunology* **180**, 5771-7 (2008).

[198] M. Zhang, G. Hutter, S.A. Kahn, T.D. Azad, S. Gholamin, C.Y. Xu, J. Liu, A.S. Achrol, C. Richard, P. Sommerkamp, M.K. Schoen, M.N. McCracken, R. Majeti, I. Weissman, S.S. Mitra, S.H. Cheshier, Anti-CD47 Treatment Stimulates Phagocytosis of Glioblastoma by M1 and M2 Polarized Macrophages and Promotes M1 Polarized Macrophages In vivo, *PLoS One* **11**, e0153550 (2016).

[199] D. Schulz, Y. Severin, V.R.T. Zanotelli, B. Bodenmiller, In-Depth Characterization of Monocyte-Derived Macrophages using a Mass Cytometry-Based Phagocytosis Assay, *Scientific Reports* **9**, 1925 (2019).

[200] M. Lingnau, C. Hoflich, H.D. Volk, R. Sabat, W.D. Docke, Interleukin-10 enhances the CD14-dependent phagocytosis of bacteria and apoptotic cells by human monocytes, *Human Immunology* **68**, 730-8 (2007).

[201] A. Mahmoudzadeh, A. Mohsenifar, T. Rahmani-Cherati, Collagen-chitosan 3-D nano-scaffolds effects on macrophage phagocytosis and pro-inflammatory cytokine release, *Journal of Immunotoxicology* **13**, 526-34 (2016).

[202] A. Das, M. Sinha, S. Datta, M. Abas, S. Chaffee, C.K. Sen, S. Roy, Monocyte and macrophage plasticity in tissue repair and regeneration, *The American Journal of Pathology* **185**, 2596-606 (2015).

[203] L. Arnold, A. Henry, F. Poron, Y. Baba-Amer, N. van Rooijen, A. Plonquet, R.K. Gherardi, B. Chazaud, Inflammatory monocytes recruited after skeletal muscle injury switch into antiinflammatory macrophages to support myogenesis, *Journal of Experimental Medicine* **204**, 1057-69 (2007).

[204] M.J. Crane, J.M. Daley, O. van Houtte, S.K. Brancato, W.L. Henry, Jr., J.E. Albina, The monocyte to macrophage transition in the murine sterile wound, *PLoS One* **9**, e86660 (2014).

[205] M.N. Michalski, A.J. Koh, S. Weidner, H. Roca, L.K. McCauley, Modulation of Osteoblastic Cell Efferocytosis by Bone Marrow Macrophages, *Journal of Cellular Biochemistry* **117**, 2697-2706 (2016).

[206] B.P. Sinder, A.R. Pettit, L.K. McCauley, Macrophages: Their Emerging Roles in Bone, *Journal of Bone and Mineral Research* **30**, 2140-2149 (2015).

[207] J. Chang, A.J. Koh, H. Roca, L.K. McCauley, Juxtacrine interaction of macrophages and bone marrow stromal cells induce interleukin-6 signals and promote cell migration, *Bone Research* **3**, 15014 (2015).

[208] S. Ma, N. Xie, W. Li, B. Yuan, Y. Shi, Y. Wang, Immunobiology of mesenchymal stem cells, *Cell Death & Differentiation* **21**, 216-25 (2014).

[209] K. English, Mechanisms of mesenchymal stromal cell immunomodulation, *Immunology & Cell Biology* **91**, 19-26 (2013).

[210] S. Maxson, E.A. Lopez, D. Yoo, A. Danilkovitch-Miagkova, M.A. Leroux, Concise review: role of mesenchymal stem cells in wound repair, *Stem Cells Translational Medicine* **1**, 142-9 (2012).

[211] R. Trindade, T. Albrektsson, P. Tengvall, A. Wennerberg, Foreign Body Reaction to Biomaterials: On Mechanisms for Buildup and Breakdown of Osseointegration, *Clinical Implant Dentistry and Related Research* **18**, 192-203 (2016).

[212] A.R. Wolfe, N.J. Trenton, B.G. Debeb, R. Larson, B. Ruffell, K. Chu, W. Hittelman, M. Diehl, J.M. Reuben, N.T. Ueno, W.A. Woodward, Mesenchymal stem cells and macrophages interact through IL-6 to promote inflammatory breast cancer in pre-clinical models, *Oncotarget*, (2016).

[213] M.V. Jackson, T.J. Morrison, D.F. Doherty, D.F. McAuley, M.A. Matthay, A. Kissenpfennig, C.M. O'Kane, A.D. Krasnodembskaya, Mitochondrial Transfer via Tunneling Nanotubes is an Important Mechanism by Which Mesenchymal Stem Cells Enhance Macrophage Phagocytosis in the In vitro and In vivo Models of ARDS, *Stem Cells* **34**, 2210-23 (2016).

[214] X. Wang, H.H. Gerdes, Transfer of mitochondria via tunneling nanotubes rescues apoptotic PC12 cells, *Cell Death & Differentiation* **22**, 1181-91 (2015).

[215] D. Torralba, F. Baixauli, F. Sanchez-Madrid, Mitochondria Know No Boundaries: Mechanisms and Functions of Intercellular Mitochondrial Transfer, *Frontiers in Cell and Developmental Biology* **4**, 107 (2016).

[216] M. Bittins, X. Wang, TNT-Induced Phagocytosis: Tunneling Nanotubes Mediate the Transfer of Pro-Phagocytic Signals from Apoptotic to Viable Cells, *Journal of Cellular Physiology*, (2016).

[217] D.G. Phinney, M. Di Giuseppe, J. Njah, E. Sala, S. Shiva, C.M. St Croix, D.B. Stolz, S.C. Watkins, Y.P. Di, G.D. Leikauf, J. Kolls, D.W. Riches, G. Deiuliis, N. Kaminski, S.V. Boregowda, D.H. McKenna, L.A. Ortiz, Mesenchymal stem cells use extracellular vesicles to outsource mitophagy and shuttle microRNAs, *Nature Communications* **6**, 8472 (2015).

[218] M. Saenz-Cuesta, I. Osorio-Querejeta, D. Otaegui, Extracellular Vesicles in Multiple Sclerosis: What are They Telling Us?, *Frontiers in Cellular Neuroscience* **8**, 100 (2014).

[219] V. Torraca, S. Masud, H.P. Spaink, A.H. Meijer, Macrophage-pathogen interactions in infectious diseases: new therapeutic insights from the zebrafish host model, *Disease Models & Mechanisms* **7**, 785-97 (2014).

[220] U. Noth, R. Tuli, A.M. Osyczka, K.G. Danielson, R.S. Tuan, In vitro engineered cartilage constructs produced by press-coating biodegradable polymer with human mesenchymal stem cells, *Tissue Engineering* **8**, 131-44 (2002).

[221] S. Gordon, P.R. Taylor, Monocyte and macrophage heterogeneity, *Nature Reviews Immunology* **5**, 953-64 (2005).

[222] C.M. Leopold Wager, F.L. Wormley, Jr., Classical versus alternative macrophage activation: the Ying and the Yang in host defense against pulmonary fungal infections, *Mucosal Immunology* **7**, 1023-35 (2014).

References

[223] T. Rőszer, Understanding the Mysterious M2 Macrophage through Activation Markers and Effector Mechanisms, *Mediators of inflammation* **2015**, 816460-816460 (2015).

[224] A. Elchaninov, T. Fatkhudinov, N. Usman, I. Arutyunyan, A. Makarov, A. Lokhonina, I. Eremina, V. Surovtsev, D. Goldshtein, G. Bolshakova, V. Glinkina, G. Sukhikh, Multipotent stromal cells stimulate liver regeneration by influencing the macrophage polarization in rat, *World Journal of Hepatology* **10**, 287-296 (2018).

[225] R. Rabani, A. Volchuk, M. Jerkic, L. Ormesher, L. Garces-Ramirez, J. Canton, C. Masterson, S. Gagnon, K.C. Tatham, J. Marshall, S. Grinstein, J.G. Laffey, K. Szaszi, G.F. Curley, Mesenchymal stem cells enhance NOX2 dependent ROS production and bacterial killing in macrophages during sepsis, *European Respiratory Journal*, (2018).

[226] J. Pajarinen, T. Lin, E. Gibon, Y. Kohno, M. Maruyama, K. Nathan, L. Lu, Z. Yao, S.B. Goodman, Mesenchymal stem cell-macrophage crosstalk and bone healing, *Biomaterials*, (2018).

[227] S.P. Bruder, A.A. Kurth, M. Shea, W.C. Hayes, N. Jaiswal, S. Kadiyala, Bone regeneration by implantation of purified, culture-expanded human mesenchymal stem cells, *Journal of Orthopaedic Research* **16**, 155-62 (1998).

[228] S. Kadiyala, R.G. Young, M.A. Thiede, S.P. Bruder, Culture expanded canine mesenchymal stem cells possess osteochondrogenic potential in vivo and in vitro, *Cell Transplantation* **6**, 125-34 (1997).

[229] M.A. Scott, V.T. Nguyen, B. Levi, A.W. James, Current methods of adipogenic differentiation of mesenchymal stem cells, *Stem Cells and Development* **20**, 1793-804 (2011).

[230] N. Takizawa, N. Okubo, M. Kamo, N. Chosa, T. Mikami, K. Suzuki, S. Yokota, M. Ibi, M. Ohtsuka, M. Taira, T. Yaegashi, A. Ishisaki, S. Kyakumoto, Bone marrow-derived mesenchymal stem cells propagate immunosuppressive/anti-inflammatory macrophages in cell-to-cell contact-independent and -dependent manners under hypoxic culture, *Experimental Cell Research* **358**, 411-420 (2017).

[231] Q.Z. Zhang, W.R. Su, S.H. Shi, P. Wilder-Smith, A.P. Xiang, A. Wong, A.L. Nguyen, C.W. Kwon, A.D. Le, Human gingiva-derived mesenchymal stem cells elicit polarization of m2 macrophages and enhance cutaneous wound healing, *Stem Cells* **28**, 1856-68 (2010).

[232] J. Tellez, I. Romero, M.J. Soares, M. Steindel, A.J. Romanha, Knockdown of Host Antioxidant Defense Genes Enhances the Effect of Glucantime on Intracellular Leishmania braziliensis in Human Macrophages, *Antimicrobial Agents and Chemotherapy* **61**, (2017).

[233] G. Valles, F. Bensiamar, L. Crespo, M. Arruebo, N. Vilaboa, L. Saldana, Topographical cues regulate the crosstalk between MSCs and macrophages, *Biomaterials* **37**, 124-33 (2015).

[234] L. Saldana, G. Valles, F. Bensiamar, F.J. Mancebo, E. Garcia-Rey, N. Vilaboa, Paracrine interactions between mesenchymal stem cells and macrophages are regulated by 1,25-dihydroxyvitamin D3, *Scientific Reports* **7**, 14618 (2017).

[235] N. Grotenhuis, S.F.H. De Witte, G.J.V.M. van Osch, Y. Bayon, J.F. Lange, Y.M. Bastiaansen-Jenniskens, Biomaterials Influence Macrophage–Mesenchymal Stem Cell Interaction In vitro, *Tissue Engineering Part A* **22**, 1098-1107 (2016).

[236] T.P. Mikolajczyk, J.E. Skrzeczynska-Moncznik, M.A. Zarebski, E.A. Marewicz, A.M. Wisniewska, M. Dzieba, J.W. Dobrucki, J.R. Pryjma, Interaction of human peripheral blood monocytes with apoptotic polymorphonuclear cells, *Immunology* **128**, 103-13 (2009).

[237] R.A. Salah, I.K. Mohamed, N. El-Badri, Development of decellularized amniotic membrane as a bioscaffold for bone marrow-derived mesenchymal stem cells: ultrastructural study, *Journal of Molecular Histology*, (2018).

[238] A. Infante, C.I. Rodriguez, Secretome analysis of in vitro aged human mesenchymal stem cells reveals IGFBP7 as a putative factor for promoting osteogenesis, *Scientific Reports* **8**, 4632 (2018).

[239] R. Mobasseri, L. Tian, M. Soleimani, S. Ramakrishna, H. Naderi-Manesh, Peptide modified nanofibrous scaffold promotes human mesenchymal stem cell proliferation and long-term passaging, *Materials Science & Engineering C-Materials for Biological Applications* **84**, 80-89 (2018).

[240] A. Altaie, T.G. Baboolal, O. Wall, E. Jones, D. McGonagle, Platelet lysate enhances synovial fluid multipotential stromal cells functions: Implications for therapeutic use, *Cytotherapy* **20**, 375-384 (2018).

[241] E. Fernandez-Rebollo, B. Mentrup, R. Ebert, J. Franzen, G. Abagnale, T. Sieben, A. Ostrowska, P. Hoffmann, P.-F. Roux, B. Rath, M. Goodhardt, J.-M. Lemaitre, O. Bischof, F. Jakob, W. Wagner, Human Platelet Lysate versus Fetal Calf Serum: These Supplements Do Not Select for Different Mesenchymal Stromal Cells, *Scientific Reports* **7**, 5132 (2017).

[242] K. Schallmoser, D. Strunk, Generation of a pool of human platelet lysate and efficient use in cell culture, *Methods in Molecular Biology* **946**, 349-62 (2013).

[243] K. Schallmoser, D. Strunk, Preparation of pooled human platelet lysate (pHPL) as an efficient supplement for animal serum-free human stem cell cultures, *Journal of Visualized Experiments*, (2009).

[244] G. Astori, E. Amati, F. Bambi, M. Bernardi, K. Chieregato, R. Schafer, S. Sella, F. Rodeghiero, Platelet lysate as a substitute for animal serum for the ex-vivo expansion of mesenchymal stem/stromal cells: present and future, *Stem Cell Research & Therapy* **7**, 93 (2016).

[245] M. Gawaz, S. Vogel, Platelets in tissue repair: control of apoptosis and interactions with regenerative cells, *Blood* **122**, 2550-4 (2013).

[246] C. Pignatelli, G. Perotto, M. Nardini, R. Cancedda, M. Mastrogiacomo, A. Athanassiou, Electrospun silk fibroin fibers for storage and controlled release of human platelet lysate, *Acta biomaterialia* **73**, 365-376 (2018).

[247] L.D.F. Almeida, P.S. Babo, C.R. Silva, M.T. Rodrigues, J. Hebling, R.L. Reis, M.E. Gomes, Hyaluronic acid hydrogels incorporating platelet lysate enhance human pulp cell proliferation and differentiation, *Journal of Materials Science: Materials in Medicine* **29**, 88 (2018).

[248] M. Camprubi-Rimblas, R. Guillamat-Prats, T. Lebouvier, J. Bringue, L. Chimenti, M. Iglesias, C. Obiols, J. Tijero, L. Blanch, A. Artigas, Role of heparin in pulmonary cell populations in an in-vitro model of acute lung injury, *Respiratory Research* **18**, 89 (2017).

[249] R. Fazzina, P. Iudicone, D. Fioravanti, G. Bonanno, P. Totta, I.G. Zizzari, L. Pierelli, Potency testing of mesenchymal stromal cell growth expanded in human platelet lysate from different human tissues, *Stem Cell Research & Therapy* **7**, 122 (2016).

[250] S. MacLauchlan, E.A. Skokos, N. Meznarich, D.H. Zhu, S. Raoof, J.M. Shipley, R.M. Senior, P. Bornstein, T.R. Kyriakides, Macrophage fusion, giant cell formation, and the foreign body response require matrix metalloproteinase 9, *Journal of Leukocyte Biology* **85**, 617-26 (2009).

[251] S. Clasper, S. Vekemans, M. Fiore, M. Plebanski, P. Wordsworth, G. David, D.G. Jackson, Inducible expression of the cell surface heparan sulfate proteoglycan syndecan-2 (fibroglycan) on human activated macrophages can regulate fibroblast growth factor action, *Journal of Biological Chemistry* **274**, 24113-23 (1999).

[252] J. Liu, L.C. Pedersen, Anticoagulant heparan sulfate: structural specificity and biosynthesis, *Applied Microbiology and Biotechnology* **74**, 263-72 (2007).

[253] D.J. Holt, L.M. Chamberlain, D.W. Grainger, Cell-cell signaling in co-cultures of macrophages and fibroblasts, *Biomaterials* **31**, 9382-9394 (2010).

References

[254] G. Zhou, H. Loppnow, T. Groth, A macrophage/fibroblast co-culture system using a cell migration chamber to study inflammatory effects of biomaterials, *Acta biomaterialia* **26**, 54-63 (2015).

[255] H. Pan, H. Jiang, S. Kantharia, W. Chen, A fibroblast/macrophage co-culture model to evaluate the biocompatibility of an electrospun Dextran/PLGA scaffold and its potential to induce inflammatory responses, *Biomedical Materials* **6**, 065002 (2011).

[256] H.C. Cohen, E.J. Joyce, W.J. Kao, Biomaterials Selectively Modulate Interactions between Human Blood-Derived Polymorphonuclear Leukocytes and Monocytes, *The American Journal of Pathology* **182**, 2180-2190 (2013).

[257] M.C. Ramello, J. Tosello Boari, F.P. Canale, H.A. Mena, S. Negrotto, B. Gastman, A. Gruppi, E.V. Acosta Rodríguez, C.L. Montes, Tumor-induced senescent T cells promote the secretion of pro-inflammatory cytokines and angiogenic factors by human monocytes/macrophages through a mechanism that involves Tim-3 and CD40L, *Cell Death and Disease* **5**, e1507 (2014).

[258] S.M. Melief, C.L.M. Schrama, H. Roelofs, Monocyte-MSC Co-cultures, *Bio-protocol* **5**, e1384 (2015).

[259] C. Witherel, P. Kubinski, K. L. Spiller, In vitro Model of Macrophage-Biomaterial Interactions, 161-176 (2018).

[260] T. Woodford-Thomas, M.L. Thomas, The leukocyte common antigen, CD45 and other protein tyrosine phosphatases in hematopoietic cells, *Seminars in Cell Biology* **4**, 409-418 (1993).

[261] E.T. Camilleri, M.P. Gustafson, A. Dudakovic, S.M. Riester, C.G. Garces, C.R. Paradise, H. Takai, M. Karperien, S. Cool, H.-J.I. Sampen, A.N. Larson, W. Qu, J. Smith, A.B. Dietz, A.J. van Wijnen, Identification and validation of multiple cell surface markers of clinical-grade adipose-derived mesenchymal stromal cells as novel release criteria for good manufacturing practice-compliant production, *Stem Cell Research & Therapy* **7**, 107-107 (2016).

[262] L.M. Doyle, M.Z. Wang, Overview of Extracellular Vesicles, Their Origin, Composition, Purpose, and Methods for Exosome Isolation and Analysis, *Cells* **8**, (2019).

[263] L.M.A. Murray, A.D. Krasnodembskaya, Concise Review: Intercellular Communication Via Organelle Transfer in the Biology and Therapeutic Applications of Stem Cells, *Stem Cells* **37**, 14-25 (2019).

[264] V.T.M. Dos Santos, A. Mizukami, M.D. Orellana, S.R. Caruso, F.B. da Silva, F. Traina, K. de Lima Prata, D.T. Covas, K. Swiech, Characterization of Human AB Serum for Mesenchymal Stromal Cell Expansion, *Transfusion Medicine and Hemotherapy* **44**, 11-21 (2017).

[265] K. Tateishi, W. Ando, C. Higuchi, D.A. Hart, J. Hashimoto, K. Nakata, H. Yoshikawa, N. Nakamura, Comparison of Human Serum with Fetal Bovine Serum for Expansion and Differentiation of Human Synovial MSC: Potential Feasibility for Clinical Applications, *Cell Transplantation* **17**, 549-557 (2008).

[266] M. Pereira, T.D. Chen, N. Buang, A. Olona, J.H. Ko, M. Prendecki, A.S.H. Costa, E. Nikitopoulou, L. Tronci, C.D. Pusey, H.T. Cook, S.P. McAdoo, C. Frezza, J. Behmoaras, Acute Iron Deprivation Reprograms Human Macrophage Metabolism and Reduces Inflammation In vivo, *Cell Reports* **28**, 498-511 e5 (2019).

[267] D. Pilling, E. Galvis-Carvajal, T.R. Karhadkar, N. Cox, R.H. Gomer, Monocyte differentiation and macrophage priming are regulated differentially by pentraxins and their ligands, *BMC Immunology* **18**, 30 (2017).

[268] A.B. Vasandan, S. Jahnavi, C. Shashank, P. Prasad, A. Kumar, S.J. Prasanna, Human Mesenchymal stem cells program macrophage plasticity by altering their metabolic status via a PGE2-dependent mechanism, *Scientific Reports* **6**, 38308 (2016).

[269] N. Espagnolle, A. Balguerie, E. Arnaud, L. Sensebe, A. Varin, CD54-Mediated Interaction with Pro-inflammatory Macrophages Increases the Immunosuppressive Function of Human Mesenchymal Stromal Cells, *Stem Cell Reports* **8**, 961-976 (2017).

[270] F. Swieringa, H.M.H. Spronk, J.W.M. Heemskerk, P.E.J. van der Meijden, Integrating platelet and coagulation activation in fibrin clot formation, *Research and practice in thrombosis and haemostasis* **2**, 450-460 (2018).

[271] A. Gros, V. Ollivier, B. Ho-Tin-Noé, Platelets in inflammation: regulation of leukocyte activities and vascular repair, *Frontiers in immunology* **5**, 678-678 (2015).

[272] C. Wang, MODULATING MACROPHAGE BEHAVIOUR AT THE BIOMATERIALS-TISSUE INTERFACE FOR ENHANCED OSTEOGENESIS AND OSSEOINTEGRATION, *Orthopaedic Proceedings* **100-B**, 113-113 (2018).

[273] T.B. Wissing, V. Bonito, E.E. van Haaften, M. van Doeselaar, M.M.C.P. Brugmans, H.M. Janssen, C.V.C. Bouten, A.I.P.M. Smits, Macrophage-Driven Biomaterial Degradation Depends on Scaffold Microarchitecture, *Frontiers in Bioengineering and Biotechnology* **7**, (2019).

[274] J.E. Rayahin, R.A. Gemeinhart, Activation of Macrophages in Response to Biomaterials, *Macrophages: Origin, Functions and Biointervention*, Springer International Publishing Cham, 317-351 (2017).

[275] L.B. Moore, T.R. Kyriakides, Molecular Characterization of Macrophage-Biomaterial Interactions, *Advances in experimental medicine and biology* **865**, 109-122 (2015).

Appendix

A.1. Abbreviations

2D	Two-dimensional
3D	Three-dimensional
7AAD	7-aminoactinomycin D
ATP	Adenosintriphosphat
BSA	Bovine serum albumin
CCL	Chemokine (C-C motif) ligand
CD	Cluster of differentiation
cDNA	Copy/complementary deoxyribonucleic acid
COX2	Cytochrome c oxidase subunit 2
CXCR/L	C-X-C chemokine receptor/ligand
DAPI	4',6-diamidino-2-phenylindole
DC	Dendritic cells
Dex	Dexamethasone
DMEM	Dulbecco's Modified Eagle's Medium
DMEM/F-12	Dulbecco's Modified Eagle's Medium/Ham's F-12
DMSO	Dimethyl sulfoxide
DNA	Deoxyribonucleic acid
ECM	Extracellular matrix
EDTA	Ethylenediaminetetraacetic acid
EV	Extracellular vesicles
FBGCs	Foreign body giant cells
FCS	Fetal calf serum
FITC	Fluorescein isothiocyanate
GCs	Glucocorticoids
GM-CSF	Granulocyte-macrophage colony-stimulating factor
HGF	Hepatocyte growth factor
hMSCs	Human mesenchymal stromal cells
hPL	Human platelet lysate
hPL -	Human platelet lysate without heparin
hPL +	Human platelet lysate plus heparin
hS	Human serum
IC	Immune complexes
IDO	Indoleamine2,3-dioxygenase
IFN-γ	Interferon-γ

Abbreviations

IL	Interleukin
LPS	Lipopolysaccharides
M-CSF	Macrophage colony-stimulating factor
MEW	Melt electrowriting
mRNA	Messenger Ribonucleic acid
MSC	Mesenchymal stromal/stem cells
MT-red	MitoTracker® Red
NADPH	Nicotinamide adenine dinucleotide phosphate
NK cell	Natural killer cell
PBS	Phosphate-buffered saline
PCL	Poly(ε-caprolactone)
PDGF	Platelet-derived growth factor
PGE2	Prostaglandin E2
PHEMA	Poly(2-hydroxyethyl methacrylate)
PS	Polystyrene
qPCR	Quantitative real-time polymerase chain reaction
RNA	Ribonucleic acid
ROS	Reactive oxygen species
rpm	Revolutions per minute
RPMI-1640	Roswell Park Memorial Institute 1640 (medium)
RT	Room temperature
SD	Standard deviation
SEM	Scanning electron microscopy
TGF-β1	Transforming growth factor-beta 1
Th1/2	T helper cell type 1/2
TLR	Toll-like receptor
TNF-α	Tumor necrosis factor-alpha
TNTs	Tunneling nanotubes
TSG6	TNF-α-stimulated-gene
VEGF	Vascular endothelial growth factor

A.2. Curriculum Vitae

Curriculum Vitae

A.3. Publications and Conference Contributions

Publications

1. **Tina Tylek**, Katrin Schlegelmilch, Andrea Ewald, Maximilian Rudert, Franz Jakob, Jürgen Groll, Cell communication modes and bidirectional mitochondrial exchange in direct and indirect macrophage/hMSC co-culture models, BioNanoMaterials, Issue 3-4 (2017).

2. **Tina Tylek**, Tatjana Schilling, Katrin Schlegelmilch, Maximilian Ries, Maximilian Rudert, Franz Jakob, Jürgen Groll, Platelet lysate outperforms FCS and human serum for co-culture of primary human macrophages and hMSCs, Scientific Reports, Volume 9, Article number: 3533 (2019).

3. **Tina Tylek***, Carina Blum*, Andrei Hrynevich, Katrin Schlegelmilch, Tatjana Schilling, Paul D. Dalton, Jürgen Groll, Precisely Defined Fiber Scaffolds with 40 µm Porosity Induce Elongation-driven M2-like Polarization of Human Macrophages. *Equally contributing authors. In revision (Biofabrication).

Oral Presentations

- **Tina Tylek**, Katrin Schlegelmilch, Andrea Ewald, Franz Jakob, Jürgen Groll, Makrophagen und mesenchymale Stromazellen im direkten und in-direktem Co-Kultur-System, Annual Meeting of the German Society for Biomaterials 2016, Aachen, Germany.

- **Tina Tylek,** Katrin Schlegelmilch, Andrea Ewald, Franz Jakob, Jürgen Groll, Bidirectional Communications of Macrophages and Mesenchymal Stromal Cells in Direct and Indirect Co-Culture System, Member Meeting of the German Society for Cell Biology 2017, Leipzig, Germany

- **Tina Tylek**, Katrin Schlegelmilch, Tatjana Schilling, Jürgen Groll, The effects of platelet lysate on human macrophages in *in vitro* mono- or co-culture with hBMSCs, 5th TERMIS World Congress 2018, Kyoto, Japan.

- **Tina Tylek**, Carina Blum, Tatjana Schilling, Katrin Schlegelmilch, Andrei Hrynevich, Paul D. Dalton, Jürgen Groll, Pore Size-Dependent Polarization of Human Macrophages towards the M2-Type on Melt-Electrowritten Scaffolds, TERMIS European Chapter Meeting 2019, Rhodes, Greece.

Poster Presentations

- **Tina Tylek**, Katrin Schlegelmilch, Tatjana Schilling, Jürgen Groll, Platelet lysate – a serum alternative for human macrophage *in vitro* cultivation in mono- or co-culture with hBMSCs, Annual Meeting of the German Society for Biomaterials 2017, Wuerzburg, Germany.

- **Tina Tylek**, Carina Blum, Tatjana Schilling, Katrin Schlegelmilch, Andrei Hrynevich, Jürgen Groll, Assessment of macrophage reaction and polarization to melt-electrowritten scaffolds, Annual Meeting of the International Society for Biofabrication 2018, Wuerzburg, Germany.

- **Tina Tylek**, Carina Blum, Matthias Ryma, Tatjana Schilling, Katrin Schlegelmilch, Andrei Hrynevich, Paul D. Dalton, Jürgen Groll, Assessment of Human Macrophage Polarization on 3D Melt-Electrowritten Scaffolds Varying in Material and Topography, Tissue Repair and Regeneration - Gordon Research Seminar and Conference 2019, New London, NH, USA.

- **Tina Tylek**, Carina Blum, Katrin Schlegelmilch, Tatjana Schilling, Franz Jakob, Jürgen Groll, *In vitro* co-culture system of macrophages and mesenchymal stromal cells – an important tool for biomaterial assessment, 30th Annual Conference of the European Society for Biomaterials 2019, Dresden, Germany.

Discussion Leader

- Session: Biomaterials, Cell and Gene Therapy Strategies for Tissue Repair and Regeneration. Conference: Tissue Repair and Regeneration - Gordon Research Seminar and Conference 2019, New London, NH, USA.

A.4. Acknowledgment/Danksagung

Acknoweldgement/Danksagung

A.5. Affidavit

I hereby confirm that my thesis entitled "Establishment of a Co-culture System of human Macrophages and hMSCs to Evaluate the Immunomodulatory Properties of Biomaterials" is the result of my own work. I did not receive any help or support from commercial consultants. All sources and / or materials applied are listed and specified in the thesis.

Furthermore, I confirm that this thesis has not yet been submitted as part of another examination process neither in identical nor in similar form.

Place, Date   Signature

A.6. Eidesstattliche Erklärung

Hiermit erkläre ich an Eides statt, die Dissertation „Etablierung eines Co-Kultur-Systems von humanen Makrophagen und hMSCs zur Bewertung der Immunmodulatorischen Eigenschaften von Biomaterialien" eigenständig, d.h. insbesondere selbständig und ohne Hilfe eines kommerziellen Promotionsberaters, angefertigt und keine anderen als die von mir angegebenen Quellen und Hilfsmittel verwendet zu haben.

Ich erkläre außerdem, dass die Dissertation weder in gleicher noch in ähnlicher Form bereits in einem anderen Prüfungsverfahren vorgelegen hat.

Ort, Datum   Unterschrift